

**DYNAMICS OF SCHWARZ REFLECTIONS:
THE MATING PHENOMENA**

SEUNG-YEOP LEE, MIKHAIL LYUBICH, NIKOLAI G. MAKAROV,
AND SABYASACHI MUKHERJEE

ABSTRACT. In this paper, we initiate the exploration of a new class of anti-holomorphic dynamical systems generated by Schwarz reflection maps associated with quadrature domains. More precisely, we study Schwarz reflection with respect to a deltoid, and Schwarz reflections with respect to a cardioid and a family of circumscribing circles. We describe the dynamical planes of the maps in question, and show that in many cases, they arise as unique conformal matings of quadratic anti-holomorphic polynomials and the ideal triangle group.

CONTENTS

1. Introduction	2
1.1. Quadrature Domains, and Schwarz Reflections	2
1.2. Coulomb Gas Ensembles and Algebraic Droplets	3
1.3. Anti-holomorphic Dynamics	4
1.4. Ideal Triangle Group and The Reflection Map ρ	5
1.5. Dynamical Decomposition: Tiling and Non-escaping Sets	5
1.6. C&C Family	7
1.7. Organization of The Paper	10
2. Background on Holomorphic Dynamics	11
2.1. Dynamics of Complex Quadratic Polynomials: The Mandelbrot Set	11
2.2. Dynamics of Quadratic Anti-Polynomials: The Tricorn	14
3. Ideal Triangle Group	17
3.1. The Reflection Map ρ , and Symbolic Dynamics	18
3.2. The Conjugacy \mathcal{E}	19
4. Quadrature Domains and Schwarz Reflection	20
5. Dynamics of Deltoid Reflection	22
5.1. Schwarz Reflection with Respect to a Deltoid	22
5.2. Local Connectivity of The Boundary of The Tiling Set	27
5.3. Conformal Removability of The Limit Set	29
5.4. Reflection Map as a Mating	33
6. Iterated Reflections with Respect to a Cardioid and a Circle	36
6.1. Schwarz Reflection with Respect to a Cardioid	36
6.2. The Dynamical and Parameter Planes	40
6.3. Dynamical Uniformization of The Tiling Set	52
7. Geometrically Finite Maps	59
7.1. Hyperbolic and Parabolic Maps	59
7.2. Misiurewicz Maps	63

Date: April 27, 2022.

8. Examples of Mating in The Circle and Cardioid Family	65
8.1. A Combinatorial Condition for Mating	66
8.2. The Basilica Map	68
8.3. The Chebyshev Map	69
References	70

1. INTRODUCTION

1.1. Quadrature Domains, and Schwarz Reflections. Schwarz reflections associated with quadrature domains (or disjoint unions of quadrature domains) provide an interesting class of dynamical systems. In some cases such systems combine the features of the dynamics of rational maps and reflection groups.

By definition, a domain $\Omega \subsetneq \hat{\mathbb{C}}$ satisfying $\infty \notin \partial\Omega$ and $\Omega = \text{int } \bar{\Omega}$ is a *quadrature domain* if there is a continuous function $S : \bar{\Omega} \rightarrow \hat{\mathbb{C}}$ such that S is meromorphic in Ω and $S(z) = \bar{z}$ on the boundary $\partial\Omega$. Such a function S is unique (if it exists). The *Schwarz reflection* σ associated with Ω is the complex conjugate of S ,

$$\sigma = \bar{S} : \bar{\Omega} \rightarrow \hat{\mathbb{C}}.$$

It is well known that except for a finite number of *singular* points (cusps and double points), the boundary of a quadrature domain consists of finitely many disjoint real analytic curves. Every non-singular boundary point has a neighborhood where the local reflection in $\partial\Omega$ is well-defined. The (global) Schwarz reflection σ is an anti-holomorphic continuation of all such local reflections.

Round discs on the Riemann sphere are the simplest examples of quadrature domains. Their Schwarz reflections are just the usual circle reflections. Further examples can be constructed using univalent polynomials or rational functions. Namely, if Ω is a *simply connected* domain and $\varphi : \mathbb{D} \rightarrow \Omega$ is a univalent map from the unit disc onto Ω , then Ω is a quadrature domain if and only if φ is a rational function. In this case, the Schwarz reflection σ associated with Ω is semi-conjugate by φ to reflection in the unit circle.

$$\begin{array}{ccc} \bar{\mathbb{D}} & \xrightarrow{\varphi} & \bar{\Omega} \\ \downarrow 1/\bar{z} & & \downarrow \sigma \\ \hat{\mathbb{C}} \setminus \mathbb{D} & \xrightarrow{\varphi} & \hat{\mathbb{C}} \end{array}$$

FIGURE 1. The rational map φ semi-conjugates the reflection map $1/\bar{z}$ of \mathbb{D} to the Schwarz reflection map σ of Ω .

Let us mention two specific examples: the interior of the *cardioid* curve and the exterior of the *deltoid* curve,

$$\left\{ \frac{z}{2} - \frac{z^2}{4} : |z| < 1 \right\} \quad \text{and} \quad \left\{ \frac{1}{z} + \frac{z^2}{2} : |z| < 1 \right\},$$

are quadrature domains. (Incidentally, the cardioid curve and the deltoid curve bound the principal hyperbolic components of the Mandelbrot set and, respectively, of the Tricorn, see Figures 7 and 8.)

Quadrature domains play an important role in diverse areas of complex analysis such as quadrature identities [Dav74, AS76, Sak82, Gus83], extremal problems for conformal mapping [Dur83, ASS99, SS00], Hele-Shaw flows [Ric72, EV92, GV06], Richardson’s moment problem [Sak78, EV92, GHMP00], free boundary problems [Sha92, Sak91, CKS00], subnormal and hyponormal operators [BG17].

1.2. Coulomb Gas Ensembles and Algebraic Droplets. Quadrature domains naturally arise in the study of 2-dimensional Coulomb gas models. Consider N electrons located at points $\{z_j\}_{j=1}^N$ in the complex plane, influenced by a strong (2-dimensional) external electrostatic field arising from a uniform non-zero charge density. Let the scalar potential of the external electrostatic field be $N \cdot Q : \mathbb{C} \rightarrow \mathbb{R} \cup \{+\infty\}$ (note that the scalar potential is rescaled so that it is proportional to the number of electrons). We assume that $Q = +\infty$ outside some compact set L , and finite (but not identically zero) on L (see Figure 2). Since the charge density of the potential Q is assumed be uniform (and non-zero), it follows that Q has constant Laplacian on L . It follows that we can write $Q(z) = |z|^2 - H(z)$ (on L), where H is harmonic. In various physically interesting cases, the scalar potential is assumed to be *algebraic*; i.e. $\frac{\partial H}{\partial z}$ is a rational function.

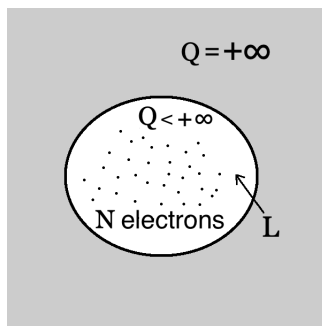


FIGURE 2. The external potential Q is infinite outside a compact set L . In the limit, the electrons condensate on a compact subset T (of L) which is called a droplet.

The combined energy of the system resulting from particle interaction and external potential is:

$$\mathcal{E}_Q(z_1, \dots, z_N) = \sum_{i \neq j} \ln |z_i - z_j|^{-1} + N \sum_{j=1}^N Q(z_j).$$

In the equilibrium, the states of this system are distributed according to the Gibbs measure with density

$$\frac{\exp(-\mathcal{E}_Q(z_1, \dots, z_N))}{Z_N},$$

where Z_N is a normalization constant known as the “partition function”.

An important topic in statistical physics is to understand the limiting behavior of the “electron cloud” as the number of electrons N grows to infinity. Under some mild regularity conditions on Q , in the limit the electrons condensate on a compact subset T of L , and they are distributed according to the normalized area measure of T [EF05, HM13]. Thus, the probability measure governing the distribution of the limiting electron cloud is completely determined by the shape of the “droplet” T .

If Q is algebraic, the complementary components of the droplet T are quadrature domains [LM16]. For example, the deltoid (the compact set bounded by the deltoid curve) is a droplet in the physically interesting case of the (localized) “cubic” external potential, see [Wie02].

The 2D Coulomb gas model described above is intimately related to logarithmic potential theory with an algebraic external field [ST97] and the corresponding random normal matrix models, where the same probability measure describes the distribution of eigenvalues [TBA⁺05, ABWZ02].

We will call any compact set $T \subset \mathbb{C}$ such that T^c is a disjoint union of quadrature domains an *algebraic droplet*, and we define the corresponding Schwarz reflection as a map $\sigma : \overline{T^c} \rightarrow \hat{\mathbb{C}}$. Iteration of Schwarz reflections was used in [LM16] to answer some questions concerning topology and singular points of quadrature domains and algebraic droplets, as well as the Hele-Shaw flow¹ of such domains. At the same time, these dynamical systems seem to be quite interesting in their own right, and in this paper we will take a closer look at them.

1.3. Anti-holomorphic Dynamics. In this paper, we will be mainly concerned with dynamics of Schwarz reflection maps (which are anti-holomorphic) with a single critical point. It is not surprising that their dynamics is closely related to the dynamics of quadratic anti-holomorphic polynomials (anti-polynomials for short).

The dynamics of quadratic anti-polynomials and their connectedness locus, the Tricorn, was first studied in [CHRSC89] (note that they called it the Mandelbar set). Their numerical experiments showed structural differences between the Mandelbrot set and the Tricorn. However, it was Milnor who first observed the importance of the Tricorn; he found little Tricorn-like sets as prototypical objects in the parameter space of real cubic polynomials [Mil92], and in the real slices of rational maps with two critical points [Mil00a]. Nakane followed up by proving that the Tricorn is connected [Nak93], in analogy to Douady and Hubbard’s classical proof of connectedness of the Mandelbrot set. Later, Nakane and Schleicher [NS03] studied the structure and dynamical uniformization of hyperbolic components of the Tricorn. It transpired from their study that while the even period hyperbolic components of the Tricorn are similar to those in the Mandelbrot set (the connectedness locus of quadratic holomorphic polynomials), the odd period ones have a completely different structure. Then, Hubbard and Schleicher [HS14] proved that the Tricorn is not pathwise connected, confirming a conjecture by Milnor. Techniques of anti-holomorphic dynamics were used in [KS03, BE16, BMMS17] to answer certain questions with physics motivation.

Recently, the topological and combinatorial differences between the Mandelbrot set and the Tricorn have been systematically studied by several people. The combinatorics of external dynamical rays of quadratic anti-polynomials was studied

¹It is a flow on the space of planar compact sets such that the normal velocity of the boundary of a compact set is proportional to its harmonic measure. This is an example of the so-called DLA or diffusion-limited aggregation process.

in [Muk15b] in terms of orbit portraits, and this was used in [MNS17] where the bifurcation phenomena, boundaries of odd period hyperbolic components, and the combinatorics of parameter rays were described. It was proved in [IM16b] that many rational parameter rays of the Tricorn non-trivially accumulate on persistently parabolic regions, and Misiurewicz parameters are not dense on the boundary of the Tricorn. These results are in stark contrast with the corresponding features of the Mandelbrot set. In this vein, Gauthier and Vigny [GV16] constructed a bifurcation measure for the Tricorn, and proved an equidistribution result for Misiurewicz parameter with respect to the bifurcation measure. As another fundamental difference between the Mandelbrot set and the Tricorn, it was proved in [IM16a] that the Tricorn contains infinitely many baby Tricorn-like sets, but these are not dynamically homeomorphic to the Tricorn. Tricorn-like sets also showed up in the recent work of Buff, Bonifant, and Milnor on the parameter space of a family of rational maps with real symmetry [BBM18] (also see [CFG15]).

1.4. Ideal Triangle Group and The Reflection Map ρ . The *ideal triangle group* \mathcal{G} is generated by the reflections in the sides of a hyperbolic triangle Π (in the open unit disk \mathbb{D}) with zero angles. Denoting the (anti-Möbius) reflection maps in the three sides of Π by ρ_1 , ρ_2 , and ρ_3 , we have

$$\mathcal{G} = \langle \rho_1, \rho_2, \rho_3 : \rho_1^2 = \rho_2^2 = \rho_3^2 = \text{id} \rangle < \text{Aut}(\mathbb{D}).$$

Π is a fundamental domain of the group. The tessellation of \mathbb{D} by images of the fundamental domain under the group elements are shown in Figure 3.

In order to model the dynamics of Schwarz reflection maps, we define a map

$$\rho : \mathbb{D} \setminus \text{int } \Pi \rightarrow \mathbb{D}$$

by setting it equal to ρ_k in the connected component of $\mathbb{D} \setminus \text{int } \Pi$ containing $\rho_k(\Pi)$ (for $k = 1, 2, 3$). The map ρ extends to an orientation-reversing double covering of $\mathbb{T} = \partial\mathbb{D}$ admitting a Markov partition $\mathbb{T} = [1, e^{2\pi i/3}] \cup [e^{2\pi i/3}, e^{4\pi i/3}] \cup [e^{4\pi i/3}, 1]$ with transition matrix

$$M := \begin{bmatrix} 0 & 1 & 1 \\ 1 & 0 & 1 \\ 1 & 1 & 0 \end{bmatrix}.$$

The anti-doubling map

$$m_{-2} : \mathbb{R}/\mathbb{Z} \rightarrow \mathbb{R}/\mathbb{Z}, \theta \mapsto -2\theta$$

(which models the dynamics of quadratic anti-polynomials on their Julia sets) admits the same Markov partition as above with the same transition matrix. This allows one to construct a circle homeomorphism $\mathcal{E} : \mathbb{T} \rightarrow \mathbb{T}$ that conjugates the reflection map ρ to the anti-doubling map m_{-2} . The conjugacy \mathcal{E} (which is a version of the Minkowski question mark function) serves as a connecting link between the dynamics of Schwarz reflections and that of quadratic anti-polynomials, and plays a crucial role in the paper (see Section 3 for details).

1.5. Dynamical Decomposition: Tiling and Non-escaping Sets. Let us now describe the basic dynamical objects associated with iteration of Schwarz reflection maps. Given an algebraic droplet T and the corresponding reflection $\sigma : \overline{T^c} \rightarrow \hat{\mathbb{C}}$, we partition $\hat{\mathbb{C}}$ into two invariant sets. The first one is an open set called the *tiling set*. It is the set of all points that eventually escape to T (where σ is no longer defined). Alternatively, the tiling set is the union of all “tiles”, the *fundamental*

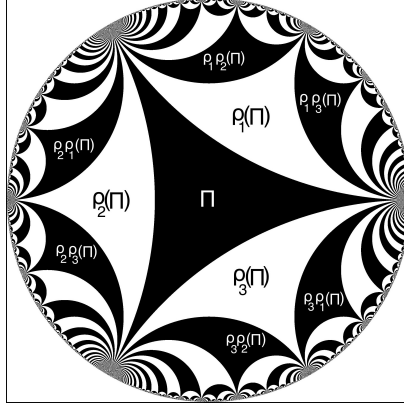


FIGURE 3. The \mathcal{G} -tessellation of \mathbb{D} and the formation of a few initial tiles are shown.

tile T (with singular points removed) and the components of all its pre-images under the iterations of σ . The second invariant set is the *non-escaping* set, the complement of the tiling set; it is analogous to the filled in Julia set in polynomial dynamics. The dynamics of σ on the non-escaping set is much like the dynamics of an anti-holomorphic rational-like map (which may be “pinched”). On the other hand, the dynamics on the tiling set exhibits features of reflection groups; this is particularly evident if the tiling set is *unramified* (i.e. if it does not contain any critical point of σ).

This is precisely the case if T is a deltoid. Figure 4 shows the tiling and the non-escaping sets as well as their common boundary, which is simultaneously analogous to the Julia set of an anti-polynomial and to the limit set of a group. In fact, the Schwarz reflection σ of the deltoid is the “mating” of the anti-polynomial $z \mapsto \bar{z}^2$ and the reflection map ρ in the following sense. As it was mentioned above, the conformal dynamical systems

$$\rho : \overline{\mathbb{D}} \setminus \text{int } \Pi \rightarrow \overline{\mathbb{D}}$$

and

$$f_0 : \hat{\mathbb{C}} \setminus \mathbb{D} \rightarrow \hat{\mathbb{C}} \setminus \mathbb{D}, z \mapsto \bar{z}^2$$

can be glued together by the circle homeomorphism \mathcal{E} (which conjugates ρ to f_0 on \mathbb{T}) to yield a (partially defined) topological map η on a topological 2-sphere. There exists a unique conformal structure on this 2-sphere which makes η an anti-holomorphic map conformally conjugate to σ .

In Section 5, we study in detail the dynamics of the Schwarz reflection map σ of the deltoid (which is one of the simplest non-trivial dynamical systems generated by Schwarz reflections), and prove the following theorem:

Theorem 1.1 (Dynamics of Deltoid Reflection). *1) The dynamical plane of the Schwarz reflection σ of the deltoid can be partitioned as*

$$\hat{\mathbb{C}} = T^\infty \sqcup \Gamma \sqcup A(\infty),$$

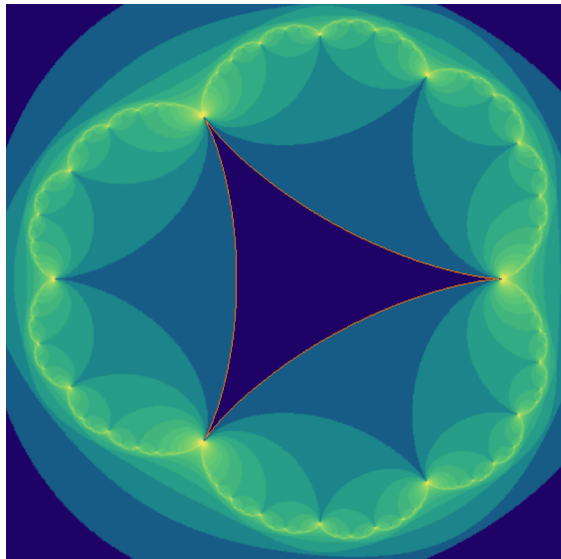


FIGURE 4. Schwarz dynamics of the deltoid with the tiles of various ranks shaded.

where T^∞ is the tiling set, $A(\infty)$ is the basin of infinity, and Γ is their common boundary (which we call the limit set). Moreover, Γ is a conformally removable Jordan curve.

2) σ is the unique conformal mating of the reflection map $\rho : \mathbb{D} \setminus \text{int } \Pi \rightarrow \mathbb{D}$ and the anti-polynomial $f_0 : \hat{\mathbb{C}} \setminus \mathbb{D} \rightarrow \hat{\mathbb{C}} \setminus \mathbb{D}$, $z \mapsto \bar{z}^2$.

This is a new occasion of a phenomenon discovered by Bullett and Penrose [BP94] (and more recently studied by Bullett and Lomonaco [BL17b, BL17a]), where matings of holomorphic quadratic polynomials and the modular group were realized as *holomorphic correspondences*.

Schwarz reflections associated with quadrature domains provide us with a general method of constructing such correspondences. In this paper, we apply this method to produce a family of conformal matings between the ideal triangle group and quadratic anti-polynomials $\bar{z}^2 + c$.

1.6. C&C Family. One of the principal goals of this paper is to study the dynamics of the following one-parameter family of Schwarz reflection maps. We consider a fixed cardioid, and for each complex number a , we consider the circle centered at a circumscribing the cardioid (see Figure 19 and Figure 20). Let T_a denote the resulting algebraic droplet (the closed disc minus the open cardioid), and let F_a denote the corresponding Schwarz reflection (the circle reflection σ_a in its exterior, and the reflection σ with respect to the cardioid in its interior). We denote this family of Schwarz reflections maps F_a by \mathcal{S} and call it the C&C family (“circle & cardioid”).

The Schwarz reflection map F_a is unicritical; indeed, the circle reflection map σ_a is univalent, while the cardioid reflection map σ has a unique critical point at the origin. Note that the droplet T_a has two singular point on its boundary. Removing these two singular point from T_a , we obtain the *desingularized droplet* T_a^0 (which is

also called the *fundamental tile*). Recall that the *non-escaping set* of F_a (denoted by K_a) consists of all points that do not escape to the fundamental tile T_a^0 under iterates of F_a , while the *tiling set* of F_a (denoted by T_a^∞) is the set of points that eventually escape to T_a^0 . The boundary of the tiling set is called the *limit set*, and is denoted by Γ_a .

As in the case of quadratic polynomials, the non-escaping set of F_a is *connected* if and only if it contains the unique critical point of F_a ; i.e. the critical point does not escape to the fundamental tile. On the other hand, if the critical point escapes to the fundamental tile, the corresponding non-escaping set is totally disconnected (see Figure 20 for various connected non-escaping sets, and Figure 25 for a totally disconnected non-escaping set).

Theorem 1.2 (Connectivity of The Non-escaping Set). *1) If the critical point of F_a does not escape to the fundamental tile T_a^0 , then the Riemann map ψ_a from T_a^0 onto Π extends to a biholomorphism between the tiling set T_a^∞ and the unit disk \mathbb{D} . Moreover, the extended map ψ_a conjugates F_a to the reflection map ρ . In particular, K_a is connected.*

2) If the critical point of F_a escapes to the fundamental tile, then the corresponding non-escaping set K_a is a Cantor set.

This leads to the notion of the *connectedness locus* $\mathcal{C}(\mathcal{S})$ as the set of parameters with connected non-escaping sets. Equivalently, $\mathcal{C}(\mathcal{S})$ is exactly the set of parameters for which the tiling set is unramified.

The geometrically finite maps (i.e. maps with attracting/parabolic cycles, and maps with strictly pre-periodic critical point) of \mathcal{S} are of particular importance. They belong to the connectedness locus $\mathcal{C}(\mathcal{S})$, and their topological and analytic properties are more tractable.

Theorem 1.3 (Limit Sets of Geometrically Finite Maps). *Let F_a be geometrically finite.*

1) The limit set Γ_a of F_a is locally connected. Moreover, the area of Γ_a is zero.

2) The iterated pre-images of the cardioid cusp are dense in the limit set Γ_a . Moreover, repelling periodic points of F_a are dense in Γ_a .

A good understanding of the dynamics of geometrically finite maps in the C&C family allow us to produce plenty of examples of conformal matings between the reflection map ρ and quadratic anti-polynomials. While this matter will be pursued in greater detail in a sequel to this work [LLMM18], here we describe the simplest examples of conformal matings appearing in the C&C family.

For any c_0 in the Tricorn with a locally connected Julia set, one can glue the conformal dynamical systems

$$\rho : \overline{\mathbb{D}} \setminus \text{int } \Pi \rightarrow \overline{\mathbb{D}}$$

and

$$f_{c_0} : \mathcal{K}_{c_0} \rightarrow \mathcal{K}_{c_0}, \quad z \mapsto \bar{z}^2 + c_0$$

(where \mathcal{K}_{c_0} is the filled Julia set of f_{c_0}) by (a factor of) the circle homeomorphism \mathcal{E} yielding a (partially defined) topological map η on a topological 2-sphere. We say that F_{a_0} is the unique conformal mating of ρ and the quadratic anti-polynomial f_{c_0} if this topological 2-sphere admits a unique conformal structure that turns η into an anti-holomorphic map conformally conjugate to F_{a_0} .

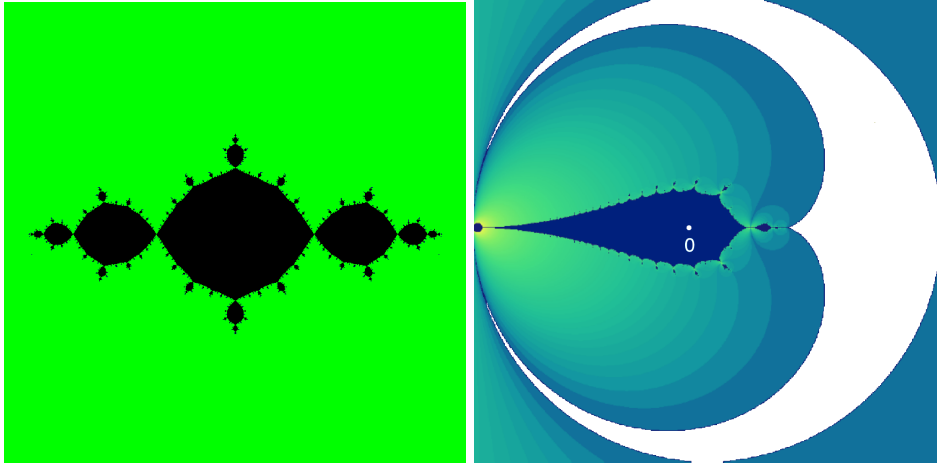


FIGURE 5. Left: The filled Julia set of the map $\bar{z}^2 - 1$. The map has a super-attracting cycle of period 2. Right: The part of the non-escaping set of F_0 inside the cardioid (in dark blue) with the critical point 0 marked. The map has a super-attracting cycle of period 2.

Theorem 1.4 (Basilica and Chebyshev Maps as Mating). 1) Let $a_0 = 0$. Then, F_{a_0} is the unique conformal mating of the reflection map ρ and the Basilica anti-polynomial $\bar{z}^2 - 1$.

2) Let $a_0 = \frac{1}{4}$. Then, F_{a_0} is the unique conformal mating of the reflection map ρ and the Chebyshev anti-polynomial $\bar{z}^2 - 2$.

The non-escaping sets and the filled Julia sets of the maps appearing in Theorem 1.4 are shown in Figure 5 and Figure 6.



FIGURE 6. Left: The Julia set $[-2, 2]$ of the Chebyshev anti-polynomial $\bar{z}^2 - 2$. The critical point of the map lands on the non-separating fixed point 2 in two iterates. Right: A part of the dynamical plane of the Misiurewicz parameter $a = \frac{1}{4}$. The corresponding limit set is the interval $[-\infty, \frac{1}{4}]$. The critical point of the map lands on the non-separating fixed point $\frac{1}{4}$ in two iterates.

Let us now state the main results of the sequel of this work. We will show that there exists a natural combinatorial bijection between the post-critically finite maps in the family \mathcal{S} and those in the *basilica limb* \mathcal{L} of the Tricorn (see [LLMM18, §2.4]). The combinatorial models of the corresponding maps are related by the circle homeomorphism \mathcal{E} . Moreover, we will show that every post-critically finite map in \mathcal{S} is a mating of a post-critically finite quadratic anti-polynomial and the reflection map ρ arising from the ideal triangle group. Using the combinatorial bijection between post-critically finite maps mentioned above, we will further show that the locally connected topological model of $\mathcal{C}(\mathcal{S})$ is naturally homeomorphic to that of the basilica limb \mathcal{L} (where the homeomorphism is induced by the map \mathcal{E}).

1.7. Organization of The Paper. In the first part of this work, we recall some fundamental facts about anti-holomorphic dynamics and quadrature domains, and study the dynamics of the C&C family. The second part is devoted to a detailed study of the parameter space of the C&C family culminating in the description of post-critically finite maps of the family as matings and a topological model of the parameter space [LLMM18].

Let us now detail the contents of the first part. In Section 2, we collect some useful results on the dynamics and parameter spaces of quadratic polynomials and anti-polynomials. Subsection 2.1 gathers some fundamental facts about the dynamics of quadratic polynomials and their connectedness locus, the Mandelbrot set. Since Schwarz reflection maps are anti-holomorphic, they are closer relatives of quadratic anti-polynomials. In Subsection 2.2, we briefly recall some dynamical objects associated with quadratic anti-polynomials. This motivates the introduction of analogous dynamical objects for the C&C family, which are extensively used to study the dynamics of Schwarz reflection maps.

As in the case of the deltoid, the ideal triangle group models the ‘external’ dynamics of the maps in \mathcal{S} . In Section 3, we give a self-contained description of the ideal triangle group, the associated tessellation of the unit disk, and the reflection map ρ . We also construct a topological conjugacy \mathcal{E} (an analogue of the Minkowski question mark function) between the map ρ (which models the external dynamics of F_a) and the anti-doubling map $\theta \mapsto -2\theta$ on the circle (which models the external dynamics of quadratic anti-polynomials). This conjugacy plays a crucial role in the paper.

In Section 4, we briefly review some general properties of quadrature domains and Schwarz reflection maps.

In Section 5, we study the dynamics of Schwarz reflection with respect to a deltoid. This yields the simplest example of a mating of an anti-polynomial and the ideal triangle group. We introduce the Schwarz reflection map of a deltoid and study its basic mapping properties in Subsection 5.1. We also show that the corresponding dynamical plane can be partitioned into three completely invariant subsets: the tiling set, the basin of attraction of infinity, and the limit set (which is the common boundary of the former two sets). Subsections 5.2 and 5.3 are devoted to the proof of the fact that the limit set of the deltoid dynamics is a conformally removable Jordan curve. Finally in Subsection 5.4, we interpret the Schwarz reflection of the deltoid as the unique conformal mating of the anti-polynomial \bar{z}^2 and the reflection map ρ coming from the ideal triangle group. We then put all these results together to deduce Theorem 1.1.

In Section 6, we turn our attention to the C&C family. In Subsection 6.1, we focus on the cardioid as a quadrature domain, and establish some basic mapping properties of the associated Schwarz reflection. Subsection 6.2 contains a detailed discussion of the elementary dynamical properties of F_a and the associated dynamically relevant sets. Here we also prove a classification theorem for Fatou components (connected components of the interior of the non-escaping set), and the interaction between various types of Fatou components and the post-critical orbits of F_a (see Propositions 6.25 and 6.26). In Subsection 6.3, we introduce an analogue of Böttcher coordinate for the maps in \mathcal{S} . We show that for maps in the connectedness locus, the dynamics on the tiling set is conformally conjugate to the reflection map ρ arising from the ideal triangle group. This allows us to introduce a combinatorial model (quotient of the unit disk by a geodesic lamination) for the non-escaping set of the maps in the connectedness locus. For maps outside $\mathcal{C}(\mathcal{S})$, such a conjugacy still exists on a subset of the tiling set containing the critical value. We conclude the subsection with the proof of Theorem 1.2.

In Section 7, we focus on a class of ‘nice’ maps in \mathcal{S} . More precisely, we study topological and combinatorial properties of geometrically finite maps in the family \mathcal{S} . We discuss some basic topological, analytic and measure-theoretic properties for hyperbolic and parabolic maps in Subsection 7.1 and for Misiurewicz maps in Subsection 7.2. This completes the proof of Theorem 1.3.

The final Section 8 contains two examples of conformal matings in the family \mathcal{S} . In Subsection 8.1, we describe a general condition on the combinatorial model (i.e. lamination) of a post-critically finite map F_a (in \mathcal{S}) which ensures a mating description of F_a . In Subsection 8.2 (respectively, Subsection 8.3), we verify this combinatorial condition for the *basilica map* $a = 0$ (respectively, the *Chebyshev map* $a = \frac{1}{4}$), and conclude that it is the unique conformal mating of the reflection map ρ and the Basilica anti-polynomial $\bar{z}^2 - 1$ (respectively, the Chebyshev anti-polynomial $\bar{z}^2 - 2$). This completes the proof of Theorem 1.4.

2. BACKGROUND ON HOLOMORPHIC DYNAMICS

Notation: We will denote the complex conjugation map on the Riemann sphere by ι . The complex conjugate of a set U will be denoted by $\iota(U)$, while \bar{U} will stand for the topological closure of U . By $B(a, r)$ (respectively $\bar{B}(a, r)$), we will denote the open (respectively closed) disk centered at a with radius r .

This preliminary section will be a brief survey of several fundamental results on the dynamics and parameter spaces of quadratic polynomials and anti-polynomials. The results collected in this section will be repeatedly used in the rest of the paper.

2.1. Dynamics of Complex Quadratic Polynomials: The Mandelbrot Set.

The quadratic polynomial family is undoubtedly the most well-studied family of maps in holomorphic dynamics. Although it is the simplest family of nonlinear holomorphic maps, their dynamics and parameter space turn out to be highly non-trivial. In particular, many powerful methods were developed to study the parameter space of these maps leading to remarkable theorems. These results and methods laid the foundation of the study of general parameter spaces of holomorphic maps, and act as a strong motivational factor in our investigation.

With this in mind, we will briefly review some aspects of the dynamics and parameter space of complex quadratic polynomials in this subsection. We will

mainly touch upon the concepts and results that are directly (or indirectly) related to our study of the dynamics and parameter spaces of Schwarz reflections.

Any complex quadratic polynomial can be affinely conjugated to a map of the form $p_c(z) = z^2 + c$. The *filled Julia set* $K(p_c)$ is defined as the set of all points which remain bounded under all iterations of p_c . The boundary of the filled Julia set is defined to be the *Julia set* $J(p_c)$. The complement of the filled Julia set is called the *basin of infinity*, and is denoted by $A_\infty(c)$.

For a periodic orbit (equivalently, a cycle) $\mathcal{O} = \{z_1, z_2, \dots, z_n\}$ of p_c , we denote by $\lambda(c, \mathcal{O}) := (p_c^{o_n})'(z_1)$ the *multiplier* of \mathcal{O} (the definition is independent of the choice of z_i). A periodic orbit \mathcal{O} of p_c is called *super-attracting*, *attracting*, *neutral*, or *repelling* if $\lambda(c, \mathcal{O}) = 0$, $0 < |\lambda(c, \mathcal{O})| < 1$, $|\lambda(c, \mathcal{O})| = 1$, or $|\lambda(c, \mathcal{O})| > 1$ (respectively). A neutral cycle is called *parabolic* if the associated multiplier is a root of unity. Otherwise, it is called *irrational*.

Every quadratic polynomial p_c has two finite fixed points, and the sum of the multipliers of these two fixed points is 2.

We now recall the existence of local uniformizing coordinates for attracting cycles of holomorphic maps. Let z_0 be an attracting fixed point of a holomorphic map g ; i.e. $0 < |g'(z_0)| < 1$. By a classical theorem of Koenigs, there exists a conformal change of coordinates κ in a neighborhood U of z_0 such that $\kappa(z_0) = 0$ and $\kappa \circ g(z) = g'(z_0)\kappa(z)$, for all z in U . The map κ is known as Koenigs linearizing coordinate, and it is unique up to multiplication by a non-zero complex number [Mil06, Theorem 8.2].

For every quadratic polynomial, ∞ is a super-attracting fixed point. It is well-known that there is a conformal map φ_c near ∞ such that $\lim_{z \rightarrow \infty} \varphi_c(z)/z = 1$ and $\varphi_c \circ p_c(z) = \varphi_c(z)^2$ [Mil06, Theorem 9.1]. The map φ_c is called the *Böttcher coordinate* for p_c . The function $G_c(z) := \log |\varphi_c|$ can be extended as a subharmonic function to the entire complex plane such that it vanishes precisely on $K(p_c)$ and has a logarithmic singularity at ∞ . In other words, G_c is the Green's function of $K(p_c)$ [Mil06, Corollary 9.2, Definition 9.6]. The level curves of G_c are called *equipotentials* of p_c . As for the conformal map φ_c itself, it extends as a conformal isomorphism to an equipotential containing c , when $K(p_c)$ is disconnected, and extends as a biholomorphism from $\hat{\mathbb{C}} \setminus K(p_c)$ onto $\hat{\mathbb{C}} \setminus \bar{\mathbb{D}}$ when $K(p_c)$ is connected [Mil06, Theorem 9.3, Theorem 9.5]. The *dynamical ray* $R_c(t)$ of p_c at an angle $t \in \mathbb{R}/\mathbb{Z}$ is defined as the pre-image of the radial line at angle t under φ_c . Evidently, p_c maps the dynamical ray $R_c(t)$ to the dynamical ray $R_c(2t)$.

We say that the dynamical ray $R_c(t)$ of p_c lands if $\overline{R_c(t)} \cap K(p_c)$ is a singleton; this unique point is called the landing point of $R_c(t)$. It is worth mentioning that for a quadratic polynomial with connected filled Julia set, every dynamical ray at a periodic angle (under multiplication by 2) lands at a repelling or parabolic periodic point, and conversely, every repelling or parabolic periodic point is the landing point of at least one periodic dynamical ray [Mil06, §18].

The filled Julia set $K(p_c)$ of a quadratic polynomial is either connected, or totally disconnected. In fact, $K(p_c)$ is connected if and only if the unique critical point 0 does not lie in the basin of infinity $A_\infty(c)$ [DH07, Exposé III, §1, Proposition 1] [CG93, Chapter VIII, Theorem 1.1]. This dichotomy leads to the notion of the connectedness locus.

Definition 2.1 (Mandelbrot Set). The *Mandelbrot set* \mathcal{M} is the connectedness locus of complex quadratic polynomials; i.e.

$$\mathcal{M} := \{c \in \mathbb{C} : K(p_c) \text{ is connected}\}.$$

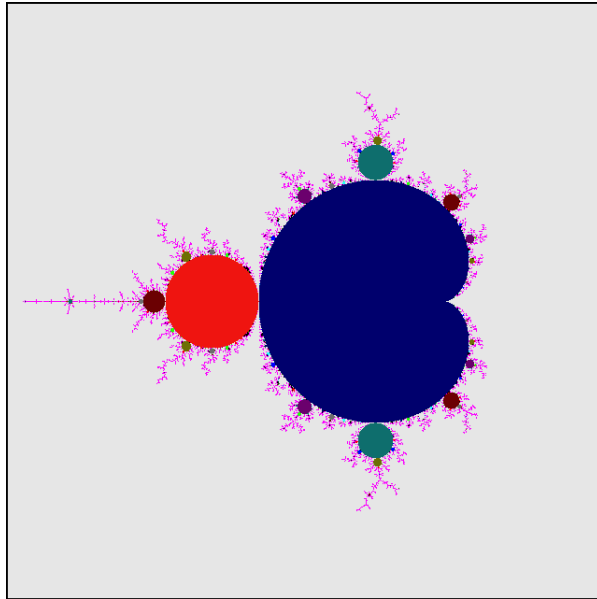


FIGURE 7. Mandelbrot set, the connectedness locus of quadratic holomorphic polynomials $z^2 + c$.

A parameter $c \in \mathcal{M}$ is called *hyperbolic* if p_c has a (necessarily unique) attracting cycle. A connected component H of the set of all hyperbolic parameters is called a *hyperbolic component* of \mathcal{M} . The following classical result is a consequence of holomorphic parameter dependence of the maps p_c [DH85, Exposé XIX, Theorem 1] [CG93, Chapter VIII, Theorem 1.4, Theorem 2.1].

Theorem 2.2 (Hyperbolic Components of \mathcal{M}). *Every hyperbolic component of \mathcal{M} is a connected component of the interior of \mathcal{M} . For every hyperbolic component H , there exists some $n \in \mathbb{N}$ such that each p_c in H has an attracting cycle of period n . The multiplier of the unique attracting cycle of p_c (where $c \in H$) defines a biholomorphism from H onto the open unit disk \mathbb{D} in the complex plane. This map is called the multiplier map of H , and is denoted by λ_H .*

Moreover, every parameter on the boundary of a hyperbolic component H has a unique neutral cycle of period dividing n . The derivative of p_c^{on} at this neutral cycle defines a continuous extension of λ_H up to ∂H .

The above proposition directly leads to the notion of centers and roots of hyperbolic components.

Definition 2.3 (Roots and Centers of Hyperbolic Components). The *center* of a hyperbolic component H is the unique parameter in H which has a super-attracting cycle (equivalently, where the multiplier map vanishes).

The *root* of H is the unique parameter $c \in \partial H$ with $\lambda_H(c) = 1$.

The unique hyperbolic component of period one (also called the principal hyperbolic component of \mathcal{M}) will be of particular importance to us. We denote it by \heartsuit . A straightforward computation shows that the inverse of the multiplier map of \heartsuit takes the form

$$\begin{aligned}\varphi : \mathbb{D} &\rightarrow \heartsuit \\ \varphi(\lambda) &= \lambda/2 - \lambda^2/4.\end{aligned}$$

Roots of hyperbolic components are intimately related to bifurcation phenomena in \mathcal{M} . If c is a parabolic parameter of \mathcal{M} such that p_c has a k -periodic cycle of multiplier $e^{2\pi ip/q}$ (where $\gcd(p, q) = 1$ and $q \geq 2$), then c lies on the boundary of a hyperbolic component H of period k and a hyperbolic component H' of period kq . Moreover, c is the root of H' [DH85, Exposé XIV, §5, Proposition 5].

The following theorem plays a basic role in the study of \mathcal{M} . For a proof, see [DH07, Exposé VIII, §I.3, Theorem 1].

Theorem 2.4 (Connectedness of \mathcal{M}). *The map $\Phi : \mathbb{C} \setminus \mathcal{M} \rightarrow \mathbb{C} \setminus \overline{\mathbb{D}}$, defined by $c \mapsto \varphi_c(c)$ (where φ_c is the Böttcher coordinate for p_c) is a biholomorphism. In particular, the Mandelbrot set is compact, connected, and full.*

The above theorem allows one to define parameter rays of the Mandelbrot set as pre-images of radial lines under Φ . More precisely, the *parameter ray* of \mathcal{M} at angle θ is defined as

$$\mathcal{R}_\theta := \{\Phi^{-1}(re^{2\pi i\theta}), r > 1\}.$$

If $\lim_{r \rightarrow 1^+} \Phi^{-1}(re^{2\pi i\theta})$ exists, we say that \mathcal{R}_θ lands. The parameter rays of the Mandelbrot set have been profitably used to reveal its combinatorial and topological structure. In particular, it is known that all parameter rays of \mathcal{M} at rational angles land. For a complete description of landing patterns of rational parameter rays and the corresponding structure theorem of the Mandelbrot set, see [Sch00, Theorem 1.1].

One of the most conspicuous features of the Mandelbrot set is its self-similarity. In [DH85], Douady and Hubbard developed the theory of polynomial-like maps to study this self-similarity. They proved the “straightening theorem” that, under certain circumstances, allows one to study a sufficiently large iterate of a polynomial by associating a simpler dynamical system, namely a polynomial of smaller degree, to it [DH85, Chapter I, Theorem 1]. They used it to explain the existence of infinitely many small homeomorphic copies of the Mandelbrot set in itself [DH85, Chapter II, Proposition 14]. It is worth mentioning that continuity of the straightening map from a baby Mandelbrot set to the original Mandelbrot set is an essential consequence of quasiconformal rigidity of parameters on the boundary of \mathcal{M} [DH85, Chapter I, Proposition 7]. In fact, straightening maps are typically discontinuous in the parameter spaces of higher degree polynomials [Ino09].

For a more general and comprehensive discussion of straightening of quadratic-like families, see [Lyu17, Chapter 6].

We refer the readers to [DH07] for an account of the early development of the subject, and to [Lyu17] for a more comprehensive account containing many sophisticated results on the Mandelbrot set.

2.2. Dynamics of Quadratic Anti-Polynomials: The Tricorn. In this subsection, we define some basic dynamical and combinatorial objects associated with quadratic anti-polynomials.

Any quadratic anti-polynomial, after an affine change of coordinates, can be written in the form $f_c(z) = \bar{z}^2 + c$ for $c \in \mathbb{C}$. In analogy to the holomorphic case, the set of all points which remain bounded under all iterations of f_c is called the *filled Julia set* \mathcal{K}_c . The boundary of the filled Julia set is defined to be the *Julia set* \mathcal{J}_c . This leads, as in the holomorphic case, to the notion of *connectedness locus* of quadratic anti-polynomials:

Definition 2.5. The *Tricorn* is defined as $\mathcal{T} = \{c \in \mathbb{C} : \mathcal{K}_c \text{ is connected}\}$.

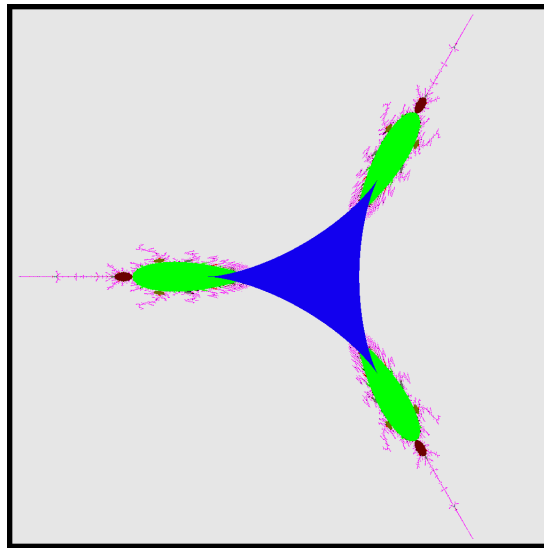


FIGURE 8. Tricorn, the connectedness locus of quadratic anti-polynomials $\bar{z}^2 + c$.

Remark 1. The anti-polynomials f_c and $f_{\omega c}$ are conformally conjugate via the linear map $z \mapsto \omega z$, where $\omega = \exp(\frac{2\pi i}{3})$. It follows that \mathcal{T} has a 3-fold rotational symmetry (see Figure 8).

Similar to the holomorphic case, we have a notion of Böttcher coordinates for anti-polynomials. By [Nak93, Lemma 1], there is a conformal map φ_c near ∞ that conjugates f_c to \bar{z}^2 . As in the holomorphic case, φ_c extends conformally to an equipotential containing c , when $c \notin \mathcal{T}$, and extends as a biholomorphism from $\hat{\mathbb{C}} \setminus \mathcal{K}_c$ onto $\hat{\mathbb{C}} \setminus \bar{\mathbb{D}}$ when $c \in \mathcal{T}$.

Definition 2.6 (Dynamical Ray). The dynamical ray $R_c(\theta)$ of f_c at an angle θ is defined as the pre-image of the radial line at angle θ under φ_c .

The dynamical ray $R_c(\theta)$ maps to the dynamical ray $R_c(-2\theta)$ under f_c . It follows that, at the level of external angles, the dynamics of f_c can be studied by looking at the simpler map

$$m_{-2} : \mathbb{R}/\mathbb{Z} \rightarrow \mathbb{R}/\mathbb{Z}, \quad m_{-2}(\theta) = -2\theta.$$

We refer the readers to [NS03, §3], [Muk15b] for details on the combinatorics of the landing pattern of dynamical rays for unicritical anti-polynomials.

For an anti-holomorphic germ g fixing a point z_0 , the quantity $\frac{\partial g}{\partial \bar{z}}|_{z_0}$ is called the *multiplier* of g at the fixed point z_0 . One can use this definition to define multipliers of periodic orbits of anti-holomorphic maps (compare [Muk15a, §1.1]). A cycle is called attracting (respectively, super-attracting or parabolic) if the associated multiplier has absolute value between 0 and 1 (respectively, is 0 or a root of unity). A map f_c is called hyperbolic (respectively, parabolic) if it has a (super-)attracting (respectively, parabolic) cycle.

It is well-known that a (super-)attracting cycle of f_c belongs to the interior of \mathcal{K}_c , and a parabolic cycle lies on the boundary of \mathcal{K}_c (see [Mil06, §5, Theorem 5.2]). Moreover, a parabolic periodic point necessarily lies on the boundary of a Fatou component (i.e. a connected component of $\text{int } \mathcal{K}_c$) that contains an attracting petal of the parabolic germ such that the forward orbit of every point in the component converges to the parabolic cycle. In the attracting (respectively, parabolic) case, the forward orbit of the critical point 0 converges to the attracting (respectively, parabolic) cycle. In either case, the unique Fatou component containing the critical value is called the *characteristic* Fatou component.

It is well-known that if f_c has a connected Julia set, then all rational dynamical rays of f_c land at repelling or parabolic (pre-)periodic points. This allows us to introduce an important combinatorial object that will play a key role later in the paper.

Definition 2.7 (Rational Lamination). The rational lamination of a quadratic anti-polynomial f_c (with connected Julia set) is defined as an equivalence relation on \mathbb{Q}/\mathbb{Z} such that $\theta_1 \sim \theta_2$ if and only if the dynamical rays $R_c(\theta_1)$ and $R_c(\theta_2)$ land at the same point of $J(f_c)$. The rational lamination of f_c is denoted by $\lambda(f_c)$.

The next proposition lists the basic properties of rational laminations.

Proposition 2.8. *The rational lamination $\lambda(f_c)$ of a quadratic anti-polynomial f_c satisfies the following properties.*

- (1) $\lambda(f_c)$ is closed in $\mathbb{Q}/\mathbb{Z} \times \mathbb{Q}/\mathbb{Z}$.
- (2) Each $\lambda(f_c)$ -equivalence class A is a finite subset of \mathbb{Q}/\mathbb{Z} .
- (3) If A is a $\lambda(f_c)$ -equivalence class, then $m_{-2}(A)$ is also a $\lambda(f_c)$ -equivalence class.
- (4) If A is a $\lambda(f_c)$ -equivalence class, then $A \mapsto m_{-2}(A)$ is consecutive reversing.
- (5) $\lambda(f_c)$ -equivalence classes are pairwise unlinked.

Proof. The proof of [Kiw01, Theorem 1.1] applies mutatis mutandis to the anti-holomorphic setting. \square

Definition 2.9 (Formal Rational Laminations). An equivalence relation λ on \mathbb{Q}/\mathbb{Z} satisfying the conditions of Proposition 2.8 is called a *formal rational lamination* under m_{-2} .

A *Misiurewicz* parameter of the Tricorn is a parameter c such that the critical point 0 is strictly pre-periodic. It is well-known that for a Misiurewicz parameter, the critical point eventually maps on a repelling cycle. By classification of Fatou components, the filled Julia set of such a map has empty interior. Moreover, the Julia set of a Misiurewicz parameter is locally connected [DH07, Exposé III, Proposition 4, Theorem 1], and has measure zero [DH07, Exposé V, Theorem 3].

Let c_0 be a Misiurewicz parameter, and \mathcal{A}' be the set of angles of the dynamical rays of f_{c_0} landing at the critical point 0. The set of angles of the dynamical rays

that land at the critical value c_0 is then given by $\mathcal{A} := m_{-2}(\mathcal{A}')$. Moreover, m_{-2} is two-to-one from \mathcal{A}' onto \mathcal{A} . Every other equivalence class of $\lambda(f_{c_0})$ is mapped bijectively onto its image class by m_{-2} . Note also that all angles in \mathcal{A}' are strictly pre-periodic. It is easy to see that the existence of a unique equivalence class (of $\lambda(f_{c_0})$) that maps two-to-one onto its image class under m_{-2} characterizes the rational lamination of Misiurewicz maps. A formal rational lamination satisfying this condition is said to be of *Misiurewicz type*.

3. IDEAL TRIANGLE GROUP

The goal of this section is to review some basic properties of the ideal triangle group and its boundary extension. This will play an important role in our study of the “escaping” dynamics of Schwarz reflection maps.

Consider the open unit disk \mathbb{D} in the complex plane. Let C_1, C_2, C_3 be the circles with centers at $(1, \sqrt{3}), (-2, 0)$, and $(1, -\sqrt{3})$ of radius $\sqrt{3}$ each. We denote the intersection of \mathbb{D} and C_i by \tilde{C}_i . Then \tilde{C}_1, \tilde{C}_2 , and \tilde{C}_3 are hyperbolic geodesics in \mathbb{D} , and they form an ideal triangle which we call \tilde{T} (see Figure 9). They bound a closed (in the topology of \mathbb{D}) region Π .

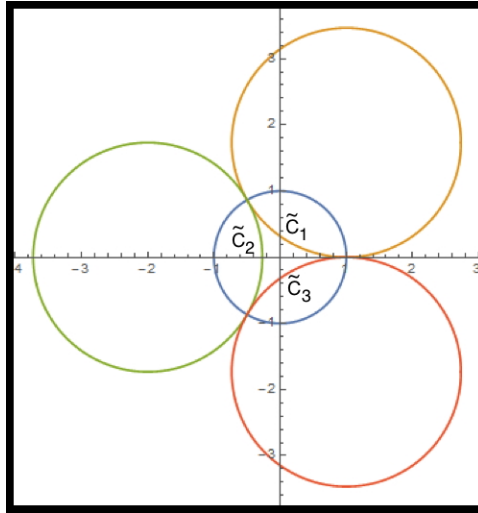


FIGURE 9. The hyperbolic geodesics \tilde{C}_1, \tilde{C}_2 and \tilde{C}_3 , which are sub-arcs of the circles C_1, C_2 and C_3 respectively, form an ideal triangle in \mathbb{D} .

Reflections with respect to the circles C_i are anti-conformal involutions (hence automorphisms) of \mathbb{D} , and we call them ρ_1, ρ_2 , and ρ_3 . The maps ρ_1, ρ_2 , and ρ_3 generate a subgroup \mathcal{G} of $\text{Aut}(\mathbb{D})$. The group \mathcal{G} is called the *ideal triangle group*. As an abstract group, it is given by the generators and relations

$$\langle \rho_1, \rho_2, \rho_3 : \rho_1^2 = \rho_2^2 = \rho_3^2 = \text{id} \rangle.$$

We will denote the connected component of $\mathbb{D} \setminus \Pi$ containing $\text{int } \rho_i(\Pi)$ by \mathbb{D}_i . Note that $\mathbb{D}_1 \cup \mathbb{D}_2 \cup \mathbb{D}_3 = \mathbb{D} \setminus \Pi$.

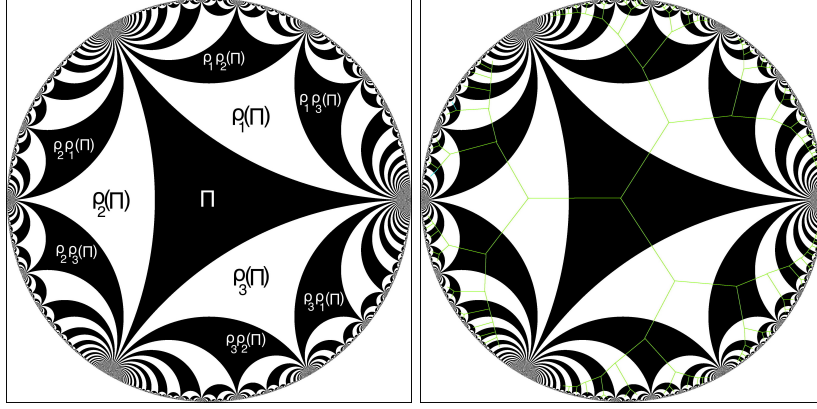


FIGURE 10. Left: The \mathcal{G} -tessellation of \mathbb{D} and the formation of a few initial tiles are shown. Right: The dual tree to the \mathcal{G} -tessellation of \mathbb{D} .

3.1. The Reflection Map ρ , and Symbolic Dynamics. We now define the reflection map $\rho : \mathbb{D} \setminus \text{int } \Pi \rightarrow \mathbb{D}$ as:

$$z \mapsto \begin{cases} \rho_1(z) & \text{if } z \in \mathbb{D}_1 \cup \tilde{\mathcal{C}}_1, \\ \rho_2(z) & \text{if } z \in \mathbb{D}_2 \cup \tilde{\mathcal{C}}_2, \\ \rho_3(z) & \text{if } z \in \mathbb{D}_3 \cup \tilde{\mathcal{C}}_3. \end{cases}$$

Then $\rho(\mathbb{D}_1) \supset \mathbb{D}_2 \cup \mathbb{D}_3$, $\rho(\mathbb{D}_2) \supset \mathbb{D}_3 \cup \mathbb{D}_1$, $\rho(\mathbb{D}_3) \supset \mathbb{D}_2 \cup \mathbb{D}_1$, and $\rho(\mathbb{D}_i) \cap \mathbb{D}_i = \emptyset$, for $i = 1, 2, 3$. Thus, the dynamics of ρ on $\mathbb{D} \setminus \text{int } \Pi$ is encoded by the transition matrix

$$M := \begin{bmatrix} 0 & 1 & 1 \\ 1 & 0 & 1 \\ 1 & 1 & 0 \end{bmatrix}.$$

Remark 2. The Markov map ρ is closely related to the \mathcal{G} -action on \mathbb{T} , compare [BS79].

Let $W := \{1, 2, 3\}$. An element $(i_1, i_2, \dots) \in W^{\mathbb{N}}$ is called M -admissible if $M_{i_k, i_{k+1}} = 1$, for all $k \in \mathbb{N}$. We denote the set of all M -admissible words in $W^{\mathbb{N}}$ by M^∞ . One can similarly define M -admissibility of finite words.

Note that Π is a fundamental domain of \mathcal{G} . The tessellation of \mathbb{D} arising from \mathcal{G} will play an important role in this paper (see Figure 10).

Definition 3.1 (Tiles). The images of the fundamental domain Π under the elements of \mathcal{G} are called *tiles*. More precisely, for any M -admissible word (i_1, \dots, i_k) , we define the tile

$$T^{i_1, \dots, i_k} := \rho_{i_1} \circ \dots \circ \rho_{i_k}(\Pi).$$

It follows from the definition that T^{i_1, \dots, i_k} consists of all those $z \in \mathbb{D}$ such that $\rho^{o(n-1)}(z) \in \mathbb{D}_{i_n}$, for $n = 1, \dots, k$ and $\rho^{ok}(z) \in \Pi$. In other words,

$$T^{i_1, \dots, i_k} = \bigcap_{n=1}^k \rho^{-(n-1)}(\mathbb{D}_{i_n}) \cap \rho^{-k}(\Pi).$$

Clearly, ρ extends as an orientation-reversing C^1 double covering of \mathbb{T} (real-analytic away from the fixed points 1 , $e^{2\pi i/3}$, and $e^{4\pi i/3}$) with associated Markov partition $\mathbb{T} = (\partial\mathbb{D}_1 \cap \mathbb{T}) \cup (\partial\mathbb{D}_2 \cap \mathbb{T}) \cup (\partial\mathbb{D}_3 \cap \mathbb{T})$. The corresponding transition matrix is M as above.

Recall that the set of all M -admissible words in $W^{\mathbb{N}}$ is denoted by M^∞ . Since the limit set of \mathcal{G} is the entire circle $\partial\mathbb{D}$, it follows that for any element of M^∞ , the corresponding infinite sequence of tiles shrinks to a single point of $\partial\mathbb{D}$. This allows us to define a continuous surjection

$$Q : M^\infty \rightarrow \mathbb{T},$$

$$(i_1, i_2, \dots) \mapsto \bigcap_{n \in \mathbb{N}} \rho^{-(n-1)}(\partial\mathbb{D}_{i_n} \cap \mathbb{T})$$

which semi-conjugates the (left-)shift map on M^∞ to the map ρ on \mathbb{T} .

It is not hard to see that two elements $(i_1, i_2, \dots), (j_1, j_2, \dots) \in M^\infty$ lie in the same fiber of Q if and only if the sequences of tiles $\{T^{i_1}, T^{i_1, i_2}, \dots\}$ and $\{T^{j_1}, T^{j_1, j_2}, \dots\}$ have the point $Q((i_1, i_2, \dots)) = Q((j_1, j_2, \dots)) \in \mathbb{T}$ as their common ω -limit. In fact, the non-trivial fibers of Q correspond to parabolic fixed points of elements of \mathcal{G} (equivalently, pre-images of the fixed points of ρ). Consequently, the set of all fibers of Q is in bijective correspondence with the set of all accesses to \mathbb{T} through infinite sequences of tiles. We will denote the fiber of Q containing (i_1, i_2, \dots) by $[(i_1, i_2, \dots)]$, and the set of all fibers of Q by \mathfrak{F} ; i.e.

$$\mathfrak{F} := \{[(i_1, i_2, \dots)] : (i_1, i_2, \dots) \in M^\infty\}.$$

Evidently, if $z_0 \in \mathbb{T}$ is (pre-)periodic under ρ , then every sequence in $Q^{-1}(z_0)$ is (pre-)periodic under the shift map, and vice versa. We will call such a fiber a (pre-)periodic fiber. The set of all (pre-)periodic fibers of Q will be denoted by $\mathfrak{F}^{\text{Per}}$. On the other hand, the set of all points of \mathbb{T} that are (pre-)periodic under ρ will be denoted by $\text{Per}(\rho)$. It follows that Q induces a bijection between $\mathfrak{F}^{\text{Per}}$ and $\text{Per}(\rho)$.

Let us set $d_{\mathbb{D}}(0, \rho_1(0)) = d_{\mathbb{D}}(0, \rho_2(0)) = d_{\mathbb{D}}(0, \rho_3(0)) =: \ell$. For any M -admissible sequence (i_1, i_2, \dots) , let us consider the sequence $\{0, \rho_{i_1}(0), \rho_{i_1} \circ \rho_{i_2}(0), \dots\}$. Clearly, the hyperbolic distance (in \mathbb{D}) of any two consecutive points in this sequence is ℓ . Connecting consecutive points of this sequence by hyperbolic geodesics of \mathbb{D} , we obtain a curve in \mathbb{D} that lands at $Q((i_1, i_2, \dots))$.

Definition 3.2 (Rays). The curve constructed above is called a \mathcal{G} -ray at angle $Q((i_1, i_2, \dots))$.²

Remark 3. The set of all \mathcal{G} -rays form a dual tree to the \mathcal{G} -tessellation of \mathbb{D} . As an abstract graph, it is isomorphic to the undirected Cayley graph of \mathcal{G} with respect to the generating set $\{\rho_1, \rho_2, \rho_3\}$.

3.2. The Conjugacy \mathcal{E} . Note that the expanding double covering of the circle

$$m_{-2} : \mathbb{R}/\mathbb{Z} \rightarrow \mathbb{R}/\mathbb{Z}, \theta \mapsto -2\theta,$$

which is the action of quadratic anti-polynomials on angles of external dynamical rays, is closely related to ρ . The map m_{-2} admits the same Markov partition as ρ ; namely $\mathbb{R}/\mathbb{Z} = I_1 \cup I_2 \cup I_3$, where $I_1 = \left[0, \frac{1}{3}\right]$, $I_2 = \left[\frac{1}{3}, \frac{2}{3}\right]$, $I_3 = \left[\frac{2}{3}, 1\right]$. Moreover,

²Here, we identify \mathbb{T} with \mathbb{R}/\mathbb{Z} .

the associated transition matrix coincides with that of ρ . This allows us to define a continuous surjection

$$P : M^\infty \rightarrow \mathbb{R}/\mathbb{Z},$$

$$(i_1, i_2 \cdots) \mapsto \bigcap_{n \in \mathbb{N}} m_{-2}^{-(n-1)}(I_{i_n})$$

which semi-conjugates the shift map on M^∞ to the map m_{-2} on \mathbb{R}/\mathbb{Z} . The two coding maps Q and P have precisely the same fibers. It follows that $P \circ Q^{-1}$ induces a homeomorphism of the circle conjugating ρ to m_{-2} . We will denote this conjugacy by \mathcal{E} (see Figure 11).

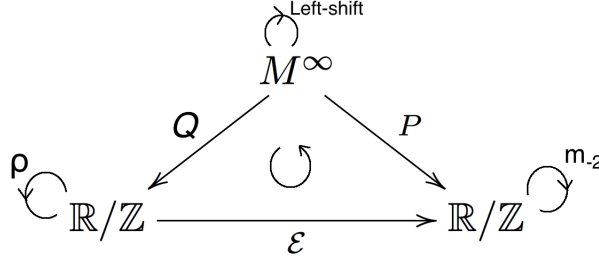


FIGURE 11. Symbolic representations of orbits of ρ and m_{-2} with respect to the common Markov partition $\mathbb{R}/\mathbb{Z} = [0, \frac{1}{3}] \cup [\frac{1}{3}, \frac{2}{3}] \cup [\frac{2}{3}, 1]$ induce the topological conjugacy \mathcal{E} between ρ and m_{-2} .

4. QUADRATURE DOMAINS AND SCHWARZ REFLECTION

We now come to a general description of the main objects of this paper. We are interested in studying the dynamics and parameter space of Schwarz reflection with respect to a cardioid and a circle. While Schwarz reflections with respect to real-analytic curves are only locally defined, it is possible to extend this reflection map to a semi-global map in certain cases (e.g. reflection with respect to a circle extends to $\hat{\mathbb{C}}$).

Recall that ι denotes the complex conjugation map.

Definition 4.1 (Schwarz Function). Let $\Omega \subsetneq \hat{\mathbb{C}}$ be a domain such that $\infty \notin \partial\Omega$ and $\text{int } \bar{\Omega} = \Omega$. A *Schwarz function* of Ω is a meromorphic extension of $\iota|_{\partial\Omega}$ to all of Ω . More precisely, a continuous function $S : \bar{\Omega} \rightarrow \hat{\mathbb{C}}$ of Ω is called a Schwarz function of Ω if it satisfies the following two properties:

- (1) S is meromorphic on Ω ,
- (2) $S = \iota$ on $\partial\Omega$.

It is easy to see from the definition that a Schwarz function of a domain (if it exists) is unique.

Definition 4.2 (Quadrature Domains). A domain $\Omega \subsetneq \hat{\mathbb{C}}$ with $\infty \notin \partial\Omega$ and $\text{int } \bar{\Omega} = \Omega$ is called a *quadrature domain* if Ω admits a Schwarz function.

Therefore, for a quadrature domain Ω , the map $\sigma := \iota \circ S : \bar{\Omega} \rightarrow \hat{\mathbb{C}}$ is an anti-meromorphic extension of the Schwarz reflection map with respect to $\partial\Omega$ (the reflection map fixes $\partial\Omega$ pointwise). We will call σ the *Schwarz reflection map* of Ω .

We now define the notion of a quadrature function for a domain.

Definition 4.3 (Quadrature Functions). Let $\Omega \subsetneq \hat{\mathbb{C}}$ be a domain with $\infty \notin \partial\Omega$ and $\text{int } \bar{\Omega} = \Omega$. Functions in $H(\Omega) \cap C(\bar{\Omega})$ are called *test functions* for Ω (if Ω is unbounded, we further require test functions to vanish at ∞). A rational map R_Ω is called a *quadrature function* of Ω if all poles of R_Ω are inside Ω (with $R_\Omega(\infty) = 0$ if Ω is bounded), and the identity

$$\int_{\Omega} f dA = \frac{1}{2i} \oint_{\partial\Omega} f(z) R_\Omega(z) dz$$

holds for every test function of Ω .

The following theorem is classical (see [AS76, Lemma 2.3] [LM16, Lemma 3.1]).

Theorem 4.4 (Characterization of Quadrature Domains). *For a domain $\Omega \subsetneq \hat{\mathbb{C}}$ with $\infty \notin \partial\Omega$ and $\text{int } \bar{\Omega} = \Omega$, the following are equivalent.*

- (1) Ω is a quadrature domain; i.e. it admits a Schwarz function,
- (2) Ω admits a quadrature function R_Ω ,
- (3) The Cauchy transform $\hat{\chi}_\Omega$ of the characteristic function χ_Ω (of Ω) is rational outside Ω .

We call $d_\Omega := \deg(R_\Omega)$ the *order* of the quadrature domain Ω . The poles of R_Ω are called *nodes* of Ω .

We now state an important theorem which guarantees that boundaries of quadrature domains are real-algebraic [Gus83].

Theorem 4.5 (Real-algebraicity of Boundaries of Quadrature Domains). *If Ω (with $\infty \notin \partial\Omega$, $\text{int } \bar{\Omega} = \Omega$) is a quadrature domain, then $\partial\Omega$ is contained in a real-algebraic curve. In particular, the only singularities on $\bar{\Omega}$ are double points and cusps.*

The next proposition characterizes simply connected quadrature domains (see [AS76, Theorem 1]).

Proposition 4.6 (Simply Connected Quadrature Domains). *A simply connected domain $\Omega \subsetneq \hat{\mathbb{C}}$ with $\infty \notin \partial\Omega$ and $\text{int } \bar{\Omega} = \Omega$ is a quadrature domain if and only if the Riemann map $\varphi : \mathbb{D} \rightarrow \Omega$ is rational.*

For a simply connected quadrature domain Ω , the rational map φ (that restricts to a Riemann map $\varphi : \mathbb{D} \rightarrow \Omega$ of Ω) semi-conjugates the reflection map $1/\bar{z}$ of \mathbb{D} to the Schwarz reflection map σ of Ω (see the commutative diagram in Figure 1). This allows us to compute the Schwarz reflection map of a simple connected quadrature domain. Moreover, the order of a simply connected quadrature domain is equal to $\deg \varphi$.

Lee and Makarov studied topology of quadrature domains using iteration of Schwarz reflection maps in [LM16, Theorem A.1, Theorem A.2]. They also established a connection between algebraic droplets (supports of equilibrium measures for suitable classes of external fields) and quadrature domains [LM16, Theorem 3.3, Theorem 3.4].

For a comprehensive account on quadrature domains and their applications, we refer the readers to [EGKP05].

5. DYNAMICS OF DELTOID REFLECTION

The goal of this Section is to carry out a detailed study of the dynamics of Schwarz reflection with respect to a deltoid.

5.1. Schwarz Reflection with Respect to a Deltoid. In this subsection, we introduce the Schwarz reflection map of a deltoid, study its basic mapping properties, and prove some fundamental topological properties of the dynamically meaningful sets associated with the Schwarz reflection map.

5.1.1. *Deltoid.*

Proposition 5.1. *The map $\varphi(w) = w + \frac{1}{2w^2}$ is univalent in $\hat{\mathbb{C}} \setminus \bar{\mathbb{D}}$.*

We define

$$\Omega := \varphi(\hat{\mathbb{C}} \setminus \bar{\mathbb{D}}), \quad T := \Omega^c.$$

$$\begin{array}{ccc} \hat{\mathbb{C}} \setminus \bar{\mathbb{D}} & \xrightarrow{\varphi} & \bar{\Omega} \\ \downarrow 1/\bar{z} & & \downarrow \sigma \\ \bar{\mathbb{D}} & \xrightarrow{\varphi} & \hat{\mathbb{C}} \end{array}$$

FIGURE 12. The rational φ restricts to a conformal isomorphism from $\hat{\mathbb{C}} \setminus \bar{\mathbb{D}}$ onto Ω . The Schwarz reflection map σ is defined via the commutative diagram shown in the figure.

By Proposition 4.6, Ω is an unbounded quadrature domain. It follows from [LM16, Theorem 3.4] that T is an algebraic droplet. Since φ commutes with multiplication by ω (where $\omega = e^{\frac{2\pi i}{3}}$), it follows that T is symmetric under rotation by $\frac{2\pi}{3}$. Moreover, as φ has simple critical points at ω^k (for $k = 0, 1, 2$), ∂T has three $\frac{3}{2}$ -cusp points (see Figure 13). It is also worth mentioning that ∂T is a deltoid curve in the sense of Euler's description with rolling circles (see [Loc61, Chapter 8] and Figure 13).

Notation: T^0 is T with the three cusp points removed.

5.1.2. *Schwarz Reflection.*

Proposition 5.2. *There exists a unique continuous map $\sigma : \bar{\Omega} \rightarrow \hat{\mathbb{C}}$ such that $\sigma(z) = z$ on $\partial\Omega$, and such that σ is anti-meromorphic in Ω . Moreover, σ has a double pole at ∞ but no other critical points in Ω .*

Proof. The first statement follows from Proposition 4.6. The statement about critical points of σ is a straightforward consequence of the commutative diagram in Figure 12 and the fact that the only critical point of φ in \mathbb{D} is at the origin. \square

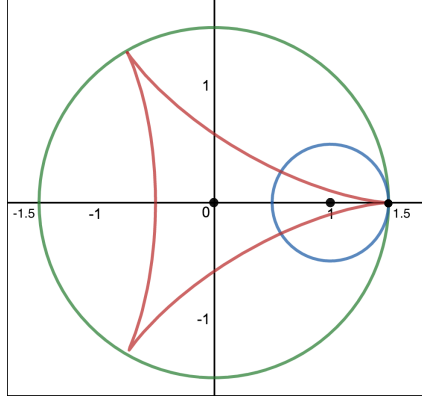


FIGURE 13. The deltoid curve ∂T (in red) is the locus of a point on the circumference of a circle of radius $\frac{1}{2}$ as it rolls inside a circle of radius $\frac{3}{2}$. There are three $\frac{3}{2}$ -cusps on ∂T .

5.1.3. Covering Properties of σ .

Proposition 5.3. $\sigma : \sigma^{-1}(\Omega) \rightarrow \Omega$ is a proper branched 2-cover (branched only at ∞). On the other hand, $\sigma : \sigma^{-1}(T^0) \rightarrow T^0$ is a 3-cover.

Proof. This follows from [LM16, Lemma 4.1] that uses the extension of the Schwarz reflection map σ to the Schottky double of Ω (see [Gus83]). Here is a more direct proof.

The degree 3 rational map φ maps $\hat{\mathbb{C}} \setminus \overline{\mathbb{D}}$ univalently onto Ω . Note that the critical points of φ (all of which are simple) are $1, \omega, \omega^2$, and 0 . They are mapped by φ to $\frac{3}{2}, \frac{3}{2}\omega, \frac{3}{2}\omega^2$, and ∞ respectively. In particular, Ω contains exactly one critical value of φ , while T^0 does not contain any critical value of φ . Let us set $X_1 := \varphi^{-1}(T^0) \cap \overline{\mathbb{D}}$, and $X_2 = \varphi^{-1}(\Omega) \cap \overline{\mathbb{D}}$ (see Figure 14). It now readily follows that $\varphi : X_1 \rightarrow T^0$ is a proper covering of degree 3, and $\varphi : X_2 \rightarrow \Omega$ is proper branched covering of degree 2 (branched only at 0).

Finally, the description of σ given in the Diagram 12 implies that $\sigma^{-1}(T^0) = (\varphi \circ \tilde{\iota})(X_1)$, and $\sigma : (\varphi \circ \tilde{\iota})(X_1) \rightarrow T^0$ is a proper 3-cover (where $\tilde{\iota}$ is reflection in the unit circle). The same description also shows that $\sigma^{-1}(\Omega) = (\varphi \circ \tilde{\iota})(X_2)$, and $\sigma : (\varphi \circ \tilde{\iota})(X_2) \rightarrow \Omega$ is proper branched 2-cover branched only at ∞ . \square

Corollary 5.4. The maps $\sigma^{on} : \sigma^{-n}(\Omega) \rightarrow \Omega$ are proper branched covers of degree 2^n (branched only at ∞).

5.1.4. Tiling Set. By definition,

$$T^\infty = \bigcup_{n \geq 0} \sigma^{-n}(T^0).$$

In Figure 4, the bounded complementary component of the green curve is T^∞ . We will call it the *tiling set*. We will call the components of $\sigma^{-n}T^0$ tiles of rank n . The next proposition directly follows from the construction of tiles.

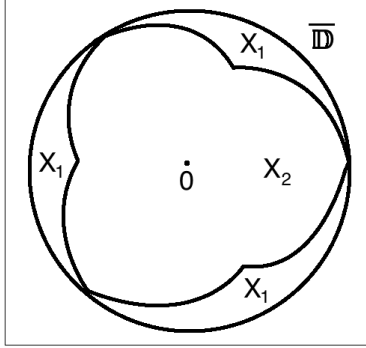


FIGURE 14. Each connected component of X_1 is mapped univalently onto T^0 by φ . Moreover, φ is a two-to-one branched covering from the connected set X_2 onto Ω , and the only ramification point is the origin.

Proposition 5.5. *There are $3 \cdot 2^{n-1}$ tiles of rank n . The union of tiles of rank $\leq n$ is a “polygon” with $3 \cdot 2^n$ vertices (cusps).*

Proposition 5.6. *T^∞ is a simply connected domain.*

Proof. If $z \in T^\infty$ belongs to the interior of a tile, then it clearly belongs to $\text{int } T^\infty$. On the other hand, if $z \in T^\infty$ belongs to the boundary of a tile of rank n , then z lies in $\text{int} \left(\bigcup_{k=0}^{n+1} \sigma^{-k} T^0 \right) \subset \text{int } T^\infty$. Hence, T^∞ is open.

The above argument also shows that T^∞ is the increasing union of the connected, simply connected domains $\left\{ \text{int} \left(\bigcup_{k=0}^n \sigma^{-k} T^0 \right) \right\}_{n \geq 1}$. Hence, T^∞ itself is connected and simply connected. \square

Note that $\sigma : T^\infty \setminus T^0 \rightarrow T^\infty$ is not a covering map as the degree of $\sigma : \sigma^{-1}(T^0) \rightarrow T^0$ is three, while the degree of $\sigma : T^\infty \setminus (T^0 \cup \sigma^{-1}(T^0)) \rightarrow T^\infty \setminus T^0$ is two. For this reason, some care should be taken to define inverse branches of the iterates of σ on T^∞ .

For a subset X of the plane, we denote by $N_\varepsilon(X)$ the ε -neighborhood of X . Let us fix some small $\varepsilon > 0$ and define the set

$$T^{\text{hyp}} := N_\varepsilon(\overline{T^\infty}) \setminus \overline{N_{2\varepsilon}(T)}.$$

The next result, which follows from the mapping properties of σ , tells us that σ is hyperbolic near the boundary of the tiling set away from the cusp points.

Proposition 5.7. *All inverse branches of $\sigma^{\circ n}$ (for $n \geq 1$) are well-defined locally on T^{hyp} . Moreover, σ is hyperbolic on T^{hyp} .*

Proof. Note that $\overline{T^{\text{hyp}}} \subset \Omega$. The first part of the proposition follows from the fact that $\sigma : \sigma^{-1}(\Omega) \rightarrow \Omega$ is a branched covering (see Proposition 5.3) and T^{hyp} does not intersect the post-critical set of σ .

For the second assertion, first recall that $\sigma(\varphi(w)) = \varphi(\frac{1}{w})$, $|w| > 1$. Taking the $\bar{\partial}$ -derivative of this relation yields

$$(1) \quad \bar{\partial}\sigma(\varphi(w)) \cdot \left(1 - \frac{1}{w^3}\right) = -\frac{1}{w^2} + \bar{w},$$

for $|w| > 1$. It follows from Relation (1) that

$$(2) \quad |\bar{\partial}\sigma(\varphi(w))| = |w|,$$

for $|w| > 1$. Since T^{hyp} is compactly contained in Ω , it follows that there exists $\lambda_0 > 1$ such that

$$|\bar{\partial}\sigma| > \lambda_0 > 1$$

on T^{hyp} . □

Remark 4. While we used the explicit formula of σ in the proof of hyperbolicity given above (which makes it look somewhat accidental), a more general argument can be given using the shrinking lemma for inverse branches.

5.1.5. *Non-escaping Set, Basin of Infinity.* The openness and complete invariance of the tiling set yields the following corollary.

Corollary 5.8. $\mathbb{C} \setminus T^\infty$ is a closed, completely invariant set.

Since every point in $T^\infty \setminus T^0$ escapes to T^0 under some iterate of σ , we can think of T^∞ as the *escaping set* of σ . On the other hand, $\hat{\mathbb{C}} \setminus T^\infty$ consists of points that never land in T^0 and we call it the *non-escaping set* of σ .

We denote the basin of attraction of ∞ (recall that ∞ is super-attracting) by $A \equiv A(\infty)$. Clearly,

$$A \subset \hat{\mathbb{C}} \setminus \overline{T^\infty}.$$

Remark 5. Note that the tiling set (where points escape to T^0) of σ plays the role of the basin of infinity (where points escape to infinity) of a polynomial. Moreover, the non-escaping set (where points never escape to T^0) of σ is the analogue of the filled Julia set (where points never escape to infinity) of a polynomial. Note that the filled Julia set of a polynomial is a compact subset of \mathbb{C} , while the non-escaping set of σ is unbounded in \mathbb{C} (but compact in $\hat{\mathbb{C}}$).

Proposition 5.9. A is a simply connected, completely invariant domain.

Proof. Since A is the basin of attraction of a super-attracting fixed point, it is necessarily open and completely invariant.

Let A_0 be the connected component of A containing ∞ . If $A \setminus A_0 \neq \emptyset$, then every connected component of $A \setminus A_0$ would eventually map onto A_0 under some iterate of σ . Therefore, every connected component of $A \setminus A_0$ must contain an iterated pre-image of ∞ . But $\sigma^{-1}(\infty) = \{\infty\}$ (by Proposition 5.3). Hence A_0 must be equal to A . This shows that A is connected and completely invariant.

It remains to prove simple connectivity of A . Let $U \subset A$ be a small neighborhood of ∞ . Clearly, A is the increasing union of the domains $\{\sigma^{-k}(U)\}_{k \geq 0}$. Since ∞ is the only critical point of σ , it follows from the Riemann-Hurwitz formula that each $\sigma^{-k}(U)$ is simply connected. Thus, A is an increasing union of simply connected domains, and hence itself is such. □

5.1.6. *Singular Points.* Denote

$$S = \bigcup \sigma^{-n}(T \setminus T^0),$$

so S is the collection of the cusp points of all tiles. It is clear, that $S \subset \partial T^\infty$. We also have

Proposition 5.10. $S \subset \partial A$.

Proof. It is enough to show that $\frac{3}{2}$, a cusp point of Ω , is in ∂A . For a real $x > 1$ we have (from $\sigma(\varphi(w)) = \varphi(1/\bar{w})$)

$$(3) \quad \sigma\left(x + \frac{1}{2x^2}\right) = \frac{1}{x} + \frac{x^2}{2} > x + \frac{1}{2x^2}$$

because at $x = 1$ we have equality in the last relation, and for the corresponding derivatives we have

$$-x^{-2} + x > 1 - x^{-3} \quad (x > 1).$$

Thus, the forward σ -orbit of any real $w > \frac{3}{2}$ must converge to ∞ (otherwise, the orbit would converge to a fixed point of σ in $(\frac{3}{2}, +\infty)$, which contradicts Inequality (3)). Hence, $(\frac{3}{2}, +\infty) \subset A$, and we are done. \square

5.1.7. *Main Results.*

Theorem 5.11. *We have*

$$\partial T^\infty = \partial A = \text{clos}(S),$$

and this set, which we denote by Γ , is a Jordan curve. Also,

$$\hat{\mathbb{C}} = T^\infty \sqcup \Gamma \sqcup A.$$

Lemma 5.12. ∂T^∞ is locally connected.

We will give a detailed proof of Lemma 5.12 in Subsection 5.2 (this lemma is crucial and the techniques that will go into the proof will be used elsewhere in the paper too). The derivation of the main theorem from the main lemma is explained below.

5.1.8. *Proof of Theorem 5.11.* Let $\psi^{\text{in}} : \mathbb{D} \rightarrow T^\infty$ be the Riemann map such that $\psi^{\text{in}}(0) = 0$, $\psi^{\text{in}}(1) = \frac{3}{2}$. This map can be constructed from the conformal map of the filled ideal triangle Π (see Section 3) onto T^0 by the reflection principle. Note that ψ^{in} conjugates $\rho : \mathbb{D} \setminus \text{int } \Pi \rightarrow \mathbb{D}$ to $\sigma : T^\infty \setminus \text{int } T^0 \rightarrow T^\infty$. Since the cusp points of the ideal triangle group are dense in \mathbb{T} , we have

$$\text{clos}(S) = \psi^{\text{in}}(\mathbb{T}) = \partial T^\infty,$$

where we used local connectivity of ∂T^∞ .

Recall that $S \subset \partial A$ (see Proposition 5.10), and therefore

$$\partial T^\infty = \text{clos}(S) \subset \partial A.$$

It remains to prove the opposite inclusion, $\partial A \subset \partial T^\infty$. (Then we would have $\partial A = \partial T^\infty$ for two disjoint simply connected domains with a locally connected boundary, so the domains are Jordan.) Let $a \in \partial A \setminus \partial T^\infty$. Then $a \notin \bar{T}^\infty$, and there

is an open set U such that $a \in U \subset \mathbb{C} \setminus T^\infty$. All iterates of σ are defined in U and form a normal family (since they avoid T). It follows that $a \in A$, a contradiction. \square

Remark 6. Here is an outline of an alternative proof of the statement that $\hat{\mathbb{C}} = \overline{T^\infty} \sqcup A$. Our knowledge of the singular values of σ and the well-defined inverse branches of the iterates of σ allow us to rule out the existence of bounded complementary components of $\overline{T^\infty}$ (modifying classical arguments of Fatou to our setting). Therefore, $\hat{\mathbb{C}} \setminus \overline{T^\infty}$ is an invariant domain, and hence $\{\sigma^{\circ n}\}_n$ form a normal family there. It follows that the sequence of functions $\{\sigma^{\circ n}\}_n$ converges locally uniformly to ∞ on $\hat{\mathbb{C}} \setminus \overline{T^\infty}$; i.e. $A = \hat{\mathbb{C}} \setminus \overline{T^\infty}$.

Definition 5.13 (The Limit Set). The Jordan curve Γ , which is the common boundary of the tiling set T^∞ and the basin of infinity A , is called the *limit set* of σ .

5.2. Local Connectivity of The Boundary of The Tiling Set. Here we discuss the proof of Lemma 5.12.

5.2.1. Local Dynamics Near Cusp Points. The dynamics of σ near $\frac{3}{2}$ (and the other two cusps of T) is essentially parabolic. In particular, on a slit domain $B(\frac{3}{2}, \varepsilon) \setminus (\frac{3}{2} - \varepsilon, \frac{3}{2})$ (where $\varepsilon > 0$ is small enough), we have the following Puiseux series expansion

$$\sigma\left(\frac{3}{2} + \delta\right) = \frac{3}{2} + \bar{\delta} + k\bar{\delta}^{\frac{3}{2}} + O(\bar{\delta}^2),$$

where k is a positive constant, and the chosen branch of square root sends positive reals to positive reals. It is easy to see that $(\frac{3}{2}, \frac{3}{2} + \varepsilon)$ is the unique repelling direction of σ at $\frac{3}{2}$ (compare the proof of Proposition 5.10).

For $\varepsilon > 0$ let us denote

$$B := B\left(\frac{3}{2}, \varepsilon\right), \quad B^- := B \cap \left\{ \operatorname{Re}(z) < \frac{3}{2} \right\}, \quad B^+ := B \setminus B^-.$$

The following facts are straightforward consequences of the local dynamical description of σ near $\frac{3}{2}$.

Proposition 5.14. *If ε is sufficiently small, then*

$$B^- \subset T^\infty,$$

and

$$\sigma^{-n} B^+ \rightarrow \left\{ \frac{3}{2} \right\}.$$

(Here σ^{-n} is the branch in B^+ which fixes $\frac{3}{2}$; convergence is in the Hausdorff topology.)

In fact, a sharpened version of Proposition 5.14 holds true. Although we do not need it for the proof of Lemma 5.12, let us record it for future reference.

Proposition 5.15. *For every $\delta \in (0, \pi)$, there exists $R > 0$ such that*

$$W := U \cup \omega U \cup \omega^2 U \subset T^\infty,$$

where

$$U := \left\{ \frac{3}{2} + r e^{i\theta} : 0 < r < R, \delta < \theta < 2\pi - \delta \right\},$$

and ω is a primitive third root of unity.

The following proposition essentially follows from the observation that locally near the cusps, ∂T^∞ is contained in the “repelling petals” of the cusp points.

Proposition 5.16. $\exists \varepsilon > 0$ such that if an orbit in ∂T^∞ stays ε -close to a cusp of T , then the orbit lands on this cusp.

5.2.2. Puzzle Pieces. Let us denote the Green function of A with pole at infinity by G ($G \equiv 0$ on A^c). It is easy to see that for any $\rho > 0$, σ maps the equipotential (or level curve) $\{G = \rho\}$ to the equipotential $\{G = 2\rho\}$.

Let Δ_n be a tile of rank $n \geq 1$. It is a “triangle”; one of its sides is a side of a tile of rank $n - 1$; we will call it (the side) the *base* of Δ_n . The vertices of the base are iterated pre-images of the cusps of T . Since $\frac{3}{2}$ is accessible from ∞ (see the proof of Proposition 5.10), it follows that the vertices of the base of Δ_n are landing points of two external rays in $A(\infty)$. We denote by $P(\Delta_n)$ the closed region bounded by the base of Δ_n , the two rays, and the equipotential $\{G = \frac{1}{2^n}\}$ (so $\Delta_n \subset P(\Delta_n)$), and call it a *puzzle piece* of rank n .

Remark 7. A similar construction of puzzles in the context of polynomials with a parabolic fixed point can be found in [Roe10, PR10].

The following propositions are immediate from the previous construction (see Figure 4), and are first indications of the usefulness of puzzle pieces.

Proposition 5.17. For each $n \geq 1$, the sets $\partial T^\infty \cap P(\Delta_n)$ are connected.

Proposition 5.18. The puzzle pieces separate the impressions of the internal rays (of T^∞) landing at points of S from each other.

5.2.3. Local Connectivity at “Radial” Points.

Proposition 5.19. If $x \in \partial T^\infty \setminus S$, then ∂T^∞ is locally connected at x .

Proof. Note first that if ∂T^∞ is locally connected at x , then ∂T^∞ is locally connected at $\sigma(x)$ and at every pre-image of x .

Consider the orbit $x_n = \sigma^{on}(x)$ of some $x \in \partial T^\infty \setminus S$. If $\text{dist}(x_n, T) \rightarrow 0$, then $\text{dist}(x_n, T \setminus T^0) \rightarrow 0$, and therefore the orbit converges to one of the cusps of T (by continuity of σ). By Proposition 5.16, this would imply that $x \in S$. But this contradicts our choice of x .

Thus there is a subsequence of $\{x_n\}$ at a positive distance from T . Let ζ be a cluster point of this subsequence, so $\zeta \in \partial T^\infty$ is not a cusp of T . Thanks to Proposition 5.18, we can assume that ζ does not lie in the impression of the rays at angles $0, \frac{1}{3}$, and $\frac{2}{3}$ (possibly after replacing ζ by one of its iterated pre-images, which is also a subsequential limit of $\{x_n\}$).

The above assumption on ζ allows us to choose a puzzle piece P of sufficiently high rank such that

$$\zeta \in \text{int } P \subset P \subset \text{int } P_1,$$

where P_1 is a rank one puzzle piece. By construction, we have $x_n \in \text{int } P$ for infinitely many n 's. The puzzle piece P will play a key role in the rest of the proof as

suitably chosen iterated pre-images of $\text{int } P$ will produce a basis of open, connected neighborhoods of x in ∂T^∞ .

In order to achieve this, we use Proposition 5.7 to define (for each n with $x_n \in \text{int } P$) the inverse branches

$$\sigma^{-n} : \text{int } P_1 \rightarrow \mathbb{C}, \quad x_n \mapsto x.$$

These inverse branches form a normal family on $\text{int } P_1$, and by a standard argument (see next paragraph) we have $(\sigma^{-n})' \rightarrow 0$ (along a subsequence) locally uniformly on $\text{int } P_1$, so uniformly on $P \cap \partial T^\infty$. Thus

$$\text{diam}[\sigma^{-n}(\text{int } P \cap \partial T^\infty)] \rightarrow 0 \quad \text{along a subsequence.}$$

The sets $\sigma^{-n}(\text{int } P \cap \partial T^\infty)$ are open connected neighborhoods of x in ∂T^∞ , and we have local connectivity at x .

Finally, here is the ‘‘standard argument’’. We have $\sigma^{-n_k} \rightarrow g$ on $\text{int } P_1$, and we need to show that $g' = 0$ on some open set $V \subset P_1$. For V we can take any small disc inside the rank one tile contained in P_1 . Note that the pre-images $V_k := \sigma^{-n_k} V$ are disjoint (they sit inside tiles of different rank), and that by Koebe distortion,

$$\text{area}(V_k) \asymp [\text{diam}(V_k)]^2,$$

so $\text{diam}(V_k) \rightarrow 0$. Hence we are done! \square

5.2.4. Local Connectivity at The Cusp Point $\frac{3}{2}$. To finish the proof of Lemma 5.12 it remains to check local connectivity at the point $\frac{3}{2}$. Let Δ_n^\pm (for $n \geq 1$) be the two tiles of rank n which have $\frac{3}{2}$ as a common vertex. Let

$$\tilde{P}_n := \text{int}(P(\Delta_n^+) \cup P(\Delta_n^-)).$$

Note that for $n \geq 2$,

$$\sigma : \tilde{P}_n \rightarrow \tilde{P}_{n-1}$$

is a bijection. In what follows, we will work with the corresponding inverse branch of σ defined on \tilde{P}_1 .

We have $\sigma^{-1}(\tilde{P}_1) \subset \tilde{P}_1$, and $\frac{3}{2}$ is the only common boundary point. The sets $(\partial T^\infty \cap \tilde{P}_n) \cup \{\frac{3}{2}\}$ are open (in ∂T^∞) and connected. Moreover, their diameters go to zero by Proposition 5.14 (and Denjoy-Wolff). Hence, they form a basis of open, connected neighborhoods of $\frac{3}{2}$ (in the relative topology of ∂T^∞).

This completes the proof of Lemma 5.12.

5.3. Conformal Removability of The Limit Set. By Lemma 5.12, the Riemann map $\psi^{\text{in}} : \mathbb{D} \rightarrow T^\infty$ (constructed in Theorem 5.11) is continuous up to the boundary. We now prove a stronger version of this result.

Definition 5.20 (John Domain). A domain $D \subset \mathbb{C}$ is called a John domain if there exists $c > 0$ such that for any $z_0 \in D$, there exists an arc γ joining z_0 to some fixed reference point $w_0 \in D$ satisfying

$$(4) \quad \delta(z) \geq c|z - z_0|, \quad z \in \gamma,$$

where $\delta(z)$ stands for the Euclidean distance between z and ∂D .

Intuitively, Condition (4) means that the arc γ is “protected” from the boundary of the domain D .

For us, the importance of John domains stems from the fact that boundaries of John domains are conformally removable [Jon95, Corollary 1] implying uniqueness in the mating theory (see Subsection 5.4.3). Moreover, the Riemann map of a John domain extends as a Hölder continuous map to $\partial\mathbb{D}$.

Let us now state a condition that is equivalent to the John condition for a simply connected domain D . For $z \in D$, we denote by γ^z the part of the hyperbolic geodesic of D (passing through z and a fixed base-point w_0) that runs from z to ∂D . A simply connected domain D is a John domain if and only if there exists $M > 0$ such that for all $z \in D$,

$$(5) \quad w \in \gamma^z, \quad d_D(z, w) \geq M \quad \implies \quad \delta(w) \leq \frac{1}{2}\delta(z),$$

where d_D is the hyperbolic distance in D .

Theorem 5.21. *T^∞ is a John domain.*

Corollary 5.22. *∂T^∞ is conformally removable, and the Riemann map ψ^{in} is Hölder continuous up to the boundary.*

To prove Theorem 5.21, we will sometimes use the conformal model $\rho|_{\mathbb{D}}$ of $\sigma|_{T^\infty}$.

Wheels (of cheese) are just discs of radius say $1/10$ centered at the singular points $\frac{3}{4}$, $\frac{3}{4}\omega$, and $\frac{3}{4}\omega^2$ for σ (respectively, $1, \omega, \omega^2$ in the case of ρ). The *cheese slices* are sectors of the wheels contained in T^∞ (or \mathbb{D} in the case of ρ). In the case of σ , W_0 denotes the slice of angle π and W the slice of angle $2\pi - \theta$ (compare Proposition 5.15). For the model map ρ , the angles are twice smaller. If necessary we modify W and W_0 in an obvious way so that the slices are invariant under σ or ρ (on the part where the maps are defined).

5.3.1. *Quasi-rays.* Let $\gamma_1(\tau)$ and $\gamma_2(\tau)$ be paths in \mathbb{D} , $0 \leq \tau < \infty$, and let $C > 0$. We say that the paths *shadow* each other (with a constant C) if

$$\forall \tau > 0, \quad d_{\mathbb{D}}(\gamma_1(\tau), \gamma_2(\tau)) \leq C;$$

notation: $\gamma_1 \approx \gamma_2$.

We will now state a “shadowing” lemma for the model map ρ .

Let us fix a small number $\eta > 0$. Let $\mathbf{z}_0 \in \mathbb{D} \setminus W$ with $d(\mathbf{z}_0, \mathbb{T}) < \eta$, and $\gamma^{\mathbf{z}_0}$ be the segment $[\mathbf{z}_0, \zeta_0]$, where $\zeta_0 = \frac{\mathbf{z}_0}{|\mathbf{z}_0|}$. We parametrize $\gamma^{\mathbf{z}_0}$ so that

$$d_{\mathbb{D}}(\mathbf{z}_0, \gamma^{\mathbf{z}_0}(\tau)) = \tau.$$

We denote $\mathbf{z}_n := \rho^{\circ n}(\mathbf{z}_0)$ (assuming that it is defined), $\zeta_n := \rho^{\circ n}(\zeta_0)$, and $\mathbf{z}'_n = |\mathbf{z}_n| \zeta_n$ (see Figure 15). Let N be a positive integer such that $d(\mathbf{z}_k, \mathbb{T}) < \eta$ and $\mathbf{z}_k \notin W$, for $k = 1, \dots, N$.

Lemma 5.23.

$$\rho^{\circ N} \circ \gamma^{\mathbf{z}_0} \approx \gamma^{\mathbf{z}'_N}.$$

Proof. Let $\tilde{\iota}$ be reflection in the unit circle. Since ρ fixes \mathbb{T} as a set, we can extend it to the “symmetrized” open set $\mathcal{V} := \widehat{\mathbb{C}} \setminus \overline{\Pi \cup \tilde{\iota}(\Pi)}$ by the Schwarz reflection principle.

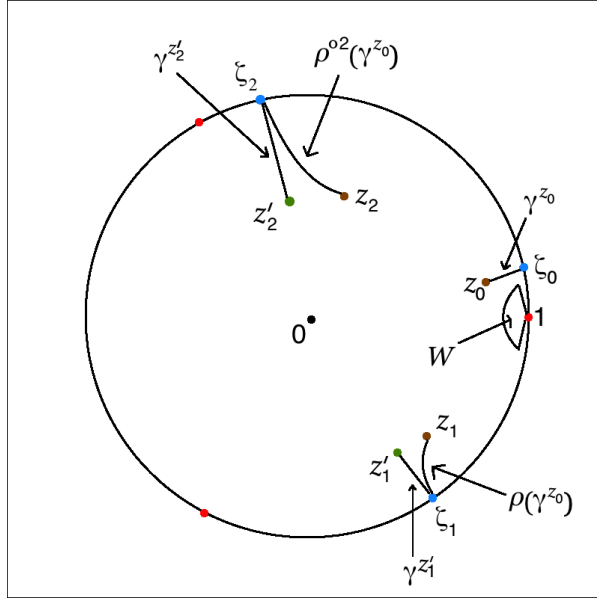


FIGURE 15. The image of the geodesic ray γ^{z_0} under $\rho^{\circ N}$ shadows the actual geodesic ray $\gamma^{z'_N}$.

Note that there exists some $C > 0$ such that $\mathbf{z}_N, \mathbf{z}'_N \in B(\zeta_N, C\eta) \cap \mathbb{D}$, and $B(\zeta_N, C\eta)$ is symmetric with respect to \mathbb{T} . Choosing C suitably large, we can assume that the inverse of branch of $\rho^{\circ N}$ that sends ζ_N to ζ_0 is defined on $B(\zeta_N, C\eta)$, and

$$\mathcal{A} := B(\zeta_N, C\eta) \setminus \overline{(\rho^{\circ N}(\gamma^{z_0}) \cup \tilde{\iota}(\rho^{\circ N}(\gamma^{z_0})))}$$

is an annulus of definite modulus (independent of \mathbf{z}_0).

ρ^{-N} is an isometry from $B(\zeta_N, C\eta)$ onto $\rho^{-N}(B(\zeta_N, C\eta))$ where both domains are equipped with the corresponding hyperbolic metrics. Hence, $\rho^{-N}(\mathcal{A})$ is an annulus of definite modulus (independent of \mathbf{z}_0) surrounding the symmetrized radial line segment $\tilde{\gamma}^{z_0} \cup \tilde{\iota}(\tilde{\gamma}^{z_0})$ in $\rho^{-N}(B(\zeta_N, C\eta))$.

It follows that the hyperbolic metric of \mathbb{D} and that of $\rho^{-N}(B(\zeta_N, C\eta) \cap \mathbb{D})$ are uniformly comparable on $\tilde{\gamma}^{z_0}$ (respectively, the hyperbolic metric of \mathbb{D} and that of $B(\zeta_N, C\eta) \cap \mathbb{D}$ are uniformly comparable on $\rho^{\circ N}(\tilde{\gamma}^{z_0})$). Therefore, $\rho^{\circ N} : \tilde{\gamma}^{z_0} \rightarrow \rho^{\circ N}(\tilde{\gamma}^{z_0})$ is a quasi-isometry with respect to the hyperbolic distance $d_{\mathbb{D}}$ of the unit disk (with quasi-isometry constants independent of \mathbf{z}_0). Therefore, $\rho^{\circ N} \circ \tilde{\gamma}^{z_0}$ is shadowed by a hyperbolic geodesic of \mathbb{D} with one end-point at ζ_N . Since ρ is expanding away from the third roots of unity, we conclude that the other end-point of this shadowing geodesic is bounded away from ζ_N . It follows that $\rho^{\circ N} \circ \tilde{\gamma}^{z_0}$ is shadowed by the geodesic arc $\tilde{\gamma}^{z'_N}$, with a shadowing constant independent of \mathbf{z}_0 . \square

Remark 8. 1) We get the same constant in \approx for all choices of $\theta \leq \theta_0$ in the definition of W .

2) We will use the notation boldface \mathbf{z} (respectively, $\boldsymbol{\gamma}^{\mathbf{z}}$) for ρ -dynamics, and ordinary z (respectively, γ^z) for σ -dynamics.

5.3.2. *Two Uniform Estimates.* We will now state a couple of uniform estimates for the σ -dynamics which are needed for the proof of Theorem 5.21. Recall that $0 \in T^\infty$ corresponds to $0 \in \mathbb{D}$ (for the model map ρ) under ψ^{in} . The curves γ^z in T^∞ are now geodesic rays through the origin.

The following assertion is straightforward.

Lemma 5.24. $\forall \varepsilon > 0, \exists M > 0$ such that if $\delta(z') \geq \eta$, $w' \in \gamma^{z'}$, and $d_{T^\infty}(w', z') \geq M$, then

$$\delta(w') \leq \varepsilon \delta(z').$$

The next estimate follows from the geometry of the limit set near a parabolic point (see Proposition 5.15).

Lemma 5.25. $\forall \varepsilon > 0, \exists M > 0$ such that if $\sigma(z') \in W$, $w' \in \gamma^{z'}$, and $d_{T^\infty}(w', z') \geq M$, then

$$\delta(w') \leq \varepsilon \delta(z').$$

Remark 9. We use the notation z' and w' (instead of just z and w) to make it consistent with the notation in the next subsection.

5.3.3. *Proof of Theorem 5.21.* Recall that our goal is to prove the existence of $M > 0$ such that for all $z \in T^\infty$,

$$w \in \gamma^z, d_{T^\infty}(z, w) \geq M \implies \delta(w) \leq \frac{1}{2} \delta(z).$$

For all $z \in T^\infty$ with $\delta(z) < \eta$, we define the *stopping time* $N = N(z)$ as the largest integer n such that

$$\delta(z_i) < \eta, i = 1, \dots, n, \quad \text{and} \quad z_{n-1} \notin W,$$

where $z_i = \sigma^{oi}(z)$. The stopping time N is well-defined because of expansiveness of σ . So we either have $\delta(z_{N+1}) \geq \eta$ (“Case 1”) or/and $z_N \in W$ (“Case 2”).

Case 1. Let $z_N \notin W$. We first observe that $\delta(z_N) \asymp \eta$ with a constant in \asymp independent of z . By Lemma 5.23, we have

$$\sigma^{\circ N} \circ \gamma^z \approx \gamma^{z'_N}$$

(z'_N is defined via the model map ρ); in particular, $d_{T^\infty}(z_N, z'_N) \leq C$. It then follows that $\delta(z'_N) \asymp \eta$ and we can apply Lemma 5.24 with $z' := z'_N$. Let ε be a small number to be specified at the end of the argument, and let M be as in Lemma 5.24. Let $w \in \gamma^z$ satisfy $d_{T^\infty}(z, w) > M$. Define $w_N := \sigma^{\circ N}(w)$, and $w'_N \in \gamma^{z'_N}$ by the condition

$$d_{T^\infty}(z, w) = d_{T^\infty}(z'_N, w'_N).$$

Then we have $d_{T^\infty}(z'_N, w'_N) > M$ and (by Lemma 5.24)

$$\delta(w'_N) \leq \varepsilon \delta(z'_N).$$

Since the hyperbolic metric (of T^∞) at a point is comparable to the reciprocal of its Euclidean distance to the boundary ∂T^∞ , and the curves $\sigma^{\circ N} \circ \gamma^z$ and $\gamma^{z'_N}$ shadow each other (with a constant C independent of z), it follows that $\delta(w_N)$ and $\delta(w'_N)$ (respectively, $\delta(z_N)$ and $\delta(z'_N)$) are uniformly comparable. So we get

$$\delta(w_N) \leq C\varepsilon \delta(z_N).$$

If θ is sufficiently small, then the (Euclidean) distance between $\sigma^{\circ N}(\gamma^z)$ and W_0 is uniformly comparable to η . A straightforward application of the Koebe distortion theorem (applied to a suitable inverse branch of $\sigma^{\circ N}$) now gives us

$$\delta(w) \leq \tilde{C}\varepsilon\delta(z) = \frac{1}{2}\delta(z)$$

(\tilde{C} is independent of z and ε is defined by the last equation).

Case 2. We now consider the case $z_N \in W$. By construction, we have $z_{N-1} \notin W$ and $\delta(z_{N-1}) < \eta$. By Lemma 5.23, we have

$$\sigma^{\circ(N-1)}(\gamma^z) \approx \gamma^{z'_{N-1}}.$$

At the same time, we can apply Lemma 5.25 with $z' = z'_{N-1}$ to obtain

$$\delta(w'_{N-1}) \leq \varepsilon\delta(z'_{N-1}).$$

The rest of the argument is exactly the same as in Case 1.

This completes the proof of Theorem 5.21.

5.4. Reflection Map as a Mating. We will now show that the Schwarz reflection of the deltoid arises as the unique conformal mating of the anti-polynomial \bar{z}^2 and the reflection map ρ coming from the ideal triangle group.

5.4.1. *Dynamical Systems Associated with σ .*

(a) *Action on the non-escaping set $\mathbb{C} \setminus T^\infty = \bar{A} = A \sqcup \Gamma$.*

By Proposition 5.9, the basin of infinity A (of σ) is simply connected. Let $\psi^{\text{out}} : \hat{\mathbb{C}} \setminus \mathbb{D} \rightarrow \bar{A}$ be the Riemann map such that $\infty \mapsto \infty$ and $1 \mapsto \frac{3}{2}$.

Proposition 5.26. $\sigma : \bar{A} \rightarrow \bar{A}$ is (conformally) equivalent to the polynomial

$$f_0 : \hat{\mathbb{C}} \setminus \mathbb{D} \rightarrow \hat{\mathbb{C}} \setminus \mathbb{D}, \quad f_0(z) = \bar{z}^2.$$

The conjugacy is given by ψ^{out} .

Proof. The (continuous extension of the) Riemann map ψ^{out} from $\hat{\mathbb{C}} \setminus \mathbb{D}$ to \bar{A} (normalized as in the statement of the proposition) conjugates σ to a degree two anti-Blaschke product with a fixed critical point at ∞ . Clearly, the conjugated map is f_0 . \square

(b) *Action on the tiling set T^∞ .* The tessellation of T^∞ by the pre-images of the droplet T corresponds to the action of the deltoid group $\mathcal{G}_\Delta \subset \text{Aut}(T^\infty)$.

Proposition 5.27. Let T_j^1 ($j=1,2,3$) be the three tiles of rank 1, so

$$\sigma^{-1}T^0 = T_1^1 \sqcup T_2^1 \sqcup T_3^1.$$

Then each map $\sigma : T_j^1 \rightarrow T^0$ extends to an automorphism $\sigma_j : T^\infty \rightarrow T^\infty$. The deltoid group $\mathcal{G}_\Delta := \langle \sigma_1, \sigma_2, \sigma_3 \rangle \subset \text{Aut}(T^\infty)$ has a presentation

$$\langle \sigma_1, \sigma_2, \sigma_3 : \sigma_1^2 = \sigma_2^2 = \sigma_3^2 = \text{id} \rangle,$$

and T^0 is a fundamental domain of \mathcal{G}_Δ .

Let us recall some notations from Section 3: Π is a filled ideal triangle with vertices at $\sqrt[3]{1}$; $\mathcal{G} \subset \text{Aut}(\mathbb{D})$ is the *ideal triangle group* (it is generated by the reflections in the sides of Π); and $\rho : \mathbb{D} \setminus \text{int } \Pi \rightarrow \mathbb{D}$ is the *reflection map*.

Proposition 5.28. *The deltoid group \mathcal{G}_Δ is conformally equivalent to the ideal triangle group \mathcal{G} . The conjugacy is given by the Riemann map $\psi^{\text{in}} : \overline{\mathbb{D}} \rightarrow \overline{T^\infty}$ such that $\psi^{\text{in}}(0) = 0$, $\psi^{\text{in}}(1) = \frac{3}{2}$. The Riemann map ψ^{in} takes Π onto T^0 .*

Proof. Since ψ^{in} was constructed in the proof of Theorem 5.11 by iterated lifting via σ and ρ , it conjugates the two groups \mathcal{G}_Δ and \mathcal{G} . In particular, ψ^{in} conjugates $\rho : \overline{\mathbb{D}} \setminus \text{int } \Pi \rightarrow \overline{\mathbb{D}}$ to $\sigma : \overline{T^\infty} \setminus \text{int } T^0 \rightarrow \overline{T^\infty}$. \square

(c) *Action on the limit set, $\sigma : \Gamma \rightarrow \Gamma$.* This is the common boundary of the systems described in (a) and (b). On the one hand, $\sigma : \Gamma \rightarrow \Gamma$ is topologically equivalent to $f_0 : \mathcal{J} \rightarrow \mathcal{J}$, where $\mathcal{J} = \mathbb{T}$ is the Julia set of f_0 . On the other hand, $\sigma : \Gamma \rightarrow \Gamma$ is topologically equivalent to the Markov map $\rho : \Lambda \rightarrow \Lambda$ where $\Lambda = \mathbb{T}$ is the limit set of the ideal triangle group \mathcal{G} .

Proposition 5.29. *There is a unique orientation preserving homeomorphism $\mathcal{E} : \mathbb{T} \rightarrow \mathbb{T}$, $1 \mapsto 1$, that conjugates ρ and f_0 on \mathbb{T} , i.e.*

$$\mathcal{E} \circ \rho = f_0 \circ \mathcal{E}.$$

Proof. The existence of the conjugacy \mathcal{E} was demonstrated at the end of Section 3. The uniqueness of such a conjugacy follows from the fact that the only orientation preserving automorphism of \mathbb{T} commuting with $f_0 : \mathbb{T} \rightarrow \mathbb{T}$ and fixing 1 is the identity map. \square

We can summarize this discussion as follows. The Schwarz reflection σ is a (conformal) mating between the polynomial dynamics f_0 on $\hat{\mathbb{C}} \setminus \mathbb{D}$ and the ideal triangle group \mathcal{G} on \mathbb{D} (or more accurately, the reflection map ρ associated with the group). The precise meaning of the term “mating” is explained in Subsection 5.4.3 below.

5.4.2. *Aside: The Question Mark Function.* The homeomorphism $\mathcal{E} : \mathbb{T} \rightarrow \mathbb{T}$ is a close relative of the famous Minkowski’s question mark function

$$? : [0, 1] \rightarrow [0, 1].$$

One way to define this function is to set $?(0) = 0$ and $?(1) = 1$ and then use the recursive formula

$$(6) \quad ?\left(\frac{p+r}{q+s}\right) = \frac{1}{2} \left(?\left(\frac{p}{q}\right) + ?\left(\frac{r}{s}\right) \right)$$

which gives us the values of $?$ on all Farey numbers in $[0, 1]$. In particular, $?$ is an increasing homeomorphism of $[0, 1]$ that sends the vertices of level n of the Farey tree to the vertices of level n of the dyadic tree (see Figure 16).

It is not hard to see that the map

$$x \mapsto \begin{cases} \frac{x}{1-x} & x \in [0, \frac{1}{2}), \\ \frac{2x-1}{x} & x \in [\frac{1}{2}, 1), \end{cases}$$

sends the vertices of level n of the Farey tree to the vertices of level $(n-1)$ (of the same tree). Also note that the doubling map

$$x \mapsto \begin{cases} 2x & x \in [0, \frac{1}{2}), \\ 2x-1 & x \in [\frac{1}{2}, 1). \end{cases}$$

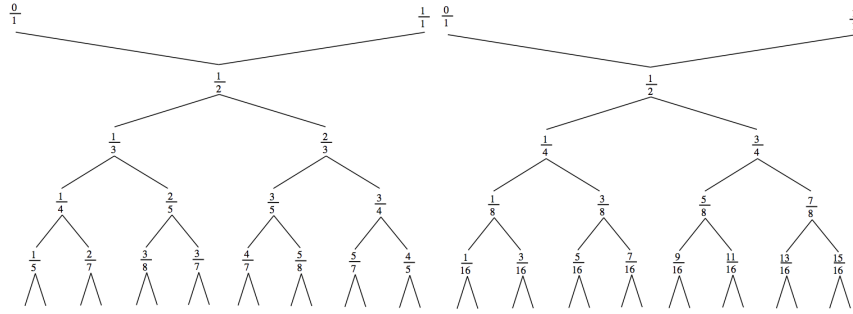


FIGURE 16. Left: The Farey tree. Right: The dyadic tree.

sends the vertices of level n of the dyadic tree to the vertices of level $(n - 1)$ (of the same tree). It follows that τ conjugates the former degree 2 map to the latter.

Formula (6) can be described in terms of the action of an ideal triangle group in the upper half-plane \mathbb{H} . Let Π' be the ideal triangle with vertices $0, 1, \infty$ (counterclockwise). Then Π' is a fundamental domain of the corresponding reflection group \mathcal{G}' . The corresponding tessellation of \mathbb{H} consists of ideal triangles of rank 0, 1, 2, etc. The rank zero triangle is Π' . There is exactly one rank 1 triangle with vertices in $[0, 1]$; the vertices are $\frac{0}{1}, \frac{1}{2}, \frac{1}{1}$. The only new vertex is $\frac{1}{2}$, which is the unique level 1 vertex of the Farey tree. The map τ sends this vertex to $\frac{1}{2}$, which is the unique level 1 vertex of the dyadic tree. There are exactly two rank 2 triangles with vertices in $[0, 1]$; the new vertices are $\frac{1}{3}$ and $\frac{2}{3}$, these are precisely the two vertices of level 2 of the Farey tree. The map τ sends these vertices to $\frac{1}{4}$ and $\frac{3}{4}$ (respectively), which are the two vertices of level 2 of the dyadic tree.

Returning to our homeomorphism $\mathcal{E} : \mathbb{T} \rightarrow \mathbb{T}$ we note that the restriction of \mathcal{E} to each of the three components of $\mathbb{T} \setminus \sqrt[3]{1}$ is given by an analogous construction which involves the tessellation of \mathbb{D} with translates of Π and the associated reflection group \mathcal{G} . On the dynamical side, the map \mathcal{E} fixes $\sqrt[3]{1}$, and maps their ρ -pre-images to their pre-images under \bar{z}^2 in an orientation-preserving way. Hence, \mathcal{E} conjugates the reflection map ρ (of degree -2) to the anti-doubling map \bar{z}^2 .

5.4.3. *Uniqueness of Mating.* Here we will formalize the notion of mating and summarize the above discussion.

(a) *Setup.* We have two conformal dynamical systems

$$\rho : \overline{\mathbb{D}} \setminus \text{int } \Pi \rightarrow \overline{\mathbb{D}}$$

and

$$f_0 : \hat{\mathbb{C}} \setminus \mathbb{D} \rightarrow \hat{\mathbb{C}} \setminus \mathbb{D}.$$

We also have a mating tool, the homeomorphism $\mathcal{E} : \mathbb{T} \rightarrow \mathbb{T}$ which conjugates ρ on the limit set and f_0 on the Julia set, $\mathcal{E} \circ \rho = f_0 \circ \mathcal{E}$.

(b) *Topological mating.* Denote

$$X = \overline{\mathbb{D}} \vee_{\mathcal{E}} (\hat{\mathbb{C}} \setminus \mathbb{D}), \quad Y = X \setminus \text{int } \Pi,$$

so X is a topological sphere, and Y is a closed Jordan disc in X . The well-defined topological map

$$\eta \equiv \rho \vee_{\varepsilon} f_0 : Y \rightarrow X$$

is the topological mating between ρ and f_0 .

(c) *Conformal mating.* Two Riemann mappings, ψ^{in} and ψ^{out} , glue together into a homeomorphism

$$H : (X, Y) \rightarrow (\hat{\mathbb{C}}, \bar{\Omega})$$

which is conformal outside $H^{-1}(\Gamma)$ and which conjugates η to σ . It endows X with a conformal structure compatible with the one on $X \setminus H^{-1}(\Gamma)$ that turns η into an anti-holomorphic map conformally conjugate to σ . In this way, the mating η provides us with a model for σ .

Moreover, there is only one conformal structure on X compatible with the standard structure on $X \setminus H^{-1}(\Gamma)$. Indeed, another structure would result in a non-conformal homeomorphism $\hat{\mathbb{C}} \rightarrow \hat{\mathbb{C}}$ which is conformal outside Γ , contradicting the conformal removability of Γ (see Corollary 5.22). In this sense, σ is the unique conformal mating of the map ρ arising from the ideal triangle group and the anti-polynomial \bar{z}^2 .

Theorem 1.1, that we announced in the introduction, is now obvious.

Proof of Theorem 1.1. The first part of the theorem follows from Theorem 5.11 and Corollary 5.22.

The second statement is the content of Subsection 5.4.3. \square

6. ITERATED REFLECTIONS WITH RESPECT TO A CARDIOID AND A CIRCLE

This section, we carry out a detailed analysis of the dynamics and parameter space of Schwarz reflections with respect to a cardioid and a circle.

6.1. Schwarz Reflection with Respect to a Cardioid. The simplest examples of quadrature domains are interior and exterior disks $B(a, r)$ and $\bar{B}(a, r)^c$ respectively. As quadrature domains, their orders are 1 and 0 (respectively). In the rest of this section, we will focus on a particular quadrature domain of order 2 that is of interest to us.

6.1.1. Cardioid as a Quadrature Domain. The principal hyperbolic component \heartsuit of the Mandelbrot set (i.e. the unique hyperbolic component of period one) has a Riemann map

$$\begin{aligned} \varphi : \mathbb{D} &\rightarrow \heartsuit \\ \varphi(\lambda) &= \lambda/2 - \lambda^2/4 \end{aligned}$$

(compare Subsection 2.1). Its boundary $\partial\heartsuit$ is the cardioid

$$\varphi(\partial\mathbb{D}) = \{e^{i\theta}/2 - e^{2i\theta}/4 : \theta \in [0, 2\pi)\}.$$

Dynamically, this means that the quadratic map $z^2 + w$ has a fixed point of multiplier $\lambda \in \mathbb{D}$ precisely when $w = \lambda/2 - \lambda^2/4$. Since this Riemann map is rational, it follows that \heartsuit is a quadrature domain. The quadrature function of \heartsuit is $(\frac{3}{8z} - \frac{1}{16z^2})$. Hence, \heartsuit is a quadrature domain of order 2 with a unique node at 0.

6.1.2. *Schwarz Reflection of \heartsuit .* Thanks to Proposition 4.6, we have an explicit description of the Schwarz reflection map $\sigma : \overline{\heartsuit} \rightarrow \hat{\mathbb{C}}$. Indeed, the commutative diagram implies that:

$$\begin{aligned} \sigma(\varphi(\lambda)) &= \varphi(1/\bar{\lambda}) \\ (7) \quad \text{i.e. } \sigma\left(\frac{\lambda}{2} - \frac{\lambda^2}{4}\right) &= \left(\frac{2\bar{\lambda} - 1}{4\bar{\lambda}^2}\right) \end{aligned}$$

for each $\lambda \in \overline{\mathbb{D}}$.

In particular, $\sigma(\overline{\heartsuit}) = \hat{\mathbb{C}}$, and 0 is the only critical point of σ in \heartsuit . Moreover, some interesting functional values can be directly computed from this formula; e.g. $\sigma(0) = \infty$, $\sigma(\frac{3}{16}) = 0$, $\sigma(\frac{5}{36}) = -\frac{3}{4}$.

Since \heartsuit parametrizes all quadratic polynomials $z^2 + w$ with an attracting fixed point of multiplier λ , it will be useful to understand the Schwarz reflection of the cardioid in terms of its action on multipliers of quadratic polynomials. A simple computation using Relation (7) shows that if the multiplier of the non-repelling fixed point of $z^2 + w$ (where $w \in \overline{\heartsuit} \setminus \{0\}$) is λ , then the multipliers of the fixed points of $z^2 + \sigma(w)$ are $2 - \frac{1}{\lambda}$ and $\frac{1}{\lambda}$.

Therefore, for each $w \in \heartsuit \setminus \{0\}$, we have the following description of σ .

Proposition 6.1 (Multiplier Description of Schwarz Reflection). *Let $w \in \heartsuit \setminus \{0\}$ with $w = \varphi(\lambda)$ for some $\lambda \in \mathbb{D}^*$ (where φ is the dynamical Riemann map of \heartsuit). Then, $\sigma(w) = c$ if and only if the quadratic polynomial $z^2 + c$ has a fixed point of multiplier $1/\bar{\lambda}$.*

Remark 10. Note that the fixed point multipliers $\{\lambda_1, \lambda_2\}$ of a quadratic map $z^2 + c$ satisfy $\lambda_1 + \lambda_2 = 2$ and $\lambda_1\lambda_2 = 4c$. Hence, two distinct quadratic maps cannot have a common fixed point multiplier; i.e. a fixed point multiplier uniquely determines a quadratic map.

6.1.3. *Covering Properties of σ .* This description allows us to conveniently study some mapping properties of the map σ .

Proposition 6.2. *$\sigma^{-1}(\heartsuit) = \varphi(B(\frac{2}{3}, \frac{1}{3}))$, and $\sigma : \sigma^{-1}(\heartsuit) \rightarrow \heartsuit$ is an anti-holomorphic isomorphism. Moreover, $\sigma : \partial\sigma^{-1}(\heartsuit) \rightarrow \partial\heartsuit$ is an orientation-reversing homeomorphism.*

Proof. First note that σ fixed $\partial\heartsuit$ pointwise. Now let $w \in \heartsuit$ and λ be the attracting multiplier of $z^2 + w$; i.e. $w = \varphi(\lambda)$. Since $\lambda < 1$, we have that $|1/\bar{\lambda}| > 1$. Therefore, $\sigma(w) \in \heartsuit$ if and only if $|2 - 1/\bar{\lambda}| < 1$. A simple computation shows that this happens if and only if $|\lambda - \frac{2}{3}| < \frac{1}{3}$; i.e. $\lambda \in B(\frac{2}{3}, \frac{1}{3})$. This proves that $\sigma(w) \in \heartsuit \Leftrightarrow w \in \varphi(B(\frac{2}{3}, \frac{1}{3}))$. Hence, $\sigma^{-1}(\heartsuit) = \varphi(B(\frac{2}{3}, \frac{1}{3}))$ (compare Figure 17).

The above discussion also shows that the (inverse of the) Riemann map φ of \heartsuit conjugates $\sigma : \sigma^{-1}(\heartsuit) \rightarrow \heartsuit$ to the map

$$g : B(\frac{2}{3}, \frac{1}{3}) \rightarrow \mathbb{D}, \quad g(\lambda) = 2 - 1/\bar{\lambda}.$$

Since g is an anti-holomorphic isomorphism, we conclude that $\sigma : \sigma^{-1}(\heartsuit) \rightarrow \heartsuit$ is such as well.

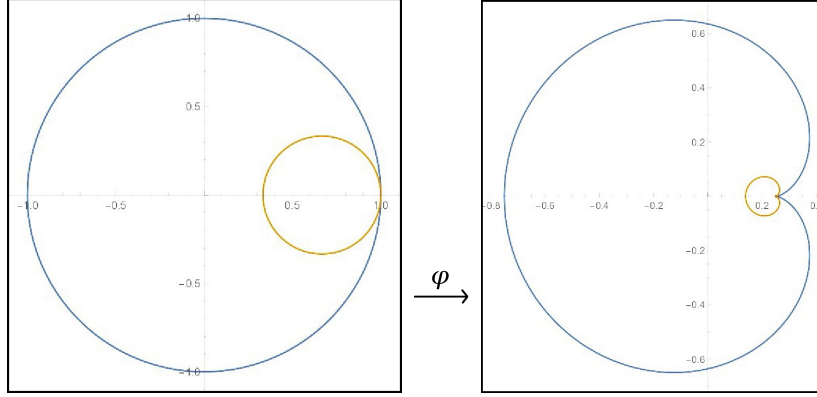


FIGURE 17. Left: The disk $B(\frac{2}{3}, \frac{1}{3})$ contained in the disk $B(0, 1)$. The smaller disk maps to the larger disk under $\lambda \mapsto 2 - 1/\bar{\lambda}$. Right: The images of the two disks under the Riemann map φ . The smaller cardioid maps univalently onto the larger cardioid, and the boundary of the smaller cardioid maps homeomorphically to the boundary of the larger cardioid under σ .

Similarly, the (inverse of the) homeomorphic boundary extension of the Riemann map φ of \heartsuit conjugates $\sigma : \partial\sigma^{-1}(\heartsuit) \rightarrow \partial\heartsuit$ to the map $g : \partial B(\frac{2}{3}, \frac{1}{3}) \rightarrow \partial\mathbb{D}$. Since g is an orientation-reversing homeomorphism, the same is true for $\sigma : \partial\sigma^{-1}(\heartsuit) \rightarrow \partial\heartsuit$. \square

Remark 11. $\sigma^{-1}(\heartsuit)$ is a smaller cardioid with its cusp at $\frac{1}{4}$ and vertex at $\frac{5}{36}$. Also, $\sigma^{-1}(\heartsuit) \cap \mathbb{R} = (\frac{5}{36}, \frac{1}{4})$.

Using Proposition 6.1, it is straightforward to see the behavior of σ outside of $\sigma^{-1}(\heartsuit)$.

Proposition 6.3. $\sigma : \heartsuit \setminus \overline{\sigma^{-1}(\heartsuit)} \rightarrow \hat{\mathbb{C}} \setminus \overline{\heartsuit}$ is a two-to-one branched covering branched at 0.

Corollary 6.4. For two points $w_1 = \varphi(\lambda_1), w_2 = \varphi(\lambda_2) \in \heartsuit \setminus (\overline{\sigma^{-1}(\heartsuit)} \cup \{0\})$, we have $\sigma(w_1) = \sigma(w_2)$ if and only if $1/\bar{\lambda}_1 + 1/\bar{\lambda}_2 = 2$.

Proof. This follows directly from the multiplier description of σ given in Proposition 6.1 and the fact that the sum of the multipliers of the two fixed points of a quadratic polynomial is 2. \square

Remark 12. The covering degrees of σ can also be computed using [LM16, Lemma 4.1] and the fact that the cardioid is a quadrature domain of order two. However, the multiplier description of σ that we used in our proofs yields additional dynamical information. In particular, shrinking of the iterated pre-images of \heartsuit (see Corollary 6.5) will be useful later in the paper.

6.1.4. Iteration of σ .

Corollary 6.5 (Iterated Pre-images of \heartsuit). $\sigma^{-n}(\heartsuit) = \varphi(B(\frac{2n}{2n+1}, \frac{1}{2n+1}))$, and $\sigma^{\circ n} : \sigma^{-n}(\heartsuit) \rightarrow \heartsuit$ is a univalent map. In particular, $\text{diam}(\sigma^{-n}(\heartsuit)) \rightarrow 0$, as $n \rightarrow +\infty$.

Proof. This is simply an extension of the arguments used in the proof of Proposition 6.2. Iterating the map σ is equivalent to iterating the univalent map $g : \lambda \mapsto 2 - 1/\bar{\lambda}$ (as long as $w \in \sigma^{-1}(\heartsuit)$ or equivalently $\lambda \in g^{-1}(\mathbb{D})$). As $(\iota \circ g)^{\circ n}(\lambda) = \frac{(n+1)\lambda - n}{n\lambda - (n-1)}$, it follows that $g^{-n}(\mathbb{D}) = B(\frac{2n}{2n+1}, \frac{1}{2n+1})$. Hence, $\sigma^{-n}(\heartsuit) = \varphi(B(\frac{2n}{2n+1}, \frac{1}{2n+1}))$. The other statements readily follow. \square

6.1.5. *An Explicit Formula for σ .* Recall that Relation (7) gives an implicit formula for σ . Choosing the branch of square root which sends positive reals to positive reals, we have the following explicit formula for σ :

$$(8) \quad \sigma(w) = \frac{1 - 2\sqrt{1 - 4\bar{w}}}{4(1 - \sqrt{1 - 4\bar{w}})^2}$$

for all $w \in \overline{\heartsuit}$.

6.1.6. A Characterization of \heartsuit as a Quadrature Domain.

Proposition 6.6 (Characterization of Cardioids and Disks as Quadrature Domains). 1) Let $\Omega \ni \infty$ be a simply connected quadrature domain with associated Schwarz reflection map σ_Ω . If $\sigma_\Omega : \sigma_\Omega^{-1}(\overline{\Omega}^c) \rightarrow \overline{\Omega}^c$ is univalent, then Ω is an exterior disk.

2) Let $\Omega \ni 0$ be a bounded simply connected quadrature domain such that $\partial\Omega$ has a cusp at $\frac{1}{4}$. Moreover, suppose that the Schwarz reflection map σ_Ω of Ω has a double pole at 0, and $\sigma_\Omega : \sigma_\Omega^{-1}(\Omega) \rightarrow \Omega$ is univalent. Then, $\Omega = \heartsuit$.

Proof. 1) By Proposition 4.6, there exists a rational map φ_Ω on $\hat{\mathbb{C}}$ such that $\varphi_\Omega : \mathbb{D} \rightarrow \Omega$ is a Riemann map of Ω . Note that by Figure 1, the degree of $\sigma_\Omega : \sigma_\Omega^{-1}(\overline{\Omega}^c) \rightarrow \overline{\Omega}^c$ is equal to the number of pre-images in $\hat{\mathbb{C}}$ of a generic point in $\overline{\Omega}^c$ under φ_Ω . Our assumption now implies that $\deg \varphi_\Omega = 1$; i.e. φ_Ω is a Möbius map. The conclusion follows.

2) As in the previous part, let φ_Ω be a rational map on $\hat{\mathbb{C}}$ such that $\varphi_\Omega : \mathbb{D} \rightarrow \Omega$ is a Riemann map of Ω . We can assume that $\varphi_\Omega(0) = 0$, and $\varphi_\Omega(1) = \frac{1}{4}$. Since $\varphi_\Omega(\partial\mathbb{D}) = \partial\Omega$ has a cusp at $\frac{1}{4}$, it follows that $\varphi'_\Omega(1) = 0$.

Since the Schwarz reflection map σ_Ω of Ω has a double pole at 0, the commutative diagram in Figure 1 readily yields that $\varphi_\Omega(\infty) = \infty$, and $D\varphi_\Omega(\infty) = 0$.

The same commutative diagram also implies that the degree of $\sigma_\Omega : \sigma_\Omega^{-1}(\Omega) \rightarrow \Omega$ is equal to the number of pre-images in $\hat{\mathbb{C}} \setminus \overline{\mathbb{D}}$ of a generic point in Ω under φ_Ω . Hence, our assumption that $\sigma_\Omega : \sigma_\Omega^{-1}(\Omega) \rightarrow \Omega$ is univalent translates to the fact that $\deg \varphi_\Omega = 2$. It follows that φ_Ω is a quadratic polynomial. Since $\varphi_\Omega(0) = 0$, $\varphi_\Omega(1) = \frac{1}{4}$, and $\varphi'_\Omega(1) = 0$, we conclude that $\varphi_\Omega(\lambda) = \frac{\lambda}{2} - \frac{\lambda^2}{4}$. Therefore, $\Omega = \heartsuit$. \square

Remark 13. The simple connectivity assumption in Proposition 6.6 can be dropped (although we will not need this improvement). However, one needs to employ more involved arguments to deduce the results without this assumption (see [Gus83] for the cardioid case, and [Eps62, ES65] for the case of disks).

6.2. The Dynamical and Parameter Planes. Let \heartsuit be the principal hyperbolic component of the Mandelbrot set. For any $a \in \mathbb{C}$, let $B(a, r_a)$ be the smallest disk containing \heartsuit and centered at a ; i.e. $\partial B(a, r_a)$ is the circumcircle to \heartsuit .

Proposition 6.7. 1) For $a \in (-\infty, -\frac{1}{12})$, the circumcircle $\partial B(a, r_a)$ touches $\partial\heartsuit$ at exactly two points. On the other hand, for any $a \in \mathbb{C} \setminus (-\infty, -\frac{1}{12})$, the circumcircle $B(a, r_a)$ touches $\partial\heartsuit$ at exactly one point.

2) For $a \neq -\frac{1}{12}$, the circle $\partial B(a, r_a)$ has a contact of order two with $\partial\heartsuit$. On the other hand, $\partial B(a, r_a)$ has a contact of order four with $\partial\heartsuit$ if $a = -\frac{1}{12}$.

Proof. 1) Note that the cardioid $\partial\heartsuit$ and its circumcircle $\partial B(a, r_a)$ can have at most two points of tangency. Since the real line is the only axis of symmetry of \heartsuit , it follows that $\partial B(a, r_a)$ can touch $\partial\heartsuit$ at two points only if a is real. Moreover, when a is real, $\partial\heartsuit \cap \partial B(a, r_a)$ is either the singleton $\{-\frac{3}{4}\}$ or consists of a pair of complex conjugate points.

It is clear that for $a \leq -\frac{3}{4}$, the circumcircle $\partial B(a, r_a)$ touches $\partial\heartsuit$ at a pair of complex conjugate points.

Now let $-\frac{3}{4} < a < -\frac{1}{12}$. For such values of a , the curvature of the circle $\partial B(a, a + \frac{3}{4})$ is larger than $\frac{3}{2}$. But the curvature of $\partial\heartsuit$ at $-\frac{3}{4}$ is $\frac{3}{2}$ (in other words, the boundary of the cardioid curves less than the circle does at $-\frac{3}{4}$). Since $\partial B(a, a + \frac{3}{4})$ is real-symmetric, we have that $B(a, a + \frac{3}{4})$ is locally contained in \heartsuit near $-\frac{3}{4}$. Hence, $\partial B(a, a + \frac{3}{4})$ is not a circumcircle to $\partial\heartsuit$. It now follows that $\partial\heartsuit \cap \partial B(a, r_a)$ consists of a pair of complex conjugate points (see Figure 18).

Finally, let $a \geq -\frac{1}{12}$. Note that the curvature of the circle $\partial B(a, a + \frac{3}{4})$ is at most $\frac{3}{2}$, while the curvature of $\partial\heartsuit$ is at least $\frac{3}{2}$ at each point (in other words, the boundary of the cardioid curves more than the circle everywhere). Since $\partial B(a, a + \frac{3}{4})$ is real-symmetric, it follows that $B(a, a + \frac{3}{4})$ contains \heartsuit . Hence, $r_a = a + \frac{3}{4}$, and $\partial B(a, a + \frac{3}{4})$ is the circumcircle to \heartsuit centered at a . In particular, $\partial\heartsuit \cap \partial B(a, a + \frac{3}{4}) = \{-\frac{3}{4}\}$.

2) The evolute (locus of centers of curvature) of $\partial\heartsuit$ is a cardioid $\frac{1}{3}$ -rd the size of $\partial\heartsuit$ with a cusp at $-\frac{1}{12}$. For any a not on the evolute, the circle $\partial B(a, r_a)$ is, by definition, not an osculating circle to $\partial\heartsuit$ (i.e. $\partial B(a, r_a)$ has a simple tangency with $\partial\heartsuit$).

Now suppose that $a \neq -\frac{1}{12}$ is a point on the evolute of \heartsuit . More precisely, let $a \neq -\frac{1}{12}$ be the center of curvature of $\partial\heartsuit$ at some point α'_a . A simple computation now shows that the radius of curvature of $\partial\heartsuit$ at α'_a is strictly smaller than the distance between a and $\overline{\alpha'_a} \in \partial\heartsuit$; i.e. $|a - \alpha'_a| < |a - \overline{\alpha'_a}|$. It follows that the osculating circle to $\partial\heartsuit$ centered at a does not circumscribe \heartsuit ; in other words, $\partial B(a, r_a)$ is not an osculating circle to $\partial\heartsuit$ for these parameters a as well.

Finally, for $a = -\frac{1}{12}$, the circle $\partial B(a, r_a)$ is indeed the osculating circle of $\partial\heartsuit$ at $-\frac{3}{4}$. Moreover, as $-\frac{3}{4}$ is a vertex of $\partial\heartsuit$ (i.e. the curvature of $\partial\heartsuit$ has a vanishing derivative at $-\frac{3}{4}$), the osculating circle of $\partial\heartsuit$ at $-\frac{3}{4}$ (which is centered at $-\frac{1}{12}$) has a third order tangency with $\partial\heartsuit$. Therefore, for all $a \in \mathbb{C} \setminus (-\infty, -\frac{1}{12}]$, the circle $\partial B(a, r_a)$ touches $\partial\heartsuit$ at exactly one point and has a contact of order two with $\partial\heartsuit$ at that point, while for $a = -\frac{1}{12}$, the circumcircle $\partial B(a, r_a)$ touches $\partial\heartsuit$ at exactly one point and has a contact of order four with $\partial\heartsuit$. \square

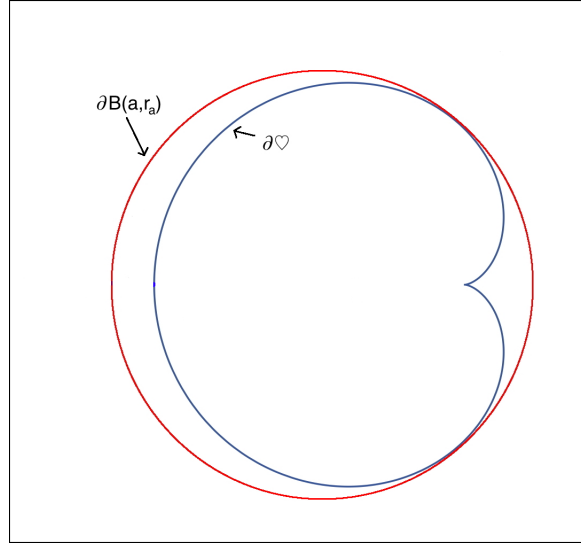


FIGURE 18. For any a in the slit $(-\infty, -\frac{1}{12})$, the disk $B(a, r_a)$ touches \heartsuit at two points.

6.2.1. *The Family \mathcal{S} .* In this paper, we will only be interested in the situation where the circumcircle to the cardioid touches it at only one point. For $a \in \mathbb{C} \setminus (-\infty, -\frac{1}{12})$, let

$$\Omega_a := \heartsuit \cup \overline{B}(a, r_a)^c.$$

We now define our dynamical system $F_a : \overline{\Omega}_a \rightarrow \hat{\mathbb{C}}$ as,

$$w \mapsto \begin{cases} \sigma(w) & \text{if } w \in \overline{\heartsuit}, \\ \sigma_a(w) & \text{if } w \in \overline{B}(a, r_a)^c, \end{cases}$$

where σ is the Schwarz reflection of \heartsuit , and σ_a is reflection with respect to the circle $|w - a| = r_a$. It follows from our previous discussion that 0 is the only critical point of F_a . We will call this family of maps \mathcal{S} ; i.e.

$$\mathcal{S} := \left\{ F_a : \overline{\Omega}_a \rightarrow \hat{\mathbb{C}} : a \in \mathbb{C} \setminus (-\infty, -\frac{1}{12}) \right\}.$$

Proposition 6.8. *For each $a \in \mathbb{C} \setminus (-\infty, -\frac{1}{12})$, the map $F_a : F_a^{-1}(\Omega_a) \rightarrow \Omega_a$ is a two-to-one branched covering, branched only at 0.*

Proof. Note that $F_a^{-1}(\Omega_a) \subset \Omega_a$ consists of three (open) connected components. Two of which, namely $\sigma^{-1}(\heartsuit)$ and $\sigma_a^{-1}(\heartsuit)$, map univalently onto \heartsuit . On the other hand, $0 \in \sigma^{-1}(\overline{B}(a, r_a)^c)$, so F_a is a 2 : 1 branched cover from $\sigma^{-1}(\overline{B}(a, r_a)^c)$ onto $\overline{B}(a, r_a)^c$. \square

Corollary 6.9. *Let $V \subset \Omega_a$ be a simply connected domain such that the forward orbit of the critical point 0 does not intersect V . Then, all inverse branches of $F_a^{\circ n}$ ($n \geq 1$) are defined on V . Moreover, the image of V under each of these branches is disjoint from T_a .*

6.2.2. *Dynamics near Singular Points.* Let $T_a := \Omega_a^c = \overline{B}(a, r_a) \setminus \heartsuit$. Note that ∂T_a has two singular points; namely α_a (a double point) and $\frac{1}{4}$ (a cusp). Both of these are fixed points of F_a . As the map F_a admits no anti-holomorphic extension in neighborhoods of these fixed points, we need to obtain local expansions of F_a in suitable relative neighborhoods of α_a and $\frac{1}{4}$.

Formula (8) shows that map F_a has no single-valued anti-holomorphic extension in a neighborhood of $\frac{1}{4}$ (extending F_a near $\frac{1}{4}$ involves choosing a branch of square root). A straightforward computation yields the following asymptotics of F_a near $\frac{1}{4}$.

Proposition 6.10 (Dynamics near Cardioid Cusp). *Choosing the branch of square root that sends positive reals to positive reals, we have*

$$F_a(w) = \bar{w} - k\left(\frac{1}{4} - \bar{w}\right)^{\frac{3}{2}} + O\left(\left(\frac{1}{4} - \bar{w}\right)^2\right)$$

where $w \in B(\frac{1}{4}, \varepsilon) \setminus (\frac{1}{4}, \frac{1}{4} + \varepsilon)$, for some $k > 0$ and $\varepsilon > 0$ small enough. Hence, $\frac{1}{4}$ repels nearby real points on its left.

Moreover, Corollary 6.5 gives a precise description of the dynamics of F_a near the fixed point $\frac{1}{4}$; in particular, all points in $\heartsuit \cap B(\frac{1}{4}, \varepsilon)$ eventually leave $\heartsuit \cap B(\frac{1}{4}, \varepsilon)$ or escape to T_a under iterations of F_a .

On the other hand, both σ and σ_a admit anti-holomorphic extensions in a neighborhood of α_a . As germs, these extensions are anti-holomorphic involutions. However, these extensions do not match up to yield a single anti-holomorphic map in a neighborhood of α_a . In this case, it will be more convenient to work with the second iterate $F_a^{\circ 2}$. Note that

$$(9) \quad F_a^{\circ 2} = \begin{cases} \sigma_a \circ \sigma & \text{on } \sigma^{-1}(\overline{B}(a, r_a)^c), \\ \sigma \circ \sigma_a & \text{on } \sigma_a^{-1}(\heartsuit). \end{cases}$$

Let us first look at the parameters $a \neq -\frac{1}{12}$. For such parameters a , the curves $\partial\heartsuit$ and $\partial B(a, r_a)$ have a simple tangency at α_a (in particular, they have common tangent and normal lines). The following simple result describes the local behavior of the maps $\sigma_a \circ \sigma$ and $\sigma \circ \sigma_a$ near α_a .

Proposition 6.11 (Dynamics near Double Point; $a \neq -\frac{1}{12}$). *Let $a \neq -\frac{1}{12}$. Then, σ and σ_a extend as local anti-holomorphic involutions near α_a such that*

$$(\sigma_a \circ \sigma)(w) = w + k_a(w - \alpha_a)^2 + O((w - \alpha_a)^3),$$

and

$$(\sigma_a \circ \sigma)^{-1}(w) = (\sigma \circ \sigma_a)(w) = w - k_a(w - \alpha_a)^2 + O((w - \alpha_a)^3)$$

for all $w \in B(\alpha_a, \varepsilon)$ and some $k_a \neq 0$. Moreover, the inward (respectively, outward) normal vector to $\partial\heartsuit$ at α_a is the repelling direction of the parabolic germ $\sigma_a \circ \sigma$ (respectively, of $\sigma \circ \sigma_a$). These are the only repelling directions for $F_a^{\circ 2}$ at α_a .

Proof. The fact that σ (respectively, σ_a) admits a local anti-holomorphic extension near α_a follows from the fact that α_a is a non-singular point of $\partial\heartsuit$ (respectively, of $\partial B(a, r_a)$). Since these local extensions are anti-holomorphic involutions, it follows that $\sigma_a \circ \sigma$ is the inverse of $\sigma \circ \sigma_a$ (as germs).

The first two terms in the local expansions of the Schwarz reflection maps σ and σ_a can be computed in terms of the slope and curvature of the corresponding curves at α_a (see [Dav74, Chapter 7]). Moreover, since $\partial\heartsuit$ and $\partial B(a, r_a)$ do not have the same curvature at α_a (recall that $\partial B(a, r_a)$ is not the osculating circle to $\partial\heartsuit$ at α_a

for $a \neq -\frac{1}{12}$), it follows that $k_a \neq 0$. The final statement on repelling directions of the parabolic germs is a consequence of the fact that $\partial\heartsuit$ has greater curvature than $\partial B(a, r_a)$ at α_a (as $\partial B(a, r_a)$ is a circumcircle of $\partial\heartsuit$). \square

Remark 14. More generally, if two real-analytic smooth curve germs γ_1 and γ_2 with associated Schwarz reflection maps σ_1 and σ_2 (respectively) have contact of order $k+1$ at the origin, then $\sigma_1 \circ \sigma_2$ is of the form $z + cz^{k+1} + \dots$.

Let us choose repelling petals P_1 and P_2 of the parabolic germs $\sigma_a \circ \sigma$ and $\sigma \circ \sigma_a$ contained in $\sigma^{-1}(\overline{B}(a, r_a)^c)$ and $\sigma_a^{-1}(\heartsuit)$ respectively (in other words, P_1 and P_2 are repelling and attracting petals for the parabolic germ $\sigma_a \circ \sigma$). Then,

$$(10) \quad \bigcap_{n \in \mathbb{N}} F_a^{-2n}(\overline{P_1}) = \bigcap_{n \in \mathbb{N}} F_a^{-2n}(\overline{P_2}) = \{\alpha_a\},$$

where we have chosen the inverse branch of $F_a^{\circ 2}$ near α_a that fixes α_a .

We now turn our attention to the parameter $a = -\frac{1}{12}$.

Proposition 6.12 (Dynamics near Double Point; $a = -\frac{1}{12}$). *Let $a = -\frac{1}{12}$. Then σ and σ_a extend as local anti-holomorphic involutions near $\alpha_a = -\frac{3}{4}$ such that*

$$(\sigma_a \circ \sigma)(w) = w - k'_a \left(w + \frac{3}{4}\right)^4 + O\left(\left(w + \frac{3}{4}\right)^5\right),$$

and

$$(\sigma_a \circ \sigma)^{-1}(w) = (\sigma \circ \sigma_a)(w) = w + k'_a \left(w + \frac{3}{4}\right)^4 + O\left(\left(w + \frac{3}{4}\right)^5\right)$$

for all $w \in B(-\frac{3}{4}, \varepsilon)$ and some $k'_a > 0$. Moreover, the positive (respectively, negative) real direction at $-\frac{3}{4}$ is an attracting vector of the former (respectively, latter) parabolic germ, and these are the only attracting directions for $F_a^{\circ 2}$ at $-\frac{3}{4}$. Thus, $-\frac{3}{4}$ attracts nearby real points under iterates of F_a .

Proof. For $a = -\frac{1}{12}$, the curves $\partial\heartsuit$ and $\partial B(a, r_a)$ have a third order tangency at $\alpha_a = -\frac{3}{4}$ (i.e. a contact of order 4), so the desired asymptotics follow from Remark 14. The fact that σ (respectively, σ_a) admits a local anti-holomorphic extension near $-\frac{3}{4}$ follows from the fact that $-\frac{3}{4}$ is a non-singular point of $\partial\heartsuit$ (respectively, of $\partial B(a, r_a)$). Since these extensions are involutions, $\sigma_a \circ \sigma$ is the inverse of $\sigma \circ \sigma_a$. The asymptotics of $\sigma_a \circ \sigma$ and $\sigma \circ \sigma_a$ near $-\frac{3}{4}$ can be explicitly computed using Formula (8). The attracting directions of the parabolic germs are readily seen from these asymptotics. The fact that these are the only attracting directions for $F_a^{\circ 2}$ at $-\frac{3}{4}$ follows from Formula (9). \square

Remark 15. We see from the above local expansions that each of the parabolic germs $\sigma_a \circ \sigma$ and $\sigma \circ \sigma_a$ has two more attracting directions at $-\frac{3}{4}$, however they lie in regions where the germs do not coincide with $F_a^{\circ 2}$, see Formula (9).

6.2.3. Tiling Set, Non-escaping set, and Limit set. We now proceed to define the dynamically relevant sets for a general map $F_a \in \mathcal{S}$. It is easy to see that the points α_a and $\frac{1}{4}$ have only two pre-images under F_a , and every point of $T_a \setminus \{\alpha_a, \frac{1}{4}\}$ has three pre-images under F_a . In order to get an honest covering map, we will therefore work with $T_a^0 := T_a \setminus \{\alpha_a, \frac{1}{4}\}$. Then, the restriction $F_a : F_a^{-1}(T_a^0) \rightarrow T_a^0$ is a degree 3 covering.

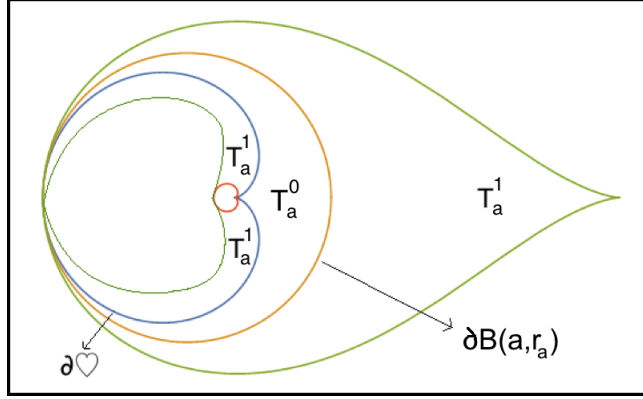


FIGURE 19. The tiles of rank 0 and 1 are labelled as T_a^0 and T_a^1 respectively. The union of the tiles of rank 0 and 1 is denoted by E_a^1 .

- Definition 6.13** (Tiling Set, Non-escaping set, and Limit set). • For any $k \geq 0$, the connected components of $F_a^{-k}(T_a^0)$ are called *tiles* (of F_a) of rank k . The unique tile of rank 0 is T_a^0 .
- The *tiling set* T_a^∞ of F_a is defined as the set of points in $\bar{\Omega}_a$ that eventually escape to T_a^0 ; i.e. $T_a^\infty = \bigcup_{k=0}^{\infty} F_a^{-k}(T_a^0)$. Equivalently, the tiling set is the union of all tiles.
 - The *non-escaping set* K_a of F_a is the complement $\hat{\mathbb{C}} \setminus T_a^\infty$. Connected components of $\text{int } K_a$ are called *Fatou components* of F_a . All iterates of F_a are defined on K_a .
 - The boundary of T_a^∞ is called the *limit set* of F_a , and is denoted by Γ_a .

Remark 16. Note that the tiling set, non-escaping set, and limit set of F_a are the analogues of basin of infinity, filled Julia set, and Julia set (respectively) of a polynomial.

The tiling set and the non-escaping set yield an invariant partition of the dynamical plane of F_a .

Proposition 6.14 (Tiling Set is Open and Connected). *For each $a \in \mathbb{C} \setminus (-\infty, -\frac{1}{12})$, the tiling set T_a^∞ is an open connected set, and hence the non-escaping set K_a is closed.*

Proof. Let us denote the union of the tiles of rank 0 through k by E_a^k (see Figure 19). Clearly, $\text{int } E_a^k$ is connected, and $\text{int } E_a^k \subsetneq \text{int } E_a^{k+1}$ for each $k \geq 0$. Moreover, we have

$$T_a^\infty = \bigcup_{k \geq 0} \text{int } E_a^k.$$

It follows that T_a^∞ is an open connected set, and hence K_a is a closed set. \square

Corollary 6.15. *Each Fatou component of F_a (i.e. connected components of $\text{int } K_a$) is simply connected.*

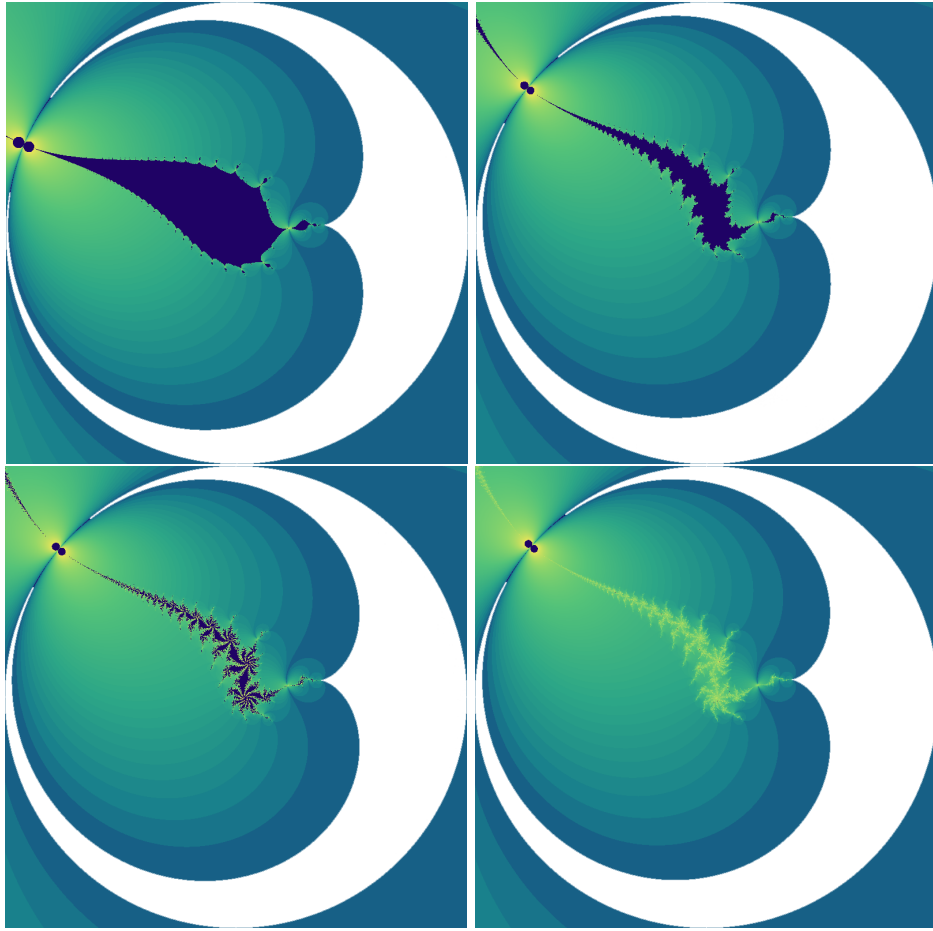


FIGURE 20. Parts of the dynamical planes of various parameters with connected limit set are shown. The white regions denote the tile of rank 0. The non-escaping set in the bottom right figure has empty interior, while the other non-escaping sets have non-empty interior.

Proposition 6.16 (Complete Invariance). *For each $a \in \mathbb{C} \setminus (-\infty, -\frac{1}{12})$, both T_a^∞ and K_a are completely invariant under F_a .*

The next proposition sheds light on the geometry of the tiling set near the singular points $\frac{1}{4}$ and α_a . It roughly says that the tiling set contains sufficiently wide angular wedges near the singular points.

Proposition 6.17. *1) Let $a \in \mathbb{C} \setminus (-\infty, -\frac{1}{12})$. Then for every $\delta \in (0, \pi)$, there exists $R > 0$ such that*

$$W_a^1 := \left\{ \frac{1}{4} + re^{i\theta} : 0 < r < R, -(\pi - \delta) < \theta < (\pi - \delta) \right\} \subset T_a^\infty.$$

2) Let $a \in \mathbb{C} \setminus (-\infty, -\frac{1}{12}]$, and θ_0 be the slope of the inward normal vector to $\partial\heartsuit$ at α_a . Then for every $\delta \in (0, \frac{\pi}{2})$, there exists $R > 0$ such that

$$W_a^2 := \alpha_a + \left\{ r e^{i(\theta_0 + \theta)} : 0 < r < R, \delta < |\theta| < \pi - \delta \right\} \subset T_a^\infty.$$

Proof. 1) This is a consequence of the ‘‘parabolic’’ behavior of F_a near $\frac{1}{4}$. The local Puiseux series expansion of F_a near $\frac{1}{4}$ (see Proposition 6.10) imply that $(\frac{1}{4} - \varepsilon, \frac{1}{4})$ is the unique repelling direction of F_a at $\frac{1}{4}$, and the iterated pre-images of the fundamental tile T_a^0 occupy a circular sector of Stolz angle $2(\pi - \delta)$ (disjoint from $(\frac{1}{4} - \varepsilon, \frac{1}{4})$) at $\frac{1}{4}$ (compare Figure 20).

2) This is a consequence of the parabolic dynamics of $F_a^{\circ 2}$ near α_a . The local power series expansions of the piecewise definitions of $F_a^{\circ 2}$ near α_a (see Formula (9) and Proposition 6.11) imply that the inward and outward normal vectors to $\partial\heartsuit$ at α_a are the only repelling directions of $F_a^{\circ 2}$ at that point, and the iterated pre-images of each of the two connected components of $T_a^0 \cap B(\alpha_a, \varepsilon)$ (for $\varepsilon > 0$ sufficiently small) occupies a circular sector of Stolz angle $(\pi - 2\delta)$ (disjoint from the repelling directions) at α_a (compare Figure 20). \square

We will now show that connectivity of the non-escaping set K_a is completely determined by the dynamics of the unique critical point 0 (as in the case of quadratic polynomials or anti-polynomials).

Proposition 6.18. *The non-escaping set K_a is connected if and only if it contains the critical point 0.*

Proof. If $0 \in T_a^\infty$, then the tile containing 0 is ramified and it disconnects K_a . On the other hand, if 0 does not escape under F_a , then every tile is unramified, and $\hat{\mathbb{C}} \setminus \text{int } E_a^k$ is a full continuum for each $k \geq 0$. Therefore,

$$K_a = \bigcap_{k \geq 0} \left(\hat{\mathbb{C}} \setminus \text{int } E_a^k \right)$$

is a nested intersection of full continua and hence is a full continuum itself. \square

6.2.4. *The Connectedness Locus.* The above proposition leads to the following definition.

Definition 6.19 (Connectedness Locus and Escape Locus). The connectedness locus of the family \mathcal{S} is defined as

$$\mathcal{C}(\mathcal{S}) = \left\{ a \in \mathbb{C} \setminus (-\infty, -\frac{1}{12}) : 0 \notin T_a^\infty \right\} = \left\{ a \in \mathbb{C} \setminus (-\infty, -\frac{1}{12}) : K_a \text{ is connected} \right\}.$$

The complement of the connectedness locus in the parameter space is called the *escape locus*.

Let us collect a few easy (but useful) facts about the connectedness locus $\mathcal{C}(\mathcal{S})$.

Proposition 6.20. $\mathcal{C}(\mathcal{S}) \subset \heartsuit \cup \{\frac{1}{4}\}$.

Proof. Note that for all $a \in \mathbb{C} \setminus (-\infty, -\frac{1}{12})$, we have $F_a^{\circ 2}(0) = a \in B(a, r_a)$. Clearly, $a \neq \alpha_a$. Therefore, if $a \notin \heartsuit \cup \{\frac{1}{4}\}$, then $F_a^{\circ 2}(0) \in T_a^0$; i.e. $0 \in T_a^\infty$. \square

Proposition 6.21. $\mathcal{C}(\mathcal{S})$ is closed in $\mathbb{C} \setminus (-\infty, -\frac{1}{12})$.

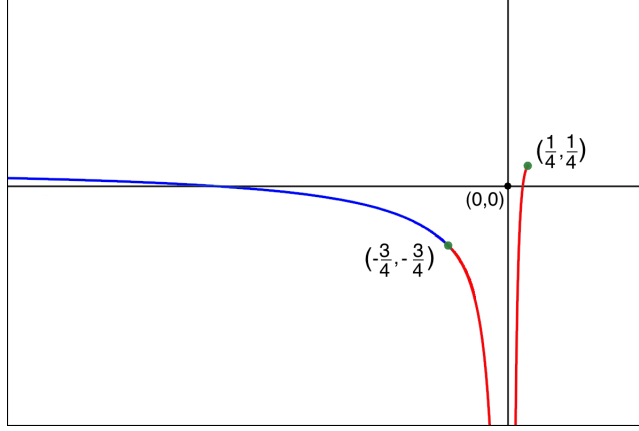


FIGURE 21. The graph of F_a restricted to $(-\infty, \frac{1}{4}]$ is shown for $a = \frac{1}{4}$. Since F_a tends to $\frac{1}{4}$ as a tends to $-\infty$, we have that F_a is a two-to-one map from $[-\infty, \frac{1}{4}]$ onto itself.

Proof. Note that the fundamental tile T_a^0 varies continuously with the parameter as a runs over $\mathbb{C} \setminus (-\infty, -\frac{1}{12})$. Now let $a_0 \in \mathbb{C} \setminus (-\infty, -\frac{1}{12})$ be a parameter outside the connectedness locus $\mathcal{C}(\mathcal{S})$. Then there exists some positive integer n_0 such that $F_{a_0}^{n_0}(0) \in T_{a_0}^0$. It follows that for all a sufficiently close to a_0 , we have $F_a^{n_0}(0) \in T_a^0$ or $F_a^{(n_0+1)}(0) \in T_a^0$. Hence, $\mathcal{C}(\mathcal{S})$ is closed in $\mathbb{C} \setminus (-\infty, -\frac{1}{12})$. \square

Proposition 6.22 (Real Slice of The Connectedness Locus). $\mathcal{C}(\mathcal{S}) \cap \mathbb{R} = [-\frac{1}{12}, \frac{1}{4}]$.

Proof. Let $a \in [-\frac{1}{12}, \frac{1}{4}]$. For such parameters a , we have $\alpha_a = -\frac{3}{4}$ and $r_a = (a + \frac{3}{4})$. Moreover, using Formula (8), we see that:

- $F_a([-\infty, -\frac{3}{4}]) = [-\frac{3}{4}, a]$ (F_a is decreasing),
- $F_a([-\frac{3}{4}, 0]) = [-\infty, -\frac{3}{4}]$ (F_a is decreasing),
- $F_a([0, \frac{1}{4}]) = [-\infty, \frac{1}{4}]$ (F_a is increasing).

In particular, the interval $[-\infty, \frac{1}{4}]$ is invariant under F_a (see Figure 21 for the graph of F_a where $a = \frac{1}{4}$). Since $[-\infty, \frac{1}{4}]$ is disjoint from T_a^0 , it follows that 0 does not escape to T_a^0 . Therefore, $[-\frac{1}{12}, \frac{1}{4}] \subset \mathcal{C}(\mathcal{S})$.

But by Proposition 6.20, we already know that $\mathcal{C}(\mathcal{S}) \subset \heartsuit \cup \{\frac{1}{4}\}$. This completes the proof. \square

The above proof also shows that for each $a \in [-\frac{1}{12}, \frac{1}{4}]$, $F_a : [-\infty, \frac{1}{4}] \rightarrow [-\infty, \frac{1}{4}]$ is a unimodal map with a simple critical point at 0.

Corollary 6.23. For each $a \in [-\frac{1}{12}, \frac{1}{4}]$, the map $F_a : [-\infty, \frac{1}{4}] \rightarrow [-\infty, \frac{1}{4}]$ is a C^1 unimodal map with a simple critical point at 0.

Proof. Since σ_a and σ are anti-meromorphic on $\overline{B}(a, a + \frac{3}{4})^c$ and \heartsuit respectively, it follows that σ_a is C^1 on $[-\infty, -\frac{3}{4}]$ and σ is C^1 on $(-\frac{3}{4}, \frac{1}{4}]$. Moreover, the real-analytic extensions of these maps (in an \mathbb{R} -neighborhood of $-\frac{3}{4}$) have a common derivative -1 at $-\frac{3}{4}$. This proves that F_a is C^1 -smooth on $[-\infty, \frac{1}{4}]$. \square

6.2.5. *Quasiconformal Deformations in \mathcal{S} .* Quasiconformal deformations play a crucial role in studying the parameter spaces of holomorphic/anti-holomorphic dynamical systems. In this spirit, we will prove a lemma that will allow us to talk about quasiconformal deformations in the family \mathcal{S} .

Lemma 6.24 (Quasiconformal Deformation of Schwarz Reflections/Changing the Mirrors). *Let μ be an F_a -invariant Beltrami coefficient on $\hat{\mathbb{C}}$, and Φ be a quasiconformal map solving μ such that Φ fixes $0, \frac{1}{4},$ and ∞ . Let $b = \Phi(a)$. Then, $b \in \mathbb{C} \setminus (-\infty, -\frac{1}{12})$, $\Phi(\Omega_a) = \Omega_b$, and $F_b = \Phi \circ F_a \circ \Phi^{-1}$ on Ω_b .*

Proof. The assumption that μ is F_a -invariant implies that $\Phi \circ F_a \circ \Phi^{-1}$ is anti-meromorphic on $\Phi(\Omega_a)$. Hence, $\Phi \circ F_a \circ \Phi^{-1}$ is an anti-meromorphic map on $\Phi(\overline{B}(a, r_a)^c)$ that continuously extends to the identity map on $\Phi(\partial\overline{B}(a, r_a)^c) = \partial\Phi(\overline{B}(a, r_a)^c)$. Since Φ fixes ∞ , it follows that $\Phi(\overline{B}(a, r_a)^c)$ is an unbounded quadrature domain with Schwarz reflection map $\Phi \circ \sigma_a \circ \Phi^{-1}$. Since F_a maps $\overline{B}(a, r_a)^c$ univalently onto $B(a, r_a)$, we conclude that $\Phi \circ F_a \circ \Phi^{-1}$ maps $\Phi(\overline{B}(a, r_a)^c)$ univalently onto $\Phi(B(a, r_a))$. It now follows by Proposition 6.6 that $\Phi(\overline{B}(a, r_a)^c)$ is an exterior disk.

Let $b = \Phi(a)$. Recall that the Schwarz reflection map of an exterior disk maps ∞ to the center of the interior part of the disk. Since $\sigma_a(\infty) = a$ and $\Phi(\infty) = \infty$, it follows that the Schwarz reflection map $\Phi \circ \sigma_a \circ \Phi^{-1}$ of $\Phi(\overline{B}(a, r_a)^c)$ maps ∞ to b . Hence, $\Phi(\overline{B}(a, r_a)^c)$ is of the form $\overline{B}(b, r)^c$, for some $r > 0$.

Again, $\Phi \circ F_a \circ \Phi^{-1}$ is an anti-meromorphic map on $\Phi(\heartsuit)$ that continuously extends to the identity map on $\Phi(\partial\heartsuit) = \partial\Phi(\heartsuit)$. As Φ fixes 0 and ∞ , it follows that $\Phi(\heartsuit) \ni 0$ is a bounded simply connected quadrature domain with associated Schwarz reflection map $\Phi \circ \sigma \circ \Phi^{-1}$. Also note that $\Phi \circ \sigma \circ \Phi^{-1}$ maps $\Phi(\sigma^{-1}(\heartsuit))$ univalently onto $\Phi(\heartsuit)$. Moreover, $\Phi \circ \sigma \circ \Phi^{-1}$ has a double pole at 0 , and $\partial\Phi(\heartsuit)$ has a cusp at $\frac{1}{4}$. Therefore by Proposition 6.6, we have that $\Phi(\heartsuit) = \heartsuit$, and $\Phi \circ \sigma \circ \Phi^{-1} \equiv \sigma$ on \heartsuit .

As $\partial B(a, r_a)$ and $\partial\heartsuit$ touch at a unique point, the same is true for $\partial\overline{B}(b, r)$ and $\partial\heartsuit$. Hence, $\partial\overline{B}(b, r)$ is a circumscribed circle of \heartsuit touching $\partial\heartsuit$ at a single point. So, $r = r_b$, and $\Phi \circ \sigma_a \circ \Phi^{-1} \equiv \sigma_b$ on $\overline{B}(b, r_b)^c$. In particular, $b \in \mathbb{C} \setminus (-\infty, -\frac{1}{12})$.

To summarize, we have proved that $\Phi(\heartsuit) = \heartsuit$ and $\Phi(\overline{B}(a, r_a)^c) = \overline{B}(b, r_b)^c$ (for some $b \in \mathbb{C} \setminus (-\infty, -\frac{1}{12})$), where $\partial\overline{B}(b, r_b)$ circumscribes $\partial\heartsuit$ and touches it at a single point. Hence, $\Phi(\Omega_a) = \Omega_b$. Furthermore, $\Phi \circ \sigma \circ \Phi^{-1} \equiv \sigma$ on \heartsuit , and $\Phi \circ \sigma_a \circ \Phi^{-1} \equiv \sigma_b$ on $\overline{B}(b, r_b)^c$. Therefore, $\Phi \circ F_a \circ \Phi^{-1} \equiv F_b$ on Ω_b .

This completes the proof. \square

6.2.6. *Classification of Fatou Components.* We will now discuss the classification of Fatou components, and their relation with the post-critical set (of the maps in \mathcal{S}).

Proposition 6.25 (Classification of Fatou Components). *Let $a \in \mathbb{C} \setminus (-\infty, -\frac{1}{12})$. Then the following hold true.*

- 1) *Every Fatou component of F_a is eventually pre-periodic.*
- 2) *For $a \neq -\frac{1}{12}$, every periodic Fatou component of F_a is either the (immediate) basin of attraction of an attracting cycle, or the (immediate) basin of attraction of a parabolic cycle, or a Siegel disk.*
- 3) *For $a = -\frac{1}{12}$, each periodic Fatou component of F_a is either the (immediate) basin of attraction of an attracting/parabolic cycle, or a Siegel disk, or the (immediate) basin of attraction of the singular point $-\frac{3}{4}$. In fact, the map F_a has a 2-cycle*

of Fatou components such that every point in these components converges (under the dynamics) to the singular point $-\frac{3}{4}$ through a period two cycle of attracting petals (intersecting the real line). Moreover, these are the only two periodic Fatou components of F_a where orbits converge to $-\frac{3}{4}$.

Remark 17. We will soon see that the only periodic Fatou components of the map $a = -\frac{1}{12}$ are the two periodic Fatou components touching at the singular point $-\frac{3}{4}$.

Proof. 1) The classical proof of non-existence of wandering Fatou components for rational maps [Sul85, Theorem 1] can be adapted to the current setting.³ This is possible because the family \mathcal{S} is quasiconformally closed (by Lemma 6.24) and the parameter space of \mathcal{S} is finite-dimensional (in fact, real two-dimensional). If F_a were to have a wandering Fatou component (such a component would necessarily be simply connected by Corollary 6.15), then one could construct an infinite-dimensional space of nonequivalent deformations of F_a (supported on the grand orbit of the wandering component), all of which would be members of \mathcal{S} . Evidently, this would contradict the fact that the parameter space of \mathcal{S} is finite-dimensional.

2) Let $a \neq -\frac{1}{12}$, and U be a periodic Fatou component of period k of $F_a^{\circ 2}$. Recall that by Corollary 6.15, U is simply connected. We can now invoke [Mil06, Theorem 5.2, Lemma 5.5] to conclude that the Fatou component U is either the (immediate) basin of attraction of an attracting cycle, or a Siegel disk, or all orbits in U converge to a unique boundary point $w_0 \in \partial U$ with $F_a^{\circ kn}(w_0) = w_0$.

To complete the proof, we only need to focus on the third case. To this end, suppose that all orbits in U converge to a unique boundary point $w_0 \in \partial U$ with $F_a^{\circ kn}(w_0) = w_0$.

Case 1: w_0 is not a singular point of T_a . In this case, $F_a^{\circ 2}$ has a holomorphic extension in a full neighborhood of w_0 . Therefore, the classical Snail Lemma (see [Mil06, Lemma 16.2]) asserts that w_0 is a parabolic fixed point of multiplier 1 of $F_a^{\circ 2k}$, and hence U is an immediate basin of attraction of a parabolic cycle.

Case 2: w_0 is a singular point of T_a . In this case, we have that $w_0 \in \{\frac{1}{4}, \alpha_a\}$. Since $F_a^{\circ 2}$ does not have a holomorphic extension in a full neighborhood of the singular points, we cannot apply the Snail Lemma.

However, the local asymptotics of F_a and the geometry of T_a^∞ near $\frac{1}{4}$ (Propositions 6.10 and 6.17) imply that $U \subset K_a$ is contained in the “repelling petal” of F_a at $\frac{1}{4}$; i.e. orbits in U cannot non-trivially converge to $\frac{1}{4}$. Hence, $w_0 \neq \frac{1}{4}$.

Again, since $a \neq -\frac{1}{12}$, the local asymptotics of $F_a^{\circ 2}$ and the geometry of T_a^∞ near α_a (Propositions 6.11 and 6.17) imply that $U \subset K_a$ is contained in one of the two “repelling petals” of $F_a^{\circ 2}$ at α_a ; i.e. orbits in U cannot non-trivially converge to α_a . Hence, $w_0 \neq \alpha_a$.

This completes the proof of the second statement of the proposition.

3) Finally, let us look at $a = -\frac{1}{12}$. For this parameter, we have $\alpha_a = -\frac{3}{4}$. We only need to prove the assertions concerning Fatou components where orbits converge to $-\frac{3}{4}$.

We have seen in Proposition 6.12 that the positive and negative real directions at $-\frac{3}{4}$ are attracting vectors for $F_a^{\circ 2}$, and in particular, $-\frac{3}{4}$ attracts nearby real points under iterations of $F_a^{\circ 2}$. These two axes are permuted by F_a .

³Proofs of nonexistence of wandering Fatou components for various classes of non-rational maps can be found in [EL84, EL92, GK86, Eps93].

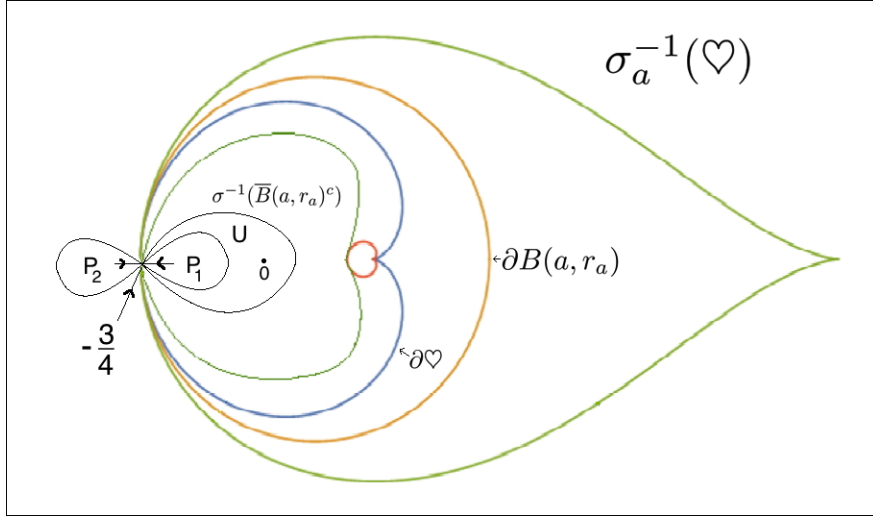


FIGURE 22. The dynamical plane of the map $a = -\frac{1}{12}$ is shown with the attracting petals P_1 and P_2 at $-\frac{3}{4}$ marked. The Fatou component $U \subset \sigma^{-1}(\overline{B}(a, r_a)^c)$ contains the petal P_1 . The $F_a^{\circ 2}$ -orbit of every point in U converges to $-\frac{3}{4}$ through the attracting petal P_1 . The critical point 0 lies in U .

Clearly, a sufficiently small attracting petal P_1 of $\sigma_a \circ \sigma$ (respectively, $P_2 := F_a(P_1)$ of $\sigma \circ \sigma_a$) containing the positive (respectively, negative) real direction at $-\frac{3}{4}$ is contained in $\text{int } K_a$. Therefore, these two petals are contained in a two-periodic cycle of Fatou components of F_a touching at the fixed point $-\frac{3}{4}$.

One of these two Fatou components is contained in $\sigma^{-1}(\overline{B}(a, r_a)^c) \subset \heartsuit$, let us call it U . Then, $P_1 \subset U$ (see Figure 22). Applying [Mil06, Lemma 5.5] to $F_a^{\circ 2}|_U$, we conclude that the $F_a^{\circ 2}$ -orbit of every point in U converges to the boundary fixed point $-\frac{3}{4}$. Moreover, $F_a^{\circ 2} \equiv \sigma_a \circ \sigma$ on U . The power series expansion of $\sigma_a \circ \sigma$ near $-\frac{3}{4}$ (see Proposition 6.12) implies that the only attracting direction of $\sigma_a \circ \sigma$ at $-\frac{3}{4}$ that is contained in $\sigma^{-1}(\overline{B}(a, r_a)^c)$ is the positive real direction. Therefore, the $F_a^{\circ 2}$ -orbit of every point in U must converge to $-\frac{3}{4}$ through the attracting petal P_1 . It follows that the $F_a^{\circ 2}$ -orbit of every point in $F_a(U)$ must converge to $-\frac{3}{4}$ through the attracting petal P_2 .

The last statement now readily follows. \square

Let us also mention the relation between (closures of) various types of Fatou components and the post-critical set.

Proposition 6.26 (Fatou Components and Critical Orbit). *1) If F_a has an attracting or parabolic cycle, then the forward orbit of the critical point 0 converges to this cycle.*

2) If U is a Siegel disk of F_a , then $\partial U \subset \overline{\{F_a^{\circ n}(0)\}_{n \geq 0}}$. Every Cremer point (i.e. an irrationally neutral, non-linearizable periodic point) of F_a is also contained in $\overline{\{F_a^{\circ n}(0)\}_{n \geq 0}}$.

3) For $a = -\frac{1}{12}$, the critical orbit of F_a converges to the singular point $-\frac{3}{4}$.

Proof. 1) The proof follows classical arguments of Fatou and is similar to the corresponding proof for rational maps [Mil06, Theorem 8.6, Theorem 10.15].

2) Let U be a Siegel disk of F_a of period k . Since U is a connected component of $\text{int } K_a$ and $K_a = \hat{\mathbb{C}} \setminus T_a^\infty$, we have that $\partial U \subset \partial T_a^\infty = \Gamma_a$.

Let us choose $w_0 \in \partial U \setminus \{\frac{1}{4}, \alpha_a\}$, and assume that w_0 is not in the closure of the post-critical set $\overline{\{F_a^{on}(0)\}_{n \geq 0}}$. Then there exists $\varepsilon_0 > 0$ such that $B(w_0, \varepsilon_0) \subset \Omega_a$ and $B(w_0, \varepsilon_0) \cap \overline{\{F_a^{on}(0)\}_{n \geq 0}} = \emptyset$. Proposition 6.9 and our assumption on $B(w_0, \varepsilon_0)$ ensure that we can define inverse branches of $F_a^{\circ kn}$ (for each $n \geq 1$) on $B(w_0, \varepsilon_0)$ such that they map $B(w_0, \varepsilon_0) \cap U$ biholomorphically into U and map $B(w_0, \varepsilon_0) \cap \partial U$ into ∂U . Moreover, all these inverse branches (defined on $B(w_0, \varepsilon_0)$) avoid T_a . Hence, they form a normal family, so some subsequence converges to a holomorphic map g . Since the maps $F_a^{\circ kn}|_U$ are conjugate to irrational rotations, it follows that g is univalent on $B(w_0, \varepsilon_0)$. Moreover, $g(w_0) \in \partial U \subset \Gamma_a$.

Let us set $V := g(B(w_0, \frac{\varepsilon_0}{2}))$. Since g is a subsequential limit of the chosen inverse branches of $F_a^{\circ kn}$ (on $B(w_0, \varepsilon_0)$), it follows that infinitely many $F_a^{\circ kn}$ map V into $B(w_0, \varepsilon_0) \subset \Omega_a$.

On the other hand, note that V is a neighborhood of $g(w_0) \in \Gamma_a$, and hence V intersects the tiling set T_a^∞ non-trivially. But every point in $V \cap T_a^\infty$ is mapped to the fundamental tile T_a^0 by a sufficiently large iterate of F_a . Clearly, this contradicts the conclusion of the previous paragraph. This contradiction implies that the assumption $w_0 \notin \overline{\{F_a^{on}(0)\}_{n \geq 0}}$ was false. Hence, $\partial U \setminus \{\frac{1}{4}, \alpha_a\} \subset \overline{\{F_a^{on}(0)\}_{n \geq 0}}$. The result (for boundaries of Siegel disks) now follows by taking topological closure on both sides.

Since a Cremer point of F_a is necessarily contained in Ω_a , the proof of the corresponding statement for Cremer points is analogous to the Siegel case (compare [Mil06, Corollary 14.4]).

3) Let $U \subset \sigma^{-1}(\overline{B(a, r_a)^c})$ be the period two Fatou component of F_a such that the $F_a^{\circ 2}$ -orbit of every point in U converges to $-\frac{3}{4}$ asymptotic to the positive real direction at $-\frac{3}{4}$ (the existence of this component was proved in Proposition 6.25(Case 3), compare Figure 22). It follows from the proof of the same proposition and [Mil06, Theorem 10.9] that $F_a^{\circ 2}$, restricted to a small attracting petal P_1 in U , is conformally conjugate to translation by $+1$ on a right half-plane. One can now argue as in [Mil06, Theorem 10.15] to conclude that the boundary of the maximal domain of definition of this conjugacy contains a critical point of $F_a^{\circ 2}$. It follows that $0 \in U$. \square

Corollary 6.27 (Counting Attracting/Parabolic Cycles). *1) Let $a \neq -\frac{1}{12}$, and F_a have an attracting (respectively, parabolic) cycle. Then the basin of attraction of this attracting (respectively, parabolic) cycle is equal to $\text{int } K_a$. In particular, F_a has no other attracting, parabolic, or Siegel cycle.*

2) Let $a = -\frac{1}{12}$. Then the basin of attraction of the singular point $-\frac{3}{4}$ is equal to $\text{int } K_a$. In particular, F_a has no attracting, parabolic, or Siegel cycle.

Proof. Both parts follow from Propositions 6.25, 6.26, and the fact that F_a has a unique critical point. \square

6.2.7. Counting Irrationally Neutral Cycles. In Proposition 6.26, we showed that the boundary of a Siegel disk is contained in the post-critical set of F_a . This, however, is not sufficient to give an upper bound on the number of Siegel cycles of the map

F_a (a priori, the unique critical point of F_a could be “shared” by various Siegel cycles of F_a). We will end this subsection with an adaptation of Shishikura’s results on rational maps [Shi87, Theorem 1] that will allow us to count the number of irrationally neutral cycles of F_a .

Proposition 6.28. *For any $a \in \mathbb{C} \setminus (-\infty, -\frac{1}{12})$, the map F_a has at most one non-repelling cycle.*

Proof. Thanks to Proposition 6.27, it suffices to prove that F_a has at most one irrationally neutral cycle.

The main idea in the proof of [Shi87, Theorem 1] is to construct a quasi-regular perturbation of the original map in Siegel disks or in a small neighborhood of Cremer points such that all the irrationally neutral cycles of the original map become attracting for the modified map. This argument, being purely local, applies equally well to the map F_a , and produces a quasi-regular map G_a with as many attracting cycles as the number of irrationally neutral cycles of F_a . Moreover, G_a is a small perturbation of F_a , and agrees with F_a outside the Siegel disks and away from the Cremer points of F_a . It follows that G_a maps $\overline{B}(a, r_a)^c$ univalently onto $B(a, r_a)$, and $G_a^{-1}(\heartsuit)$ univalently onto \heartsuit . We can now adapt the proof of Proposition 6.24 to conclude that G_a is quasiconformally conjugate to some member $F_{a'}$ of the family \mathcal{S} . Since attracting cycles are preserved under quasiconformal conjugacies, it follows from Proposition 6.27 that G_a can have at most one attracting cycle. The conclusion follows. \square

Corollary 6.29. *1) If F_a has a cycle of Siegel disks, then every Fatou component of F_a eventually maps to this cycle of Siegel disks.*

2) If F_a has a Cremer point, then $\text{int } K_a = \emptyset$; i.e. $K_a = \Gamma_a$.

Remark 18. 1) For maps with locally connected Julia sets, the Snail Lemma rules out the presence of Cremer points.

2) A weaker upper bound on the number of neutral cycles of F_a can be obtained by employing Fatou’s classical perturbation arguments (see [Mil06, Lemma 13.2])

6.3. Dynamical Uniformization of The Tiling Set. Recall that in the basin of infinity of a quadratic anti-polynomial, the dynamics is conjugate to the model map \bar{z}^2 via the Böttcher coordinate. For the maps F_a , we have the following analogue of Böttcher coordinates in the tiling set T_a^∞ that conjugates F_a to the reflection map ρ arising from the ideal triangle group \mathcal{G} (see Section 3 for definitions of the ideal triangle Π and the reflection map ρ).

6.3.1. Uniformization of The Tiling Set. Note that for $a \in \mathbb{C} \setminus ((-\infty, -\frac{1}{12}) \cup \mathcal{C}(\mathcal{S}))$, the critical value ∞ eventually escapes to the tile T_a^0 . This leads to the following definition of depth for parameters in the escape locus.

Definition 6.30 (Depth). For $a \in \mathbb{C} \setminus ((-\infty, -\frac{1}{12}) \cup \mathcal{C}(\mathcal{S}))$, the *smallest* positive integer $n(a)$ such that $F_a^{\circ n(a)}(\infty) \in T_a^0$ is called the *depth* of a .

Proposition 6.31. *1) For $a \in \mathcal{C}(\mathcal{S})$, $F_a : T_a^\infty \setminus \text{int } T_a^0 \rightarrow T_a^\infty$ is conformally conjugate to $\rho : \mathbb{D} \setminus \text{int } \Pi \rightarrow \mathbb{D}$.*

2) For $a \in \mathbb{C} \setminus ((-\infty, -\frac{1}{12}) \cup \mathcal{C}(\mathcal{S}))$, $F_a : \bigcup_{n=1}^{n(a)} F_a^{-n}(T_a^0) \rightarrow \bigcup_{n=0}^{n(a)-1} F_a^{-n}(T_a^0)$ is conformally conjugate to $\rho : \bigcup_{n=1}^{n(a)} \rho^{-n}(\Pi) \rightarrow \bigcup_{n=0}^{n(a)-1} \rho^{-n}(\Pi)$, where $n(a)$ denotes the depth of a .

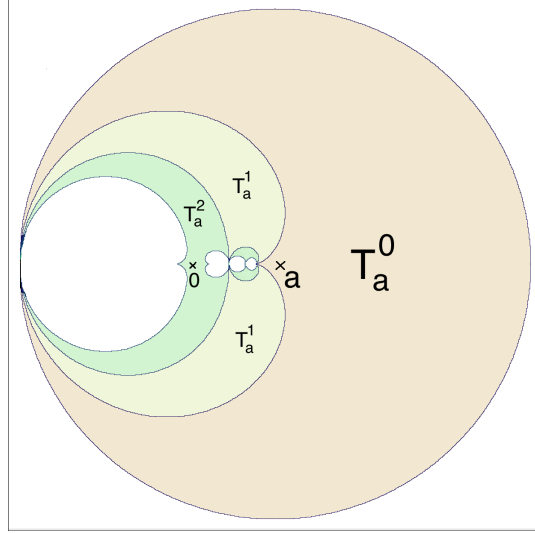


FIGURE 23. Some of the initial tiles for a parameter a in the escape locus with $n(a) = 1$ are shown. A tile of rank 2 is ramified (i.e. it contains the critical point 0) and hence disconnects the non-escaping set K_a . For such a parameter a , the external conjugacy ψ_a extends conformally to all the tiles of the first rank (and all non-degenerate tiles of higher rank).

Proof. Let ψ_a be (the homeomorphic extension of) a conformal isomorphism between T_a^0 and Π such that ψ_a maps the upper (respectively lower) half of $\partial\mathbb{H} \setminus \{\alpha_a, \frac{1}{4}\}$ onto \tilde{C}_1 (respectively \tilde{C}_3) and $\partial B(a, r_a) \setminus \{\alpha_a\}$ onto \tilde{C}_2 (compare Figure 9).

1) Since $a \in \mathcal{C}(\mathcal{S})$, the tiles (of all rank) of F_a map diffeomorphically onto T_a^0 (under iterates of F_a). Similarly, the tiles (of the tessellation of \mathbb{D}) arising from the ideal triangle group \mathcal{G} map diffeomorphically onto Π under iterates of ρ . Furthermore, F_a and ρ act as identity maps on ∂T_a^0 and $\partial\Pi$ respectively. This allows us to lift ψ_a to a conformal isomorphism from T_a^∞ (which is the union of all iterated pre-images of T_a^0 under F_a) onto \mathbb{D} (which is the union of all iterated pre-images of Π under ρ). Note that the trivial actions of F_a and ρ on ∂T_a^0 and $\partial\Pi$ (respectively) ensure that the iterated lifts match on the boundaries of the tiles. By construction, the extended map conjugates $F_a : T_a^\infty \setminus \text{int } T_a^0 \rightarrow T_a^\infty$ to $\rho : \mathbb{D} \setminus \text{int } \Pi \rightarrow \mathbb{D}$.

2) Let $a \in \mathbb{C} \setminus ((-\infty, -\frac{1}{12}) \cup \mathcal{C}(\mathcal{S}))$. By definition of depth of a , the unique critical point 0 does not lie in $\bigcup_{n=1}^{n(a)} F_a^{-n}(T_a^0)$ (compare Figure 23). So each connected

component of $F_a^{-n}(T_a^0)$, $n = 1, \dots, n(a)$ (i.e. tiles of rank 1 through $n(a)$) maps onto T_a^0 diffeomorphically under iterates of F_a . Hence, ψ_a lifts to a conformal isomorphism from $\bigcup_{n=1}^{n(a)} F_a^{-n}(T_a^0)$ onto $\bigcup_{n=1}^{n(a)} \rho^{-n}(\Pi)$ such that it conjugates $F_a : \bigcup_{n=1}^{n(a)} F_a^{-n}(T_a^0) \rightarrow \bigcup_{n=0}^{n(a)-1} F_a^{-n}(T_a^0)$ to $\rho : \bigcup_{n=1}^{n(a)} \rho^{-n}(\Pi) \rightarrow \bigcup_{n=0}^{n(a)-1} \rho^{-n}(\Pi)$. \square

Remark 19. We say that a tile is degenerate if it contains the critical point 0 or some of its iterated pre-images. For $a \notin \mathcal{C}(\mathcal{S})$, the conjugacy ψ_a extends biholomorphically to all the non-degenerate tiles of F_a .

6.3.2. Tiles and Rays. We will denote the “external” conjugacy obtained in Proposition 6.31 by ψ_a . This conjugacy allows us to associate a symbol sequence to every non-degenerate tile of F_a . Indeed, every non-degenerate tile of F_a is mapped biholomorphically by ψ_a onto some tile T^{i_1, \dots, i_k} of \mathbb{D} (see Definition 3.1).

Definition 6.32 (Coding of Dynamical Tiles). i) Let $a \in \mathcal{C}(\mathcal{S})$. For any M -admissible word (i_1, \dots, i_k) , the dynamical tile $T_a^{i_1, \dots, i_k}$ is defined as

$$T_a^{i_1, \dots, i_k} := \psi_a^{-1}(T^{i_1, \dots, i_k}).$$

ii) Let $a \in \mathbb{C} \setminus ((-\infty, -\frac{1}{12}) \cup \mathcal{C}(\mathcal{S}))$. For any M -admissible word (i_1, \dots, i_k) , the dynamical tile $T_a^{i_1, \dots, i_k}$ is defined as above, provided T^{i_1, \dots, i_k} is in the image of ψ_a .

We can use the map ψ_a to define dynamical rays for the maps F_a .

Definition 6.33 (Dynamical Rays of F_a). The pre-image of a \mathcal{G} -ray at angle θ under the map ψ_a is called a θ -dynamical ray of F_a .

Remark 20. 1) Although a \mathcal{G} -ray at angle θ is not always uniquely defined, it is easy to see that the corresponding θ -dynamical rays define the same prime end to K_a .

2) For $a \notin \mathcal{C}(\mathcal{S})$, we say that a dynamical ray of F_a at angle θ bifurcates if the corresponding sequence of tiles (of F_a) contains a degenerate tile. Otherwise, a dynamical ray is well-defined all the way to Γ_a .

6.3.3. Landing of Pre-periodic Rays. As in the case for polynomials with connected Julia sets, we will now show that for a map F_a with connected limit set, all dynamical rays at pre-periodic angles (under ρ) land on Γ_a .

Proposition 6.34 (Landing of Pre-periodic Rays). *Let $a \in \mathcal{C}(\mathcal{S})$, and $\theta \in \text{Per}(\rho)$. Then the following statements hold true.*

1) *The dynamical θ -ray of F_a lands on Γ_a .*

2) *The 0-ray of F_a lands at $\frac{1}{4}$, while the $\frac{1}{3}$ and $\frac{2}{3}$ -rays land at α_a . No other ray lands at $\frac{1}{4}$ or α_a . The iterated pre-images of the 0, $\frac{1}{3}$, and $\frac{2}{3}$ -rays land at the iterated pre-images of $\frac{1}{4}$ and α_a .*

3) *Let $\theta \in \text{Per}(\rho) \setminus \bigcup_{n \geq 0} \rho^{-n} \left(\left\{ 0, \frac{1}{3}, \frac{2}{3} \right\} \right)$. Then, the dynamical ray of F_a at angle θ lands at a repelling or parabolic (pre-)periodic point on Γ_a .*

Proof. 1) The idea of the proof is classical (see [Mil06, Theorem 18.10]). But there are subtleties related to the presence of singular points that we need to address.

Without loss of generality, we can assume that θ is periodic under ρ . Then by Section 3, there exists a shift-periodic element $(\overline{i_1, i_2, \dots, i_k}) \in M^\infty$ such that $Q(\overline{i_1, i_2, \dots, i_k}) = \theta$. Consider the sequence of points

$$w_n := \psi_a^{-1}((\rho_{i_1} \circ \dots \circ \rho_{i_k})^{\circ n}(0)), \quad n \geq 1$$

on the θ -dynamical ray of F_a . Let γ_n be the sequence of arcs on the θ -dynamical ray (of F_a) bounded by w_n and w_{n+1} . Clearly, $F_a(\gamma_n) = \gamma_{n-1}$, and there is a fixed positive constant c such that $\ell_{\text{hyp}}(\gamma_n) = c$ for all $n \geq 1$ (here, ℓ_{hyp} denotes the hyperbolic length in T_a^∞).

Since the arcs γ_n accumulate on the limit set Γ_a , it follows that the Euclidean lengths of these arcs tend to 0 as $n \rightarrow \infty$. It is now easy to see that every accumulation point of the θ -dynamical ray is either an iterated pre-image of the singular points $\frac{1}{4}, \alpha_a$ or fixed under $F_a^{\circ k}$. Note that the set of all iterated pre-images of the singular points and the fixed points of $F_a^{\circ k}$ in Γ_a is totally disconnected (as the set of fixed points of the holomorphic second iterate $F_a^{\circ 2k}$ in Γ_a is discrete). Moreover, the accumulation set of a ray is connected. Therefore, the θ -dynamical ray of F_a lands at an iterated pre-images of a singular point or at a fixed point of $F_a^{\circ k}$. But the landing point of a periodic ray cannot be strictly pre-periodic. It now follows that the θ -dynamical ray of F_a lands at a singular point or at a fixed point of $F_a^{\circ k}$.

2) Note that the landing point of a ray at a fixed angle must be a fixed point, and the only fixed points of F_a on Γ_a are $\frac{1}{4}$ and α_a . By the construction of ψ_a and the dynamical rays of F_a , we see that the tail of the 0-ray is contained in $\sigma^{-1}(\heartsuit)$. Hence, it must land at $\frac{1}{4}$. Similarly, the tails of the $\frac{1}{3}$ and $\frac{2}{3}$ -rays lie outside $\sigma^{-1}(\heartsuit)$, and hence they must land at α_a . Since the iterated pre-images of the singular points (excluding the singular points themselves) are mapped locally univalently (by suitable iterates of F_a) to the singular points, it follows that the dynamical rays at angles in $\bigcup_{n \geq 1} \rho^{-n} \left(\{0, \frac{1}{3}, \frac{2}{3}\} \right) \setminus \{0, \frac{1}{3}, \frac{2}{3}\}$ land at iterated pre-images of $\frac{1}{4}$ and α_a (excluding $\frac{1}{4}$ and α_a).

Now let $\theta \in \mathbb{R}/\mathbb{Z} \setminus \bigcup_{n \geq 0} \rho^{-n} \left(\{0, \frac{1}{3}, \frac{2}{3}\} \right)$. It remains to show that the dynamical θ -ray does not land at a singular point.

If the dynamical θ -ray of F_a lands at $\frac{1}{4}$, then so do the dynamical rays at angles $\rho^{\circ n}(\theta)$, $n \geq 1$. Clearly, all these rays (including the 0-ray) are locally contained in $\sigma^{-2}(\heartsuit)$ near $\frac{1}{4}$ (see Figure 24). Note that $F_a^{\circ 2} \equiv \sigma^{\circ 2}$ on $\sigma^{-2}(\heartsuit)$. By Corollary 6.5, $\sigma^{\circ 2}|_{\sigma^{-2}(\heartsuit)}$ extends to an orientation-preserving local homeomorphism in a neighborhood of $\frac{1}{4}$. Hence, $F_a^{\circ 2}$ acts injectively on these rays, and preserves their circular order near $\frac{1}{4}$. Applying the arguments of [Mil00b, Lemma 2.3] on $F_a^{\circ 2} = \sigma^{\circ 2}$ near $\frac{1}{4}$, one concludes that θ is fixed under $\rho^{\circ 2}$. However, there is no angle of period 2 under ρ , and θ is not a fixed angle. It follows that the dynamical θ -ray of F_a cannot land at $\frac{1}{4}$.

Now suppose that the θ -ray of F_a lands at α_a . Then the dynamical rays at angles $\rho^{\circ 2n}(\theta)$ ($n \geq 1$) also land at α_a . Locally near α_a , either all these rays are contained in $(\sigma_a \circ \sigma)^{-1}(\heartsuit)$ or all of them are contained in $(\sigma \circ \sigma_a)^{-1}(\overline{B}(a, r_a)^c)$.

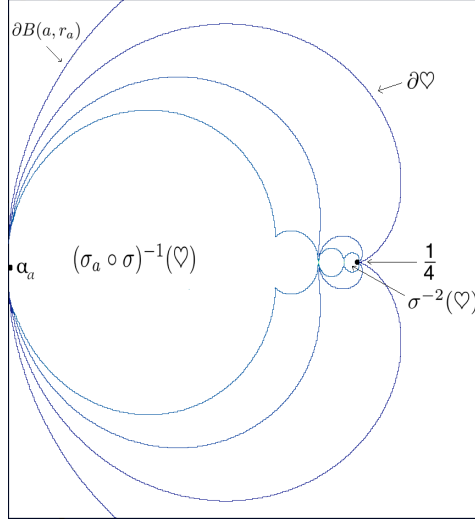


FIGURE 24. The tail of the 0-ray of F_a is trapped inside $\sigma^{-2}(\heartsuit)$, which is mapped univalently onto \heartsuit by $\sigma^{\circ 2}$. If any other ray were to land at $\frac{1}{4}$, its tail would also be contained in $\sigma^{-2}(\heartsuit)$. Similarly, there is a representative of the $\frac{1}{3}$ -ray whose tail is contained in $(\sigma_a \circ \sigma)^{-1}(\heartsuit)$. If any other θ -ray of F_a were to land at α_a , then the tail of that ray or the ray at angle $\rho(\theta)$ would be contained in $(\sigma_a \circ \sigma)^{-1}(\heartsuit)$.

For definiteness, let us assume that they are all contained in $(\sigma_a \circ \sigma)^{-1}(\heartsuit)$ (see Figure 24). We can also choose a representative of the $\frac{1}{3}$ -ray in $(\sigma_a \circ \sigma)^{-1}(\heartsuit)$. Note that $F_a^{\circ 2} \equiv \sigma_a \circ \sigma$ on $(\sigma_a \circ \sigma)^{-1}(\heartsuit)$ (see Formula (9)). By Propositions 6.11 and 6.12, $(\sigma_a \circ \sigma)|_{(\sigma_a \circ \sigma)^{-1}(\heartsuit)}$ has a holomorphic extension around α_a which is locally injective near α_a . Therefore, $F_a^{\circ 2}$ acts injectively on the rays mentioned above (including the $\frac{1}{3}$ -ray), and preserves their circular order near α_a . Applying again [Mil00b, Lemma 2.3] on $F_a^{\circ 2} = \sigma_a \circ \sigma$ near α_a , we conclude that θ must be fixed under $\rho^{\circ 2}$. Now the conclusion follows as in the previous case.

This shows that no ray lands at the singular points other than the 0, $\frac{1}{3}$, and $\frac{2}{3}$ -rays.

3) Finally, let $\theta \in \text{Per}(\rho) \setminus \bigcup_{n \geq 0} \rho^{-n} \left(\left\{ 0, \frac{1}{3}, \frac{2}{3} \right\} \right)$. Once again, we can assume that

θ is periodic under ρ . By the second part of the proposition, the landing point of the θ -ray of F_a is not an iterated pre-image of the singular points. Therefore, $F_a^{\circ 2k}$ is defined in a small neighborhood of the landing point. An application of the classical Snail Lemma now shows that the landing point of the θ -dynamical ray is repelling or parabolic (compare [Mil06, Lemma 18.9]). \square

Let us also state a converse to the previous proposition.

Proposition 6.35 (Repelling and Parabolic Points are Landing Points of Rays). *Let $a \in \mathcal{C}(\mathcal{S})$. Then, every repelling and parabolic periodic point of F_a is the landing*

point of finitely many (at least one) dynamical rays. Moreover, all these rays have the same period under $F_a^{\circ 2}$.

Proof. The proof of [Lyu17, Theorem 24.5, Theorem 24.6] applies mutatis mutandis to our situation. \square

Remark 21. Unlike in the holomorphic situation, it is not true that all rays landing at a periodic point have the same period under F_a (this is already false for quadratic anti-polynomials, see [Muk15a, Theorems 2.6, 3.1]). The combinatorics of dynamical rays landing at periodic points of F_a will be discussed in detail in [LLMM18].

6.3.4. *Locally Connected Limit Sets, and Density of Repelling Cycles.* Similar to the situation of rational maps or Kleinian groups, we have the following statements.

Proposition 6.36 (Density of Repelling Cycles). *Let $a \in \mathcal{C}(\mathcal{S})$, and Γ_a be locally connected. Then the following hold true.*

- 1) *Iterated pre-images of $\frac{1}{4}$ under F_a are dense in Γ_a .*
- 2) *Repelling periodic points of F_a are dense in Γ_a .*

Proof. 1) Since $\Gamma_a = \partial T_a^\infty$ is connected and locally connected, the inverse of the Riemann map $\psi_a^{-1} : \mathbb{D} \rightarrow T_a^\infty$ that conjugates ρ to F_a (constructed in Proposition 6.31) extends continuously to \mathbb{T} , and semi-conjugates $\rho|_{\mathbb{T}}$ to $F_a|_{\Gamma_a}$. Abusing notations, let us denote this continuous extension by ψ_a^{-1} . Note that $\psi_a^{-1}(0) = \frac{1}{4}$. Moreover, the iterated pre-images of 0 under ρ are dense in \mathbb{T} , and φ_a^{-1} maps these points to the iterated pre-images of $\frac{1}{4}$ under F_a . It now follows that $\bigcup_{k=0}^{\infty} F_a^{-k} \left(\left\{ \frac{1}{4} \right\} \right)$ is dense in Γ_a .

2) Since periodic points of ρ are dense in \mathbb{T} , one can argue as in the first part to conclude that periodic points of F_a are dense in Γ_a . The result now immediately follows from Proposition 6.28. \square

Remark 22. 1) Note that for $w \in \Gamma_a$, there exists no $\varepsilon > 0$ such that infinitely many forward iterates of F_a are defined on $B(w_0, \varepsilon)$. This prohibits us from using the standard normal family argument to prove density of iterated pre-images or density of repelling cycles in Γ_a . In the locally connected case, we circumvent this problem by working with the topological model $\rho|_{\mathbb{T}}$ for $F_a|_{\Gamma_a}$.

2) Under the local connectivity assumption, the density statement is also true for the pre-images of the double point α_a , and can be proved similarly.

6.3.5. *Landing Map and Lamination.* Let $a \in \mathcal{C}(\mathcal{S})$. Proposition 6.34 allows us to define a landing map

$$L_a : \text{Per}(\rho) \rightarrow \Gamma_a$$

that associates to every (pre-)periodic angle θ (under ρ) the landing point of the θ -dynamical ray of F_a .

Definition 6.37 (Pre-periodic Lamination of F_a). For $a \in \mathcal{C}(\mathcal{S})$, the pre-periodic lamination of F_a is defined as the equivalence relation on $\text{Per}(\rho) \subset \mathbb{R}/\mathbb{Z}$ such that $\theta, \theta' \in \text{Per}(\rho)$ are related if and only if $L_a(\theta) = L_a(\theta')$. We denote the pre-periodic lamination of F_a by $\lambda(F_a)$.

The next definition and the subsequent proposition relates pre-periodic laminations of F_a to rational laminations of quadratic anti-polynomials (see Definition 2.7). This connection will be crucial in [LLMM18], where we will establish a combinatorial bijection between the post-critically finite parameters of \mathcal{S} and those of \mathcal{L} .

Definition 6.38 (Push-forward/pullback of Laminations). The push-forward $\mathcal{E}_*(\lambda(F_a))$ of the pre-periodic lamination of F_a is defined as the image of $\lambda(F_a) \subset \text{Per}(\rho) \times \text{Per}(\rho)$ under $\mathcal{E} \times \mathcal{E}$. Clearly, $\mathcal{E}_*(\lambda(F_a))$ is an equivalence relation on \mathbb{Q}/\mathbb{Z} . Similarly, the pullback $\mathcal{E}^*(\lambda(f_c))$ of the rational lamination of a quadratic anti-polynomial f_c is defined as the pre-image of $\lambda(f_c) \subset \mathbb{Q}/\mathbb{Z} \times \mathbb{Q}/\mathbb{Z}$ under $\mathcal{E} \times \mathcal{E}$.

Proposition 6.39 (Properties of Pre-periodic Laminations). *Let $a \in \mathcal{C}(\mathcal{S})$, and $\lambda(F_a)$ be the pre-periodic lamination associated with F_a . Then, $\lambda(F_a)$ satisfies the following properties.*

- (1) $\lambda(F_a)$ is closed in $\text{Per}(\rho) \times \text{Per}(\rho)$.
- (2) Each $\lambda(F_a)$ -equivalence class A is a finite subset of $\text{Per}(\rho)$.
- (3) If A is a $\lambda(F_a)$ -equivalence class, then $\rho(A)$ is also a $\lambda(F_a)$ -equivalence class.
- (4) If A is a $\lambda(F_a)$ -equivalence class, then $A \mapsto \rho(A)$ is consecutive reversing.
- (5) $\lambda(F_a)$ -equivalence classes are pairwise unlinked.

Consequently, the push-forward $\mathcal{E}_*(\lambda(F_a))$ is a formal rational lamination (under m_{-2}).

Proof. The proof of the properties of $\lambda(F_a)$ are analogous to the proof of the corresponding statements for rational laminations of polynomials (see [Kiw01, Theorem 1.1]). The last statement follows from the fact that \mathcal{E} is a homeomorphism of the circle that conjugates m_{-2} to ρ . \square

6.3.6. *Cantor Dynamics.* Recall that for parameters c outside the Tricorn, the filled Julia set of f_c is a Cantor set. We will need an analogous statement for maps F_a outside the connectedness locus $\mathcal{C}(\mathcal{S})$.

Proposition 6.40 (Cantor outside $\mathcal{C}(\mathcal{S})$). *If $a \notin \mathcal{C}(\mathcal{S})$, then K_a is a Cantor set.*

Proof. The idea of the proof is similar to that of [DH85, Exposé III, §1, Proposition 1]. However, lack of uniform contraction of the inverse branches of F_a (around the singular points) adds some subtlety to the situation.

Let $a \notin \mathcal{C}(\mathcal{S})$ and $n(a)$ be the depth of a (see Definition 6.30). Then, some tile of rank $(n(a)+1)$ contains the critical point 0, and disconnects K_a (compare Figure 25). This is equivalent to saying that $\hat{\mathbb{C}} \setminus E_a^{n(a)+1}$ has two connected components (where E_a^k is the union of tiles of rank $\leq k$). F_a maps each of these two connected components injectively onto $\hat{\mathbb{C}} \setminus E_a^{n(a)}$. Let us denote the inverse branches of F_a defined on $\hat{\mathbb{C}} \setminus E_a^{n(a)}$ by g_1 and g_2 . Clearly, every connected component of K_a is the nested intersection of sets of the form $(g_{i_1} \circ g_{i_2} \circ \cdots \circ g_{i_k})(\hat{\mathbb{C}} \setminus E_a^{n(a)})$, where $(i_1, i_2, \dots) \in \{1, 2\}^{\mathbb{N}}$.

The fact that the connected component of K_a containing $\frac{1}{4}$ is a singleton follows from Corollary 6.5, and the same statement about α_a follows from shrinking of petals in Relation (10). Hence, every connected component of K_a containing a point of $\bigcup_{k \geq 0} F_a^{-k}(\{\frac{1}{4}, \alpha_a\})$ is a singleton.

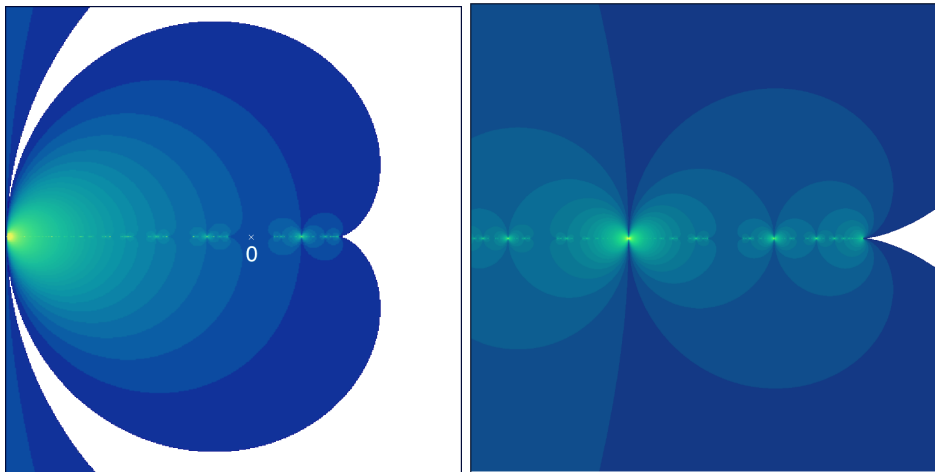


FIGURE 25. Left: A part of the dynamical plane of some parameter a outside $\mathcal{C}(\mathcal{S})$ showing a Cantor limit set. The critical point 0 is contained in a ramified tile, which disconnects K_a . Right: A blow-up of the same dynamical plane around $\sigma^{-1}(\heartsuit)$ showing disconnections of K_a at deeper levels producing a Cantor set structure.

On $\text{int}(\hat{\mathbb{C}} \setminus E_a^{n(a)})$, the sequence of anti-conformal maps $\{g_{i_1}, g_{i_1} \circ g_{i_2}, \dots\}$ forms a normal family with a constant limit function. It follows that a connected component of K_a not intersecting $\frac{1}{4}, \alpha_a$ and their pre-images is also a singleton.

This proves that every connected component of K_a is a singleton; i.e. K_a is a Cantor set. \square

Proof of Theorem 1.2. This follows from Proposition 6.31 and Proposition 6.40. \square

7. GEOMETRICALLY FINITE MAPS

In this section, we will take a closer look at the dynamical properties of a simpler subclass of maps in \mathcal{S} . More precisely, we will focus on geometrically finite maps; i.e. maps with an attracting or parabolic cycle, and maps for which the critical point is strictly pre-periodic.

Recall that for any $a \in \mathbb{C} \setminus (-\infty, -\frac{1}{12})$, the map F_a has two fixed points α_a and $\frac{1}{4}$ such that F_a does not admit an anti-holomorphic extension in a neighborhood of these points. We analyzed the dynamical behavior of F_a near these fixed points in Proposition 6.10 and Proposition 6.11. In what follows, we will refer to these fixed points as *singular points*. On the other hand, the terms *cycle/periodic orbit* will be reserved for periodic points of period greater than one (these are contained in Ω_a).

7.1. Hyperbolic and Parabolic Maps. F_a is called hyperbolic (respectively, parabolic) if it has a (super-)attracting (respectively, parabolic) cycle. It is easy to see that a (super-)attracting cycle of F_a belongs to the interior of K_a , and a parabolic cycle lies on the boundary of K_a (e.g. by [Mil06, §5, Theorem 5.2]). Moreover, a parabolic periodic point necessarily lies on the boundary of a Fatou component (i.e. a connected component of $\text{int} K_a$) that contains an attracting petal

of the parabolic germ such that the forward orbit of every point in the component converges to the parabolic cycle through the attracting petals.

7.1.1. *First Properties and Examples.* By Corollary 6.27, a hyperbolic or parabolic map F_a has a unique (super-)attracting or parabolic cycle, and the basin of attraction of this cycle coincides with all of $\text{int } K_a$. Moreover, Proposition 6.26 implies that $a \in \mathcal{C}(\mathcal{S}) \setminus \{-\frac{1}{12}\}$.

Examples. i) The simplest hyperbolic map in $\mathcal{C}(\mathcal{S})$ is $a = 0$ (see Figure 5(right)). The critical orbit of the corresponding map is given by $0 \leftrightarrow \infty$, so the map has a super-attracting cycle. This map is the analogue of the Basilica anti-polynomial $\bar{z}^2 - 1$.

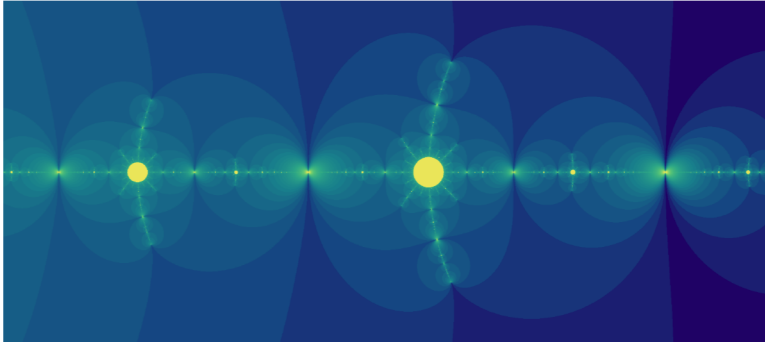


FIGURE 26. A part of the non-escaping set of F_a with $a = \frac{3}{16}$ (in yellow) bearing resemblance with the filled Julia set of the Airplane anti-polynomial $\bar{z}^2 - 1.7549\dots$.

ii) The map F_a with $a = \frac{3}{16}$ has a super-attracting 3-cycle; namely $0 \mapsto \infty \mapsto 3/16 \mapsto 0$ (by Equation (7)). This map is the analogue of the Airplane anti-polynomial $\bar{z}^2 - 1.7549\dots$ (see Figure 26).

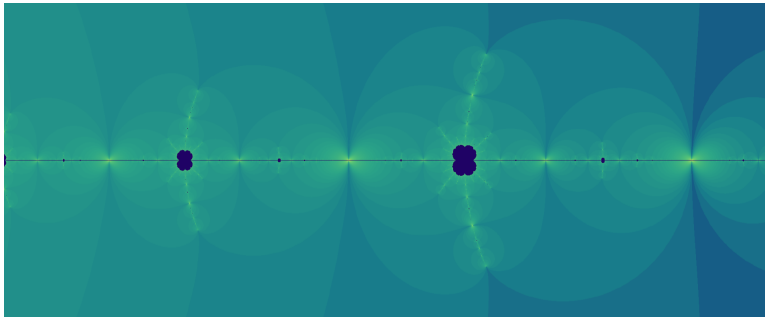


FIGURE 27. A part of the non-escaping set of F_a with $a = \frac{16\sqrt{3}-3}{132}$ (in blue) bearing resemblance with the filled Julia set of the anti-polynomial $\bar{z}^2 - \frac{7}{4}$.

iii) The map F_a with $a = \frac{16\sqrt{3}-3}{132}$ has a parabolic cycle of period 3. This map is the analogue of the anti-polynomial $\bar{z}^2 - \frac{7}{4}$, which has also has a parabolic cycle of period 3 (see Figure 27).

7.1.2. Radial Limit Set of Hyperbolic/Parabolic Maps. The following notion, which plays an important role in our study, was first introduced in [Lyu83] and later formalized in [Urb03, McM00]. (The concept was tacitly used in the proof of Lemma 5.12.)

Definition 7.1 (Radial Limit Set). A point $w \in \Gamma_a$ is called a radial point if there exists $\delta > 0$ and an infinite sequence of positive integers $\{n_k\}$ such that there exists a well-defined inverse branch of $F_a^{\circ n_k}$ defined on $B(F_a^{\circ n_k}(w), \delta)$ sending $F_a^{\circ n_k}(w)$ to w for all k . The set of all radial points of Γ_a is called the radial limit set of F_a .

It is not hard to see that for a radial point w , the sequence of inverse branches of $F_a^{\circ n_k}$ mapping $F_a^{\circ n_k}(w)$ to w are eventually contracting; in other words, we have $\lim_{k \rightarrow \infty} (F_a^{\circ n_k})'(w) = \infty$. Thus, F_a has a strong expansion property at the radial points of Γ_a . Furthermore, one can use the inverse branches of $F_a^{\circ n_k}$ to transfer information from moderate scales to microscopic scales at radial points.

The next proposition gives an explicit description of the radial limit set of hyperbolic and parabolic maps.

Proposition 7.2. 1) Let F_a have a (super-)attracting cycle. Then, the radial limit set of F_a is equal to $\Gamma_a \setminus \bigcup_{k=0}^{\infty} F_a^{-k}(\{\frac{1}{4}, \alpha_a\})$.

2) Let F_a have a parabolic cycle \mathcal{O} . Then, the radial limit set of F_a is equal to $\Gamma_a \setminus \bigcup_{k=0}^{\infty} F_a^{-k}(\mathcal{O} \cup \{\frac{1}{4}, \alpha_a\})$.

Proof. 1) If w is an iterated pre-image of a singular point, then it clearly does not belong to the radial limit set.

Let $w \in \Gamma_a \setminus \bigcup_{k=0}^{\infty} F_a^{-k}(\{\frac{1}{4}, \alpha_a\})$. Recall that by Proposition 6.17, the limit set is locally contained in the “repelling petals” at $\frac{1}{4}$ and α_a . Hence, no point in Γ_a can non-trivially converge to one of the singular points. Our assumption on w now implies that there exists $\delta > 0$ such that infinitely many forward iterates $F_a^{\circ n_k}(w)$ stay outside $B(\{\frac{1}{4}, \alpha_a\}, 2\delta)$. Since the critical orbit of F_a converges to an attracting cycle (i.e. the post-critical set stays at a positive distance away from Γ_a), it follows $B(F_a^{\circ n_k}(w), \delta) \subset \Omega_a \setminus \{F_a^{\circ r}(0)\}_{r \geq 0}$ for all $k \geq 1$ (possibly after choosing a smaller $\delta > 0$). Therefore, for each $k \geq 1$, there is a well-defined inverse branch $F_a^{-n_k} : B(F_a^{\circ n_k}(w), \delta) \rightarrow \mathbb{C}$ that sends $F_a^{\circ n_k}(w)$ to w .

2) In the parabolic situation, the only difference is that the critical orbit converges to the parabolic cycle \mathcal{O} which lies on the limit set. In particular, there is no uniform neighborhood of \mathcal{O} where infinitely many inverse branches of $F_a^{\circ n}$ are defined. Hence, the radial limit set is disjoint from $\bigcup_{k=0}^{\infty} F_a^{-k}(\mathcal{O} \cup \{\frac{1}{4}, \alpha_a\})$.

On the other hand, if $w \in \Gamma_a \setminus \bigcup_{k=0}^{\infty} F_a^{-k}(\mathcal{O} \cup \{\frac{1}{4}, \alpha_a\})$, then its forward orbit can neither converge to the parabolic cycle nor converge to the singular points. Hence, infinitely many forward iterates of $F_a^{\circ n k}(w)$ stay away from the fundamental tile and the closure of the post-critical set. Therefore, there exists $\delta > 0$ and well-defined inverse branches $F_a^{-n k} : B(F_a^{\circ n k}(w), \delta) \rightarrow \mathbb{C}$ that send $F_a^{\circ n k}(w)$ to w (for all $k \geq 1$). \square

7.1.3. Topological and Analytic Properties. Note that the Julia set of a hyperbolic or parabolic polynomial has zero area. Using the description of radial limit sets given in Proposition 7.2, we can now prove the same statement for hyperbolic and parabolic maps in \mathcal{S} .

Corollary 7.3. *If F_a is hyperbolic or parabolic, then Γ_a has zero area.*

Proof. The proof is similar to [Lyu17, Proposition 25.22] or [Urb03, Theorem 2.9], we include it for completeness.

Any small scale disk around a radial point w of F_a can be mapped with bounded distortion onto a moderate scale oval of bounded shape. As Γ_a is the boundary of T_a^∞ , it is a closed set with empty interior. Therefore, a moderate scale oval of bounded shape around a point of Γ_a contains a definite gap. But this gap can be pulled back by an inverse branch of some iterate of F_a proving that the initial small scale disk around w has a definite gap as well. Hence, no radial point is a point of Lebesgue density for Γ_a . The result now follows from the description of the radial limit set of F_a given in Proposition 7.2 and Lebesgue's density theorem. \square

Recall that the limit set of a hyperbolic or parabolic map is connected. The following proposition shows that the limit set of such maps is also locally connected.

Proposition 7.4. *If F_a is hyperbolic or parabolic, then Γ_a is locally connected.*

Proof. The proof of [DH07, Exposé X, Theorem 1] can be adapted for our situation, we only indicate the necessary modifications.

Recall that since F_a is hyperbolic or parabolic, the non-escaping set K_a is connected and every tile is unramified. In particular, there is a unique tile of rank 0, and $3 \cdot 2^{n-1}$ tiles of rank n (for $n \geq 1$). We denote the union of all tiles of rank $\leq n$ by E_a^n . Then ∂E_a^n is a closed curve contained in the union of the tiling set T_a^∞ and the iterated pre-images of the singular points $\frac{1}{4}$ and α_a . Moreover, $F_a^{\circ 2}$ is a two-to-one covering from ∂E_a^{n+2} onto ∂E_a^n . Choose a parametrization $\gamma_1 : \mathbb{T} \rightarrow \partial E_a^1$ such that $\gamma_1(0) = \frac{1}{4}$, and $\gamma_1(\theta) = \gamma_1(\theta')$ for $\theta \neq \theta'$ only if $\gamma_1(\theta)$ is a singular point (of T_a) or one of its pre-images. Now define parametrizations $\gamma_n : \mathbb{T} \rightarrow \partial E_a^{2n-1}$ inductively by lifting $\gamma_{n-1} : \mathbb{T} \rightarrow \partial E_a^{2n-3}$ (by the covering map $F_a^{\circ 2} : \partial E_a^{2n-1} \rightarrow \partial E_a^{2n-3}$) such that $\gamma_n(0) = \frac{1}{4}$.

Let B be a neighborhood of the attracting cycle A_- of F_a (if F_a is hyperbolic) or the union of attracting petals at the parabolic cycle A_0 of F_a (if F_a is parabolic) such that the post-critical set $\{F_a^{\circ n}(0)\}_{n \geq 0}$ is contained in B . We define a compact set

$$X := \hat{\mathbb{C}} \setminus (\text{int } E_a^1 \cup B).$$

Let Y be the set of singular points on ∂E_a^1 ; i.e. $Y := \{\frac{1}{4}, \alpha_a, \sigma^{-1}(\alpha_a), \sigma^{-1}(\frac{1}{4})\}$. Then, X satisfies the following properties (compare [DH07, Proposition 1]).

- (1) $X \cap \{F_a^{on}(0)\}_{n \geq 0} = \emptyset$, and in the hyperbolic case, $X \cap A_- = \emptyset$;
- (2) $A_0 \cup Y \subset \partial X$ (where $A_0 = \emptyset$ in the hyperbolic case);
- (3) Each of the sets $\Gamma_a, F_a^{-2}(X)$, and ∂E_a^n ($n \geq 1$) is contained in $\text{int } X \cup A_0 \cup Y$ (where $A_0 = \emptyset$ in the hyperbolic case).

Let $U := \text{int } X$, and μ_U the hyperbolic metric on each connected component of U . Fixing $\varepsilon > 0$ sufficiently small and $M > 0$ sufficiently large, we define a metric μ on $U \cup N_\varepsilon(A_0 \cup \{\frac{1}{4}, \alpha_a\})$ as follows

$$\mu := \begin{cases} \inf(\mu_U, M|dw|) & \text{on } U \cap N_\varepsilon(A_0 \cup \{\frac{1}{4}, \alpha_a\}), \\ \mu_U & \text{on } U \setminus N_\varepsilon(A_0 \cup \{\frac{1}{4}, \alpha_a\}), \\ M|dw| & \text{on } N_\varepsilon(A_0 \cup \{\frac{1}{4}, \alpha_a\}) \setminus U. \end{cases}$$

Finally, let us set $X' := F_a^{-2}(X)$. The arguments of [DH07, Propositions 4,5] now apply verbatim to show that if M is large enough, then $\{\gamma_n\}_n$ is a Cauchy sequence in $C(\mathbb{T}, X')$ equipped with the metric of uniform convergence for the distance d_μ on X' (associated with the Riemannian metric μ). It follows that the sequence converges uniformly for d_μ , and hence also for the Euclidean distance (as X' is compact). The limit of the sequence $\{\gamma_n\}_n$ is the Caratheodory loop of Γ_a , proving local connectivity of Γ_a . □

The following improvement will be important in the mating discussion, which will be carried out in Section 8.

Theorem 7.5. *If F_a is hyperbolic, then the tiling set T_a^∞ is a John domain. Hence, Γ_a is conformally removable.*

Proof. Since the post-critical set of a hyperbolic map F_a is bounded away from its limit set, the proof is completely analogous to that of Theorem 5.21. □

Remark 23. The tiling set of a parabolic map F_a is not a John domain as it has outward pointing cusps at the parabolic points (see Figure 27). However, we do not know if the corresponding limit sets are conformally removable.

7.2. Misiurewicz Maps. A parameter $a \in \mathbb{C} \setminus (-\infty, -\frac{1}{12})$ is called Misiurewicz if the critical point 0 of F_a is strictly pre-periodic and the post-critical orbit does not meet the desingularized droplet T_a^0 .

7.2.1. First Properties.

Proposition 7.6. *Let F_a be a Misiurewicz map.*

1) *The critical point of F_a eventually lands on a repelling cycle or on one of the singular points $\frac{1}{4}, \alpha_a$. Consequently, $a \in \mathcal{C}(\mathcal{S}) \setminus \{-\frac{1}{12}\}$.*

2) *The non-escaping set K_a of F_a has empty interior; i.e. $K_a = \Gamma_a$.*

Proof. 1) It follows from Proposition 6.26 that such a map cannot have a (super-)attracting or neutral cycle (a simple modification of the proof of Proposition 6.26 shows that a Cremer point is also an accumulation point of the orbit of 0). Hence, the critical point 0 of a Misiurewicz map must eventually land on a repelling cycle or on one of the singular points $\frac{1}{4}, \alpha_a$. In particular, the entire forward orbit of 0 (which is finite) stays in K_a ; and hence $a \in \mathcal{C}(\mathcal{S}) \setminus \{-\frac{1}{12}\}$.

2) Since the critical point of F_a is strictly pre-periodic, Proposition 6.25 and Proposition 6.26 rule out the existence of interior components of K_a ; hence $\text{int } K_a = \emptyset$. Thus, $K_a = \Gamma_a$. \square

7.2.2. *Radial Limit Set of Misiurewicz Maps.* The next proposition describes the radial limit set (see Definition 7.1) for Misiurewicz maps.

Proposition 7.7. *Let a be a Misiurewicz parameter. The radial limit set of F_a is equal to $\Gamma_a \setminus \bigcup_{k=0}^{\infty} F_a^{-k}(\{0, \frac{1}{4}, \alpha_a\})$.*

Proof. Since critical values are obstructions to the existence of inverse branches of anti-holomorphic maps (on a full disk neighborhood), and F_a does not have anti-holomorphic extensions in neighborhoods of the singular points, it follows that neither a pre-critical point nor an iterated pre-image of a singular point can be a radial limit point of F_a .

Since the critical value ∞ eventually falls on a repelling cycle, points in the forward orbit of ∞ evidently satisfy the radial limit set condition.

Finally, if $w \in \Gamma_a$ does not belong to the grand orbit of the critical point and the singular points, then infinitely many forward iterates of w stay away from the singular points and the post-critical set. The arguments of Proposition 7.2 can now be applied verbatim to conclude that such a point belongs to the radial limit set. \square

7.2.3. *Topological and Analytic Properties.* We now record a couple of basic topological and analytic properties of the non-escaping set of a Misiurewicz map.

Proposition 7.8. *Let a be some Misiurewicz parameter. Then, the area of K_a is zero.*

Proof. Note that since K_a has empty interior, we only need to show that Γ_a has measure zero. This follows from the description of the radial limit set of F_a given in Proposition 7.7, and the fact that no radial limit point is a point of Lebesgue density for Γ_a (compare Proposition 7.3). \square

Proposition 7.9. *Let a be some Misiurewicz parameter. Then, Γ_a is locally connected. Consequently, all external dynamical rays of F_a land on Γ_a . Moreover, Γ_a is a dendrite.*

Proof. The proof is similar to that of Proposition 7.4 with one important modification (since Γ_a contains the critical orbit).

Let $X := \hat{\mathbb{C}} \setminus \text{int } E_a^1$. Then X satisfies the following properties

- (1) $\{\frac{1}{4}, \alpha_a, \sigma^{-1}(\alpha_a), \sigma_a^{-1}(\frac{1}{4})\} \subset \partial X$;
- (2) $\{F_a^{\circ n}(0)\}_{n \geq 0} \subset \text{int } X$,
- (3) $\Gamma_a, \gamma_n, F_a^{-2}(X) \subset \text{int } X \cup \{\frac{1}{4}, \alpha_a, \sigma^{-1}(\alpha_a), \sigma_a^{-1}(\frac{1}{4})\}$.

Let us set $U := \text{int } X$, and define a function $v : U \rightarrow \mathbb{Z}^+$ as

$$v(w) = \begin{cases} 2 & \text{if } w \in \{F_a^{\circ k}(0)\}_{k \geq 1}, \\ 1 & \text{otherwise.} \end{cases}$$

Then, $v(F_a(w)) = \deg_w(F_a) \cdot v(w)$ for each w (where $\deg_w(F_a)$ denotes the local degree of F_a at w). Let U^* be a ramified covering of U , with ramification degree

equal to $v(w)$ for every point above w , and \tilde{U} the universal covering of U^* . Let $\pi : \tilde{U} \rightarrow U$ be the projection map.

Denote by $\mu_{\tilde{U}}$ the hyperbolic metric on \tilde{U} and μ_U the admissible Riemannian metric on U such that $\pi : \tilde{U} \rightarrow U$ is a local isometry. Now, fixing $\varepsilon > 0$ sufficiently small and $M > 0$ sufficiently large, we define a metric μ on $U \cup N_\varepsilon(\{\frac{1}{4}, \alpha_a\})$ as follows

$$\mu := \begin{cases} \inf(\mu_U, M|dw|) & \text{on } U \cap N_\varepsilon(\{\frac{1}{4}, \alpha_a\}), \\ \mu_U & \text{on } U \setminus N_\varepsilon(\{\frac{1}{4}, \alpha_a\}), \\ M|dw| & \text{on } N_\varepsilon(\{\frac{1}{4}, \alpha_a\}) \setminus U. \end{cases}$$

Once again, the arguments of [DH07, Propositions 4,5] show that if M is large enough, then $\{\gamma_n\}_n$ (see the proof of Proposition 7.4 for the definition of the curves γ_n) is a Cauchy sequence in $C(\mathbb{T}, X')$ (where $X' := F_a^{-2}(X)$) equipped with the metric of uniform convergence for the distance d_μ on X' (associated with the Riemannian metric μ). It follows that the sequence converges uniformly for d_μ , and hence also for the Euclidean distance (as X' is compact). The limit of the sequence $\{\gamma_n\}_n$ is the Caratheodory loop of Γ_a , proving local connectivity of Γ_a .

Landing of dynamical rays follows from local connectivity of Γ_a and Caratheodory's theorem. The last statement follows from the fact that K_a is full and has empty interior (see Proposition 7.6). \square

Theorem 1.3, which was announced in the introduction, follows from our analysis of geometrically finite maps.

Proof of Theorem 1.3. 1) Local connectivity of the limit sets of geometrically finite maps follows from Propositions 7.4 and 7.9. The statement on zero area of limit sets follows from Proposition 7.3 and 7.8.

2) This follows from Propositions 6.36, 7.4, and 7.9. \square

7.2.4. Examples of Misiurewicz Maps. **Examples.** i) The simplest Misiurewicz parameter in $\mathcal{C}(\mathcal{S})$ is $a = \frac{1}{4}$. The critical orbit of the corresponding map is $0 \mapsto \infty \mapsto \frac{1}{4} \circlearrowleft$. Note that $F_a : [-\infty, \frac{1}{4}] \rightarrow [-\infty, \frac{1}{4}]$ is a two-to-one surjective map (see Figure 21). Hence, $[-\infty, \frac{1}{4}]$ is a completely invariant subset of Γ_a .

By Propositions 6.36 and 7.9, the pre-images of $\frac{1}{4}$ are dense in Γ_a . It follows that $\Gamma_a = [-\infty, \frac{1}{4}]$ (see Figure 6). This map is the analogue of the Chebyshev anti-polynomial $\bar{z}^2 - 2$ whose Julia set is the interval $[-2, 2]$.

ii) For $a = \frac{5}{36}$, the critical orbit of F_a is $0 \mapsto \infty \mapsto \frac{5}{36} \mapsto -\frac{3}{4} \circlearrowleft$ (by Relation (7)). So, $\frac{5}{36}$ is a Misiurewicz parameter of $\mathcal{C}(\mathcal{S})$ (see Figure 28). This map is the analogue of the anti-polynomial $\bar{z}^2 - 1.543689\dots$, whose critical point also lands at the separating fixed point in three steps.

8. EXAMPLES OF MATING IN THE CIRCLE AND CARIOID FAMILY

Recall that in Section 5, we showed that the Schwarz reflection map of the deltoid is the unique conformal mating of the anti-polynomial \bar{z}^2 and the reflection map ρ . Here, we will demonstrate that Schwarz reflection maps in the family \mathcal{S} provide us with more examples of conformal matings between quadratic anti-polynomials and the reflection map ρ .

This section contains simple illustrations of a more general result that will be proved in [LLMM18]. Amongst other things, we will show in [LLMM18] that there

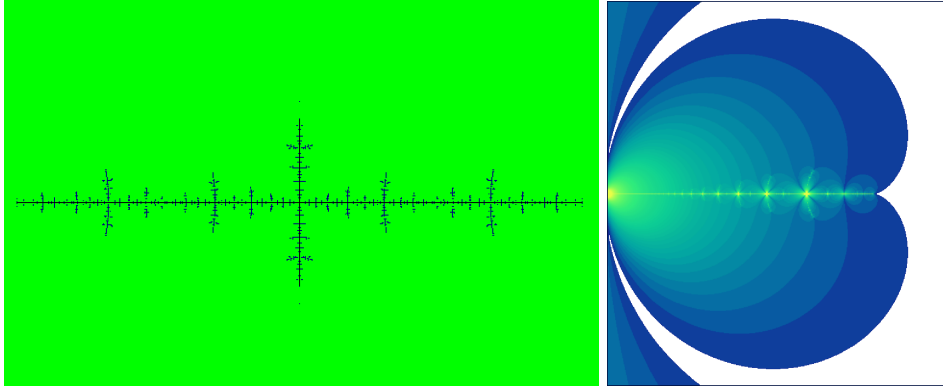


FIGURE 28. Left: The dynamical plane of the Misiurewicz map $\bar{z}^2 - 1.5437 \dots$, for which the critical point 0 lands at the α -fixed point in 3 iterates. Right: A part of the dynamical plane of the Misiurewicz map F_a where $a = \frac{5}{36}$. The critical point 0 of this map lands at the fixed point α_a in 3 iterates.

exists a bijection between the post-critically finite maps in \mathcal{S} and those in the real basilica limb of the Tricorn such that each post-critically finite map in \mathcal{S} is the conformal mating of the corresponding anti-polynomial and the reflection map ρ .

8.1. A Combinatorial Condition for Mating. Let us state and prove a general combinatorial condition that guarantees mateability of a quadratic anti-polynomial and the reflection map ρ .

Proposition 8.1. *Let $a_0 \in \mathcal{S}$ and $c_0 \in \mathcal{T}$ be post-critically finite maps satisfying $\mathcal{E}_*(\lambda(F_{a_0})) = \lambda(f_{c_0})$. Then, $F_{a_0} : K_{a_0} \rightarrow K_{a_0}$ is topologically conjugate to $f_{c_0} : \mathcal{K}_{c_0} \rightarrow \mathcal{K}_{c_0}$ such that the conjugacy is conformal in $\text{int } K_{a_0}$, and $F_{a_0} : T_{a_0}^\infty \setminus T_{a_0}^0 \rightarrow T_{a_0}^\infty$ is conformally conjugate to $\rho : \mathbb{D} \setminus \Pi \rightarrow \mathbb{D}$.*

Let us start with an intermediate lemma, which states that the homeomorphism $\mathcal{E} : \mathbb{R}/\mathbb{Z} \rightarrow \mathbb{R}/\mathbb{Z}$ induces a topological conjugacy between the maps F_{a_0} and f_{c_0} on their respective limit and Julia sets.

Lemma 8.2. *With a_0 and c_0 as in Proposition 8.1, the homeomorphism \mathcal{E} of the circle induces a topological conjugacy \mathcal{E}_{a_0} between $F_{a_0} : \Gamma_{a_0} \rightarrow \Gamma_{a_0}$ and $f_{c_0} : \mathcal{J}_{c_0} \rightarrow \mathcal{J}_{c_0}$.*

Proof. As f_{c_0} is a post-critically finite map, \mathcal{J}_{c_0} is locally connected. Hence, the inverse of the Böttcher conjugacy $\varphi_{c_0} : \widehat{\mathbb{C}} \setminus \mathcal{K}_{c_0} \rightarrow \widehat{\mathbb{C}} \setminus \overline{\mathbb{D}}$ between f_{c_0} and \bar{z}^2 extends continuously to \mathbb{R}/\mathbb{Z} , and yields a semi-conjugacy between $m_{-2} : \mathbb{R}/\mathbb{Z} \rightarrow \mathbb{R}/\mathbb{Z}$ and $f_{c_0} : \mathcal{J}_{c_0} \rightarrow \mathcal{J}_{c_0}$. The fibers of this semi-conjugacy give rise to an equivalence relation $\lambda_{\mathbb{R}}(f_{c_0})$ (on \mathbb{R}/\mathbb{Z}), which is the smallest closed equivalence relation containing the rational lamination $\lambda(f_{c_0})$ (see [Kiw01, Lemma 4.17]). Therefore, $f_{c_0} : \mathcal{J}_{c_0} \rightarrow \mathcal{J}_{c_0}$ is topologically conjugate to the quotient of $m_{-2} : \mathbb{R}/\mathbb{Z} \rightarrow \mathbb{R}/\mathbb{Z}$ by the m_{-2} -invariant lamination $\lambda_{\mathbb{R}}(f_{c_0})$.

Again, for a post-critically finite parameter a_0 , the limit set Γ_{a_0} is locally connected (see Theorem 1.3). Hence, the inverse of the external conjugacy $\psi_{a_0} : T_{a_0}^\infty \rightarrow \mathbb{D}$ between F_{a_0} and ρ extends continuously to the boundary, and yields a semi-conjugacy

between $\rho : \mathbb{R}/\mathbb{Z} \rightarrow \mathbb{R}/\mathbb{Z}$ and $F_{a_0} : \Gamma_{a_0} \rightarrow \Gamma_{a_0}$. The fibers of this semi-conjugacy give rise to an equivalence relation $\lambda_{\mathbb{R}}(F_{a_0})$ (on \mathbb{R}/\mathbb{Z}), which is the smallest closed equivalence relation on \mathbb{R}/\mathbb{Z} containing the pre-periodic lamination $\lambda(F_{a_0})$ (this can be proved following the arguments of [Kiw01, Lemma 4.17]). Therefore, $F_{a_0} : \Gamma_{a_0} \rightarrow \Gamma_{a_0}$ is topologically conjugate to the quotient of $\rho : \mathbb{R}/\mathbb{Z} \rightarrow \mathbb{R}/\mathbb{Z}$ by the ρ -invariant lamination $\lambda_{\mathbb{R}}(F_{a_0})$.

$$\begin{array}{ccccccc}
 \Gamma_{a_0} & \xrightarrow{\psi_{a_0}} & (\mathbb{R}/\mathbb{Z})/\lambda_{\mathbb{R}}(F_{a_0}) & \xrightarrow{\mathcal{E}} & (\mathbb{R}/\mathbb{Z})/\lambda_{\mathbb{R}}(f_{c_0}) & \xrightarrow{\varphi_{c_0}^{-1}} & \mathcal{J}_{c_0} \\
 \downarrow F_{a_0} & & \downarrow \rho & & \downarrow m_{-2} & & \downarrow f_{c_0} \\
 \Gamma_{a_0} & \xrightarrow{\psi_{a_0}} & (\mathbb{R}/\mathbb{Z})/\lambda_{\mathbb{R}}(F_{a_0}) & \xrightarrow{\mathcal{E}} & (\mathbb{R}/\mathbb{Z})/\lambda_{\mathbb{R}}(f_{c_0}) & \xrightarrow{\varphi_{c_0}^{-1}} & \mathcal{J}_{c_0}
 \end{array}$$

FIGURE 29. The maps ψ_{a_0} and $\varphi_{c_0}^{-1}$ in the commutative diagram denote the homeomorphisms induced by the continuous boundary extensions of the corresponding conformal maps. The composition of the three horizontal maps yields a topological conjugacy between $F_{a_0} : \Gamma_{a_0} \rightarrow \Gamma_{a_0}$ and $f_{c_0} : \mathcal{J}_{c_0} \rightarrow \mathcal{J}_{c_0}$.

Since $\mathcal{E}_*(\lambda(F_{a_0})) = \lambda(f_{c_0})$, and $\lambda(F_{a_0})$ (respectively $\lambda(f_{c_0})$) generate $\lambda_{\mathbb{R}}(F_{a_0})$ (respectively, $\lambda_{\mathbb{R}}(f_{c_0})$), we have that $\mathcal{E}_*(\lambda_{\mathbb{R}}(F_{a_0})) = \lambda_{\mathbb{R}}(f_{c_0})$ (note that \mathcal{E} is a homeomorphism of the circle). Therefore, the conjugacy \mathcal{E} between ρ and m_{-2} descends to a topological conjugacy between their quotients by $\lambda_{\mathbb{R}}(F_{a_0})$ and $\lambda_{\mathbb{R}}(f_{c_0})$ respectively. It follows that $F_{a_0} : \Gamma_{a_0} \rightarrow \Gamma_{a_0}$ is topologically conjugate to $f_{c_0} : \mathcal{J}_{c_0} \rightarrow \mathcal{J}_{c_0}$ by the composition of the above three conjugacies (see Figure 29). \square

We denote the topological conjugacy between $F_{a_0} : \Gamma_{a_0} \rightarrow \Gamma_{a_0}$ and $f_{c_0} : \mathcal{J}_{c_0} \rightarrow \mathcal{J}_{c_0}$ by \mathcal{E}_{a_0} .

Let us now proceed to prove Proposition 8.1, which gives a complete description of the dynamics of the post-critically finite map F_{a_0} as a “mating” of the reflection map ρ arising from the ideal triangle group \mathcal{G} and the anti-polynomial $\bar{z}^2 + c_0$.

Proof of Proposition 8.1. Let us first assume that a_0 is a Misiurewicz parameter. Then the corresponding pre-periodic lamination $\lambda(F_{a_0})$ is of Misiurewicz type, and hence, $\lambda(f_{c_0}) = \mathcal{E}_*(\lambda(F_{a_0}))$ is a rational lamination of Misiurewicz type. It follows that c_0 is a Misiurewicz parameter of the Tricorn. Thus we have $\Gamma_{a_0} = K_{a_0}$, and $\mathcal{J}_{c_0} = \mathcal{K}_{c_0}$. The theorem (for Misiurewicz parameters) now follows from Lemma 8.2 and Proposition 6.31.

Now let a_0 be a super-attracting parameter. We will construct a conformal conjugacy between F_{a_0} and f_{c_0} in the interior of K_{a_0} that matches continuously with the conjugacy on the limit set constructed in Lemma 8.2.

We assume that F_{a_0} has a super-attracting cycle of odd period k (the even period case is similar). Let U be the Fatou component of F_{a_0} containing the critical point 0. Since K_{a_0} is full and Γ_{a_0} is locally connected, it follows that U is a Jordan disk. Hence, the Riemann map $\mathfrak{b} : \mathbb{D} \rightarrow U$ (which is the inverse of a Böttcher coordinate) that conjugates $\bar{z}^2|_{\mathbb{D}}$ to the first return map $F_{a_0}^{\circ k}|_U$ extends homeomorphically to the boundary $\partial\mathbb{D}$. We can normalize the Riemann map so that it sends 1 to the

dynamical root on ∂U . Moreover, if \tilde{U} is the Fatou component of f_{c_0} containing 0, then the same is true for the Riemann map $\tilde{\mathfrak{b}} : \mathbb{D} \rightarrow \tilde{U}$ that conjugates $\bar{z}^2|_{\mathbb{D}}$ to the first return map $f_{c_0}^{\circ k}|_{\tilde{U}}$. Therefore, $\mathfrak{h} := \tilde{\mathfrak{b}} \circ \mathfrak{b}^{-1} : \bar{U} \rightarrow \tilde{U}$ conjugates $F_{a_0}^{\circ k}$ to $f_{c_0}^{\circ k}$.

We claim that \mathfrak{h} continuously matches with \mathcal{E}_{a_0} on ∂U . Since both \mathfrak{h} and \mathcal{E}_{a_0} conjugate $F_{a_0}^{\circ k}|_{\partial U}$ to $f_{c_0}^{\circ k}|_{\partial \tilde{U}}$, it follows that $\mathcal{E}_{a_0}^{-1} \circ \mathfrak{h} : \partial U \rightarrow \partial U$ is an orientation-preserving homeomorphism commuting with $F_{a_0}^{\circ k}|_{\partial U}$. Moreover, it fixes the dynamical root on ∂U . But $F_{a_0}^{\circ k}|_{\partial U}$ is topologically equivalent to $\bar{z}^2|_{\partial \mathbb{D}}$, and the only orientation-preserving homeomorphism of the circle commuting with \bar{z}^2 and having a fixed point is the identity map. Hence, $\mathcal{E}_{a_0}^{-1} \circ \mathfrak{h}|_{\partial U} = \text{id}$, and the claim follows.

Let us now consider another component D of $\text{int } K_{a_0}$. Since $\text{int } K_{a_0}$ is the basin of the super-attracting cycle of F_{a_0} , there exists some positive integer n such that $F_{a_0}^{\circ n}$ maps D univalently onto U . Let \tilde{D} be the Fatou component of f_{c_0} such that $\mathcal{E}_{a_0}(\partial D) = \partial \tilde{D}$, and $\tilde{D} f_{c_0}^{-n}$ be the inverse branch that maps \tilde{U} to \tilde{D} . Since \mathcal{E}_{a_0} is a conjugacy on the whole limit set, we have

$$\mathcal{E}_{a_0}|_{\partial D} = \tilde{D} f_{c_0}^{-n} \circ \mathcal{E}_{a_0}|_{\partial U} \circ F_{a_0}^{\circ n} : \partial D \rightarrow \partial \tilde{D}.$$

We now define

$$\mathfrak{h}_D := \tilde{D} f_{c_0}^{-n} \circ \mathfrak{h} \circ F_{a_0}^{\circ n} : \bar{D} \rightarrow \tilde{D}.$$

Since, \mathfrak{h} agrees with \mathcal{E}_{a_0} on ∂U , it now follows that $\mathcal{E}_{a_0}|_{\partial D} = \mathfrak{h}_D$.

Thus, we have extended the conjugacy \mathcal{E}_{a_0} (which was defined between the limit set of F_{a_0} and the Julia set of f_{c_0}) conformally and equivariantly to all of $\text{int } K_{a_0}$. Since Γ_{a_0} is locally connected, the diameters of the Fatou components of F_{a_0} tend to 0. It is now easy to verify that the extension is a homeomorphism on K_{a_0} .

This, together with Proposition 6.31, completes the proof of the theorem for super-attracting parameters. \square

8.2. The Basilica Map. Throughout this subsection, we will assume that $a_0 = 0$, and $c_0 = -1$.

The map F_{a_0} has a super-attracting 2-cycle $0 \leftrightarrow \infty$. The dynamical $\frac{1}{3}$ and $\frac{2}{3}$ -rays of F_{a_0} land at α_a , which is the unique common boundary point of the periodic super-attracting Fatou components. By [LLMM18, Proposition 6.6], iterated pull-backs of the leaf connecting $\frac{1}{3}$ and $\frac{2}{3}$ (in $\bar{\mathbb{D}}$) under ρ are pairwise disjoint and their closure in \mathbb{Q}/\mathbb{Z} is the pre-periodic lamination $\lambda(F_{a_0})$.

On the other hand, the Basilica anti-polynomial $f_{c_0}(z) = \bar{z}^2 - 1$ has a super-attracting 2-cycle $0 \leftrightarrow -1$. The dynamical $\frac{1}{3}$ and $\frac{2}{3}$ -rays of f_{c_0} land at the α -fixed point of f_{c_0} , which is the unique common boundary point of the periodic super-attracting Fatou components. By [Lyu17, Theorem 25.42], iterated pull-backs of the leaf connecting $\frac{1}{3}$ and $\frac{2}{3}$ (in $\bar{\mathbb{D}}$) under m_{-2} are pairwise disjoint and their closure in \mathbb{Q}/\mathbb{Z} is the rational lamination $\lambda(f_{c_0})$.

Since \mathcal{E} fixes $\frac{1}{3}$ and $\frac{2}{3}$, it follows that $\mathcal{E}_*(\lambda(F_{a_0})) = \lambda(f_{c_0})$.

Let us now consider the two conformal dynamical systems

$$f_{c_0} : \mathcal{K}_{c_0} \rightarrow \mathcal{K}_{c_0}$$

and

$$\rho : \bar{\mathbb{D}} \setminus \text{int } \Pi \rightarrow \bar{\mathbb{D}}.$$

We use the mating tool $\xi := \varphi_{c_0}^{-1} \circ \mathcal{E} : \mathbb{T} \rightarrow \mathcal{J}_{c_0}$ (which semi-conjugates ρ to f_{c_0}) to glue $\bar{\mathbb{D}}$ outside \mathcal{K}_{c_0} .

Denote

$$X = \overline{\mathbb{D}} \vee_{\xi} \mathcal{K}_{c_0}, \quad Y = X \setminus \text{int } \Pi.$$

We will argue that X is a topological sphere. Since \mathcal{K}_{c_0} is homeomorphic to $\overline{\mathbb{D}}/\lambda_{\mathbb{R}}(f_{c_0})$, it follows that X is topologically the quotient of the 2-sphere by a closed equivalence relation such that all equivalence classes are connected and non-separating, and not all points are equivalent. It follows by Moore's theorem that X is a topological 2-sphere [Moo25, Theorem 25]. Moreover, Y is a closed Jordan disc in X .

The well-defined topological map

$$\eta \equiv \rho \vee_{\xi} f_{c_0} : Y \rightarrow X$$

is the topological mating between ρ and f_{c_0} .

The conjugacies obtained in Proposition 8.1 glue together to produce a homeomorphism

$$H : (X, Y) \rightarrow (\hat{\mathbb{C}}, \overline{\Omega}_{a_0})$$

which is conformal outside $H^{-1}(\Gamma_{a_0})$, and which conjugates η to F_{a_0} . It endows X with a conformal structure compatible with the one on $X \setminus H^{-1}(\Gamma_{a_0})$ that turns η into an anti-holomorphic map conformally conjugate to F_{a_0} . In this way, the mating η provides us with a model for F_{a_0} .

Moreover, there is only one conformal structure on X compatible with the standard structure on $X \setminus H^{-1}(\Gamma_{a_0})$. Indeed, another structure would result in a non-conformal homeomorphism $\hat{\mathbb{C}} \rightarrow \hat{\mathbb{C}}$ which is conformal outside Γ_{a_0} , contradicting the conformal removability of Γ_{a_0} (see Theorem 7.5).

In this sense, F_{a_0} is the unique conformal mating of the map ρ arising from the ideal triangle group and the anti-polynomial $\bar{z}^2 - 1$.

8.3. The Chebyshev Map. Throughout this subsection, we will assume that $a_0 = \frac{1}{4}$, and $c_0 = -2$.

The critical point of the map F_{a_0} is strictly pre-periodic, the critical orbit is $0 \mapsto \infty \mapsto \frac{1}{4} \circlearrowleft$. We saw in Subsection 7.2 that $\Gamma_{a_0} = [-\infty, \frac{1}{4}]$. It follows by real symmetry (or by dynamical considerations) that the critical value ∞ is the landing point of the unique dynamical ray at angle $\frac{1}{2}$ (of F_{a_0}).

By Proposition 6.39, the push-forward $\mathcal{E}_*(\lambda(F_a))$ is a formal rational lamination (under m_{-2}) of Misiurewicz type. Now [LLMM18, Theorem 2.24] and its proof imply that there exists a unique Misiurewicz parameter in the Tricorn whose rational lamination is given by $\mathcal{E}_*(\lambda(F_a))$ such that in the corresponding dynamical plane, the only dynamical ray landing at the critical value has angle $\mathcal{E}(\frac{1}{2}) = \frac{1}{2}$.

The unique Misiurewicz parameter in the Tricorn satisfying the above property is $c_0 = -2$. The corresponding map is the Chebyshev anti-polynomial $f_{c_0}(z) = \bar{z}^2 - 2$. The forward orbit of its critical point is $0 \mapsto -2 \mapsto 2 \circlearrowleft$, and its Julia set is the interval $[-2, 2]$.

Since $\mathcal{E}_*(\lambda(F_{a_0})) = \lambda(f_{c_0})$ and $\Gamma_{a_0} = [-\infty, \frac{1}{4}]$ is conformally removable, the mating theory discussed in Subsection 8.2 applies to the map F_{a_0} as well. Hence, F_{a_0} is the unique conformal mating of the map ρ arising from the ideal triangle group and the anti-polynomial $\bar{z}^2 - 2$.

Proof of Theorem 1.4. Follows from Subsection 8.2 and Subsection 8.3. □

REFERENCES

- [ABWZ02] O. Agam, E. Bettelheim, P. Wiegmann, and A. Zabrodin. Viscous fingering and a shape of an electronic droplet in the quantum hall regime. *Phys. Rev. Lett.*, 88(23):236801, 2002.
- [AS76] D. Aharonov and H. S. Shapiro. Domains on which analytic functions satisfy quadrature identities. *J. Analyse Math.*, 30:39–73, 1976.
- [ASS99] D. Aharonov, H. S. Shapiro, and A. Solynin. A minimal area problem in conformal mapping. *J. Analyse Math.*, 78:157–176, 1999.
- [BBM18] A. Bonifant, X. Buff, and J. Milnor. Antipode preserving cubic maps: the fjord theorem. *Proc. London Math. Soc.*, 116:670–728, 2018.
- [BE16] W. Bergweiler and A. Eremenko. Green’s function and anti-holomorphic dynamics on a torus. *Proc. Amer. Math. Soc.*, 144:2911–2922, 2016.
- [BG17] M. Putinar B. Gustafsson. *Hypernormal quantization of planar domains*, volume 2199 of *Lect. Notes Math.* Springer, 2017.
- [BL17a] S. Bullett and L. Lomonaco. Dynamics of modular matings. <https://arxiv.org/abs/1707.04764>, 2017.
- [BL17b] S. Bullett and L. Lomonaco. Mating quadratic maps with the modular group II. <https://arxiv.org/abs/1611.05257>, 2017.
- [BMMS17] K. Bogdanov, K. Mamayusupov, S. Mukherjee, and D. Schleicher. Antiholomorphic perturbations of Weierstrass Zeta functions and Green’s function on tori. *Nonlinearity*, 30:3241–3254, 2017.
- [BP94] S. Bullett and C. Penrose. Mating quadratic maps with the modular group. *Inventiones Mathematicae*, 115:483–511, 1994.
- [BS79] R. Bowen and C. Series. Markov maps associated with fuchsian groups. *Publications Mathématiques de L’I.H.É.S.*, 50(153-170), 1979.
- [CFG15] J. Canela, N. Fagella, and A. Garijo. On a family of rational perturbations of the doubling map. *Journal of Difference Equations and Applications*, 21:715–741, 2015.
- [CG93] L. Carleson and T. W. Gamelin. *Complex Dynamics*. Springer, Berlin, 1993.
- [CHRSC89] W. D. Crowe, R. Hasson, P. J. Rippon, and P. E. D. Strain-Clark. On the structure of the Mandelbar set. *Nonlinearity*, 2, 1989.
- [CKS00] L. A. Caffarelli, L. Karp, and H. Shahgholian. Regularity of a free boundary problem with application to the pompeiu problem. *Annals of Mathematics*, 151:269–292, 2000.
- [Dav74] P. J. Davis. *The Schwarz Function and its Applications*. Number 17 in Carus Math. Monographs. Math. Assoc. Amer., 1974.
- [DH85] A. Douady and J. H. Hubbard. On the dynamics of polynomial-like mappings. *Ann. Sci. Ec. Norm. Sup.*, 18:287–343, 1985.
- [DH07] A. Douady and J. H. Hubbard. *Étude dynamique des polynômes complexes*. Société Mathématique de France, 2007.
- [Dur83] P. L. Duren. *Univalent functions*, volume 259 of *Grundlehren der mathematischen Wissenschaften*. Springer-Verlag, New York, 1983.
- [EF05] P. Elbau and G. Felder. Density of eigenvalues of random normal matrices. *Commun. Math. Phys.*, 259:433–450, 2005.
- [EGKP05] Peter Ebenfelt, Björn Gustafsson, Dmitry Khavinson, and Mihai Putinar, editors. *Quadrature Domains and Their Applications : The Harold S. Shapiro Anniversary Volume*, volume 156 of *Operator Theory: Advances and Applications*, Basel, 2005. Birkhäuser Verlag.
- [EL84] A. E. Eremenko and M. Yu. Lyubich. Iterates of entire functions. *Soviet Math. Dokl.*, 30:592–594, 1984.
- [EL92] A. E. Eremenko and M. Yu. Lyubich. Dynamical properties of some classes of entire functions. *Ann. Inst. Fourier (Grenoble)*, 42:989–1020, 1992.
- [Eps62] B. Epstein. On the mean-value property of harmonic functions. *Proc. Amer. Math. Soc.*, 13:830, 1962.
- [Eps93] A. L. Epstein. *Towers of finite type complex analytic maps*. PhD thesis, The City University of New York, 1993.
- [ES65] B. Epstein and M. Schiffer. On the mean-value property of harmonic functions. *J. Analyse Math.*, 14:109–111, 1965.

- [EV92] P. Etingof and A. Varchenko. *Why the Boundary of a Round Drop Becomes a Curve of Order Four*, volume 3 of *University Lecture Series*. American Mathematical Society, Providence, R.I., 1992.
- [GHMP00] B. Gustafsson, C. He, P. Milanfar, and M. Putinar. Reconstructing planar domains from their moments. *Inverse Problems*, 16:1053–1070, 2000.
- [GK86] L. R. Goldberg and L. Keen. A finiteness theorem for a dynamical class of entire functions. *Ergodic Theory and Dynamical Systems*, 6:183–192, 1986.
- [Gus83] B. Gustafsson. Quadrature identities and the Schottky double. *Acta Appl. Math.*, 1:209–240, 1983.
- [GV06] B. Gustafsson and A. Vasil’ev. *Conformal and Potential Analysis in Hele-Shaw Cell*. Birkhäuser Basel, 2006.
- [GV16] T. Gauthier and G. Vigny. Distribution of postcritically finite polynomials III: combinatorial continuity. <http://arxiv.org/pdf/1602.00925.pdf>, 2016.
- [HM13] H. Hedenmalm and N. Makarov. Coulomb gas ensembles and laplacian growth. *Proc. London Math. Soc.*, 106:859–907, 2013.
- [HS14] J. H. Hubbard and D. Schleicher. Multicorns are not path connected. In *Frontiers in Complex Dynamics: In Celebration of John Milnor’s 80th Birthday*, pages 73–102. Princeton University Press, 2014.
- [IM16a] H. Inou and S. Mukherjee. Discontinuity of straightening in antiholomorphic dynamics. <https://arxiv.org/abs/1605.08061>, 2016.
- [IM16b] H. Inou and S. Mukherjee. Non-landing parameter rays of the multicorns. *Inventiones Mathematicae*, 204:869–893, 2016.
- [Ino09] H. Inou. Combinatorics and topology of straightening maps II: Discontinuity. <http://arxiv.org/abs/0903.4289>, 2009.
- [Jon95] P. W. Jones. On removable sets for Sobolev spaces in the plane. In R. Fefferman, C. Fefferman and S. Wainger, editors, *Essays on Fourier Analysis in Honor of Elias M. Stein*, volume 42 of *Princeton Math. Ser.*, pages 250–267. Princeton University Press, New Jersey, 1995.
- [Kiw01] Jan Kiwi. Rational laminations of complex polynomials. In Mikhail Lyubich, John W. Milnor, and Yair N. Minsky, editors, *Laminations and Foliations in Dynamics, Geometry and Topology*, volume 269 of *Contemporary Mathematics*, pages 111–154. American Mathematical Society, 2001.
- [KS03] D. Khavinson and G. Swiatek. On the number of zeros of certain harmonic polynomials. *Proc. Amer. Math. Soc.*, 131(2):409–414, 2003.
- [LLMM18] S.-Y. Lee, M. Lyubich, N. G. Makarov, and S. Mukherjee. Dynamics of Schwarz reflections and the Tricorn. Preprint, 2018.
- [LM16] S. Y. Lee and N. G. Makarov. Topology of quadrature domains. *Journal of The American Mathematical Society*, 29:333–369, 2016.
- [Loc61] E. H. Lockwood. *A book of curves*. Cambridge University Press, 1961.
- [Lyu83] M. Lyubich. On typical behavior of the trajectories of a rational mapping of the sphere. *Soviet Math. Dokl.*, 27(1):22–25, 1983.
- [Lyu17] M. Lyubich. *Conformal Geometry and Dynamics of Quadratic Polynomials, vol I-II*. in preparation, 2017. <http://www.math.stonybrook.edu/~mlyubich/book.pdf>.
- [McM00] C. T. McMullen. Hausdorff dimension and conformal dynamics II: geometrically finite rational maps. *Commentarii Mathematici Helvetici*, 75(4):535–593, 2000.
- [Mil92] J. Milnor. Remarks on iterated cubic maps. *Experiment. Math.*, 1:5–24, 1992.
- [Mil00a] J. Milnor. On rational maps with two critical points. *Experiment. Math.*, 9:333–411, 2000.
- [Mil00b] J. Milnor. Periodic orbits, external rays and the Mandelbrot set. *Astérisque*, 261:277–333, 2000.
- [Mil06] J. Milnor. *Dynamics in one complex variable*. Princeton University Press, New Jersey, 3rd edition, 2006.
- [MNS17] S. Mukherjee, S. Nakane, and D. Schleicher. On Multicorns and Unicorns II: bifurcations in spaces of antiholomorphic polynomials. *Ergodic Theory and Dynamical systems*, 37:859–899, 2017.
- [Moo25] R. L. Moore. Concerning upper-semicontinuous collections of continua. *Transactions of the American Mathematical Society*, 27(4):416–428, 1925.

- [Muk15a] S. Mukherjee. *Antiholomorphic Dynamics: Topology of Parameter Spaces, and Discontinuity of Straightening*. PhD thesis, Jacobs University, Bremen, 2015. <http://nbn-resolving.de/urn:nbn:de:gbv:579-opus-1005222>.
- [Muk15b] S. Mukherjee. Orbit portraits of unicritical antiholomorphic polynomials. *Conformal Geometry and Dynamics of the AMS*, 19:35–50, 2015.
- [Nak93] S. Nakane. Connectedness of the tricorn. *Ergodic Theory and Dynamical Systems*, 13:349–356, 1993.
- [NS03] S. Nakane and D. Schleicher. On Multicorns and Unicorns I : Antiholomorphic dynamics, hyperbolic components and real cubic polynomials. *International Journal of Bifurcation and Chaos*, 13:2825–2844, 2003.
- [PR10] C. L. Petersen and P. Roesch. Parabolic tools. *Journal of Difference Equations and Applications*, 16:715–738, 2010.
- [Ric72] S. Richardson. Hele shaw flows with a free boundary produced by the injection of fluid into a narrow channel. *J. Fluid Mech.*, 56:609–618, 1972.
- [Roe10] P. Roesch. Cubic polynomials with a parabolic point. *Ergodic Theory and Dynamical Systems*, 30:1843–1867, 2010.
- [Sak78] M. Sakai. A moment problem in jordan domains. *Proc. Amer. Math. Soc.*, 70:35–38, 1978.
- [Sak82] M. Sakai. *Quadrature domains*, volume 934 of *Lect. Notes Math.* Springer-Verlag, Berlin-Heidelberg, 1982.
- [Sak91] M. Sakai. Regularity of a boundary having a Schwarz function. *Acta Math.*, 166:263–297, 1991.
- [Sch00] D. Schleicher. Rational parameter rays of the Mandelbrot set. *Astérisque*, 261:405–443, 2000.
- [Sha92] H. Shahgholian. On quadrature domains and the Schwarz potential. *J. Math. Anal. Appl.*, 171:61–78, 1992.
- [Shi87] M. Shishikura. On the quasiconformal surgery of rational functions. *Ann. Sci. Éc. Norm. Supér.*, 4^e série, 20(1):1–29, 1987.
- [SS00] T. Sheil-Small. *Complex Polynomials*. Cambridge University Press, 2000.
- [ST97] E. B. Saff and V. Totik. *Logarithmic Potentials with External Fields*, volume 316 of *Grundlehren der mathematischen Wissenschaften*. Springer-Verlag, Berlin, 1997.
- [Sul85] D. Sullivan. Quasiconformal homeomorphisms and dynamics I. solution of the Fatou-Julia problem on wandering domains. *Annals of Mathematics*, 122(2):401–418, 1985.
- [TBA⁺05] R. Teodorescu, E. Bettelheim, O. Agam, A. Zabrodin, and P. Wiegmann. Normal random matrix ensemble as a growth problem. *Nucl. Phys. B*, 704:407–444, 2005.
- [Urb03] M. Urbanski. Measures and dimensions in conformal dynamics. *Bull. Amer. Math. Soc.*, 40:281–321, 2003.
- [Wie02] P. Wiegmann. Aharonov-bohm effect in the quantum hall regime and laplacian growth problems. In Andrea Cappelli and Giuseppe Mussardo, editors, *Statistical Field Theories*, volume 73 of *NATO Science Series*, pages 337–349. Springer, Dordrecht, 2002.

DEPARTMENT OF MATHEMATICS AND STATISTICS, UNIVERSITY OF SOUTH FLORIDA, TAMPA, FL 33620, USA

E-mail address: lees3@usf.edu

INSTITUTE FOR MATHEMATICAL SCIENCES, STONY BROOK UNIVERSITY, NY, 11794, USA

E-mail address: mlyubich@math.stonybrook.edu

DEPARTMENT OF MATHEMATICS, CALIFORNIA INSTITUTE OF TECHNOLOGY, PASADENA, CALIFORNIA 91125, USA

E-mail address: makarov@caltech.edu

INSTITUTE FOR MATHEMATICAL SCIENCES, STONY BROOK UNIVERSITY, NY, 11794, USA

E-mail address: sabya@math.stonybrook.edu